# Investigating the potential of membranes formed by the vapor induced phase separation process

Norafiqah Ismail [a], Antoine Venault [b], Jyri-Pekka Mikkola [a,c], Denis Bouyer [d], Enrico Drioli [e], Naser Tavajohi Hassan Kiadeh [a,*]

[a] Technical Chemistry, Department of Chemistry, Chemical-Biological Centre, Umeå University, 90187, Umeå, Sweden
[b] R&D Center for Membrane Technology and Department of Chemical Engineering, Chung Yuan Christian University, Chung-Li, 32023, Taiwan
[c] Industrial Chemistry & Reaction Engineering, Johan Gadolin Process Chemistry Centre, Åbo Akademi University, Biskopsgatan 8, 20500, Åbo-Turku, Finland
[d] Institut Européen des Membranes, IEM, UMR 5635, ENSCM, CNRS, Univ Montpellier, Montpellier, France
[e] ITM-CNR, University of Calabria, Italy

## ARTICLE INFO

## ABSTRACT

About 100 years ago, Zsigmondy and Bachmann invented a new method to induce phase inversion, the so-called vapor induced phase separation (VIPS). Since then many researchers have demonstrated this method in membrane fabrication. Here we present a review on membrane fabrication *via* VIPS to provide insights into membrane formation parameters in order to achieve desired properties for different applications. The key factors upon membrane preparation including solution parameters (i.e. polymer type and concentration, type of solvent, and additives) as well as operating parameters (i.e. exposure time, relative humidity, dissolution temperature, and vapor temperature) are comprehensively discussed. Furthermore, the design of a fouling-resistance membrane by the VIPS process has recently gained attention and is elaborated in details. The applications of the produced membranes *via* VIPS in water and wastewater treatment, gas separations, electrochemical applications (i.e. secondary batteries and supercapacitors) as well as in medical and biological applications are summarized and an outlook for future investigation is presented.

## 1. Introduction

Generally, 40%–70% of chemical plant capital and operating costs are related to the separation and purification processes [1]. Among the different types of separation systems, membrane processes have superior performance. It is widely recognized that membrane separation processes can be represented as "greener" alternatives in comparison to the corresponding conventional systems [2,3]. Membrane separation systems have demonstrated promising performances in medical applications [4,5], desalination [6–8], water and wastewater treatment [9–11], water reclamation [12,13], energy production [14], energy storage [15–17] and carbon dioxide capture [18–22]. In addition, they are important tools in new concepts of engineering such as process intensification [23–26] and zero-discharge [27–29].

Membranes are typically in a flat sheet, hollow fiber or hollow capsule shape with symmetric, asymmetric, bi- or multilayer, thin-layer or mixed matrix composite cross-section structures. Membranes are made of organic polymers, inorganic materials (oxides, ceramics, and metals), mixed matrix or composite materials. There are different methods for membrane fabrication such as phase separation of a polymer, sol-gel process, interfacial reaction, stretching, extrusion, track etching, and micro-fabrication. Polymeric membranes and phase separations, respectively, are the most common materials and methods upon membrane fabrication [30].

Phase separation processes mainly encompass methods such as non-solvent induced phase separation (NIPS), thermally induced phase separation (TIPS), evaporation induced phase separation (EIPS) and vapor induced phase separation (VIPS) or the combination of these methods [31]. In all of the above-mentioned methods, a homogenous polymer solution, which may contain some additives, is at first prepared. In TIPS, changing the temperature causes a change in the solubility of the polymer in a solvent and phase inversion can happen. Depending on the thermodynamics of the polymer/solvent, an upper or lower critical temperature can be reached and, as a result, changing in the temperature leads to phase inversion. Therefore, heat transfer is the main parameter regulating phase inversion in TIPS [32–36]. In NIPS, the

---

*N. Ismail et al.*

phase inversion happens by penetration of the non-solvent to the polymer solution and substitution of the initial solvent with the non-solvent. Therefore, mass transfer phenomena play an important role in this phase inversion process [37–48]. In EIPS, the non-solvent exists in the polymeric solution. By evaporation of the volatile solvent, the casting solution will be enriched by non-volatile non-solvents, so that the phase inversion happens. Therefore, in EIPS method, the rate of volatile solvent evaporation is a critical factor controlling phase inversion [49–56]. The VIPS process was first introduced by Zsigmondy and Bachmann [57] in 1918 and then developed further by Elford in 1937 [58]. Since then many researchers used the VIPS method in membrane fabrication. In the VIPS process, the non-solvent penetrates from a vapor phase to polymer solution and induce phase inversion. Fig. 1 shows the schematic illustration of the VIPS process.

It is critical to distinguish VIPS and EIPS. The main differences between VIPS and EIPS are 1) In VIPS, non-solvent penetrates to the polymer solution while in case of EIPS the non-solvent originally exists in the solution with the polymer and a more volatile solvent. 2) In VIPS, the non-solvent inflow is responsible for phase separation while in EIPS the solvent outflow is responsible for phase inversion.

It is worthwhile to consider that among the different phase inversion methods, VIPS is more similar to the NIPS process. One can assume the VIPS as a NIPS processes by much slower mass transfer rates and more controllable parameters in the phase inversion steps. This can be attributed to slower kinetics of gaseous non-solvents in comparison to liquid non-solvents used in phase inversion [59,60]. Indeed, one of the main reasons of the interest in membrane formation by VIPS is its potential to better control the membrane morphology during the phase separation.

The importance of the fundamental knowledge about VIPS method is getting more obvious when we note that phase inversion based on VIPS mechanism is occurring in other methods of membrane fabrication approaches too. For example, there may emerge a VIPS step during the time gap between nascent flat sheet membrane casting and immersion in the coagulation bath, in the air gap during the spinning of hollow fiber membrane, and during the electrospinning of fiber under controlled humidity and temperature. In all of the above-mentioned procedures,

VIPS plays an important role in phase inversion and influences the ultimate morphology of the prepared membranes.

## 2. VIPS from a morphological perspective

Membrane fabrication by many approaches is aiming at a simple process and tunable features of the fabricated membrane. The advantage of VIPS over the other techniques is the possibility of better controlling the desired membrane morphologies. This goal can be achieved by proper monitoring and regulating of the phase inversion process during the fabrication step. Although the VIPS process like the other phase inversion processes can easily attain different morphologies such as dense, porous, symmetric or asymmetric structures, the ability to better control the rate of phase inversion and membrane morphology provide the opportunity to tailor membrane morphology more accurately in comparison with another phase inversion methods.

Generally, four main morphologies can commonly be obtained *via* the VIPS process namely symmetric cellular, asymmetric cellular, symmetric nodular as well as symmetric bi-continuous structures. Fig. 2 depicts the morphology of commonly obtained membrane fabricated *via* VIPS process.

### 2.1. Symmetric cellular morphology

Slow diffusion of non-solvent through the cross-section of nascent polymer solution makes the concentration gradient in the cross section negligible and a typical symmetric structure can be obtained [31,59, 64–67]. Since the water activity in the vapor phase is similar to that in a liquid phase, one may assume that the membrane structure should be a finger-like structure (i.e. typical NIPS structure) if the other parameters are kept constant because the thermodynamic status of all the other components is the same. However, Park et al. [68] answered this question by explaining the critical role of the kinetic aspect of phase inversion. They pointed out that the interface of vapor/liquid is critical for mass transfer (kinetic aspect) and the final structure of the membranes [59].

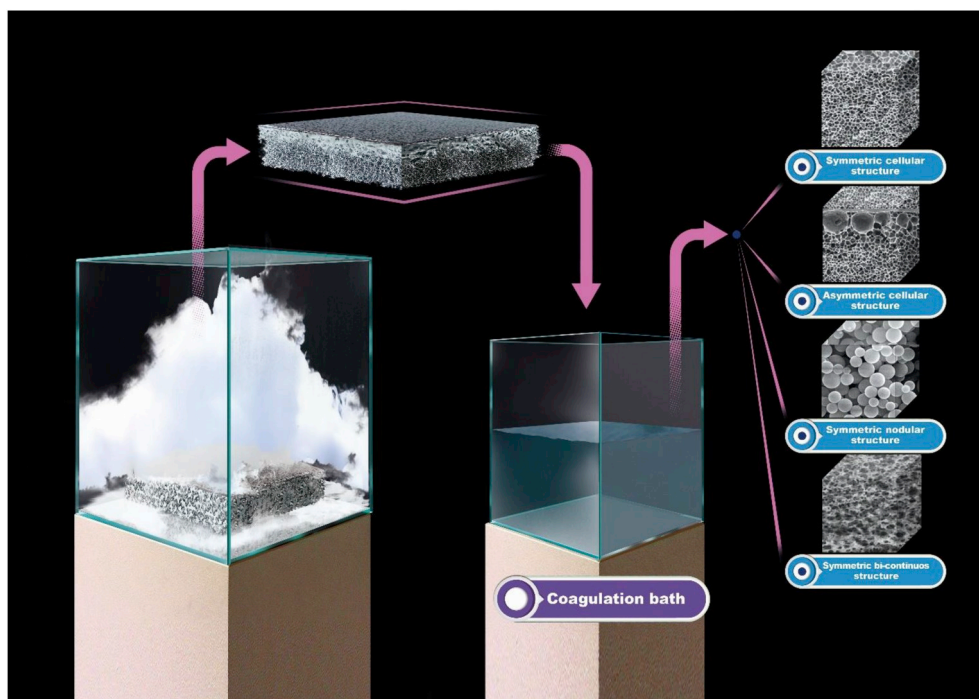In short, the differences between the structures of the membrane



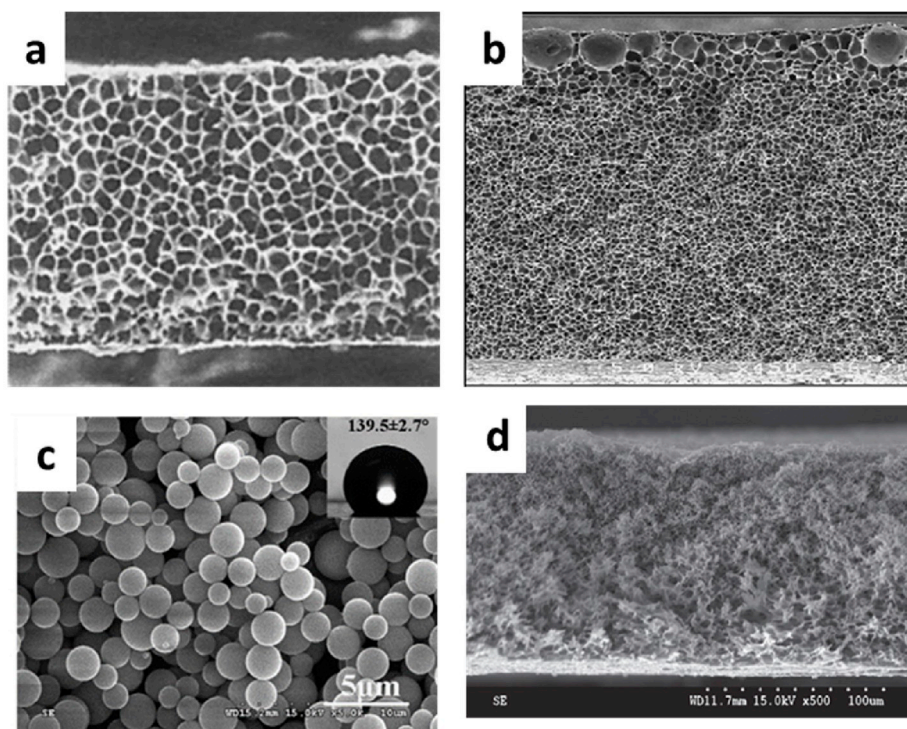**Fig. 1.** Schematic illustration of the VIPS process.

**Fig. 2.** The common membrane morphologies attained by the VIPS process a) symmetric cellular structure (Reproduced from Park et al. [59]), b) asymmetric cellular structure (Reproduced from Menut et al. [61]), c) symmetric nodular structure (Reproduced from Zhao et al. [62]), d) symmetric bi-continuous structure (Reproduced from Peng et al. [63]).

obtained by VIPS and NIPS are mainly arising from the kinetic aspect of phase inversion between these two distinguished techniques [59]. Fig. 3 depicts SEM images of the symmetric cellular structure prepared by VIPS.

### 2.2. Symmetric nodular morphology

Nodular morphology, which also is so-called as the granular or spherulitic structure, is another common morphology encountered in membrane prepared by VIPS [69–74]. This structure is typically made from semi-crystalline and crystalline polymers. This type of structure was mostly obtained over the whole cross-section of the prepared membrane. The slower non-solvent intake rate (water vapor) would make VIPS favor the polymer crystallization process over L-L demixing. In addition, this process endured the cast film in the crystallization region without being affected by L-L phase separation. This phenomenon

led to the formation of a solid sphere and granular structure [69–72, 75–77]. This morphology can be expanded to the whole of the membrane cross section Fig. 4.

### 2.3. Asymmetric cellular morphology

Apart from the symmetric structure of membrane formation, VIPS technique is also capable of producing asymmetric structures (Fig. 5). One this kind of structure is represented by the asymmetric cellular structure. Incongruent to that of a symmetric cellular structure, this asymmetric structure is caused by the surface liquid layer that eventually triggers the solvent gradient across the casted polymeric solution [61]. This occurrence strongly promotes the formation of a polymer gradient with a lower concentration towards the surface from near the top region of the polymer solution. Additionally, the low viscosity of the surface of the polymer solution eases the coarsening of the droplet as
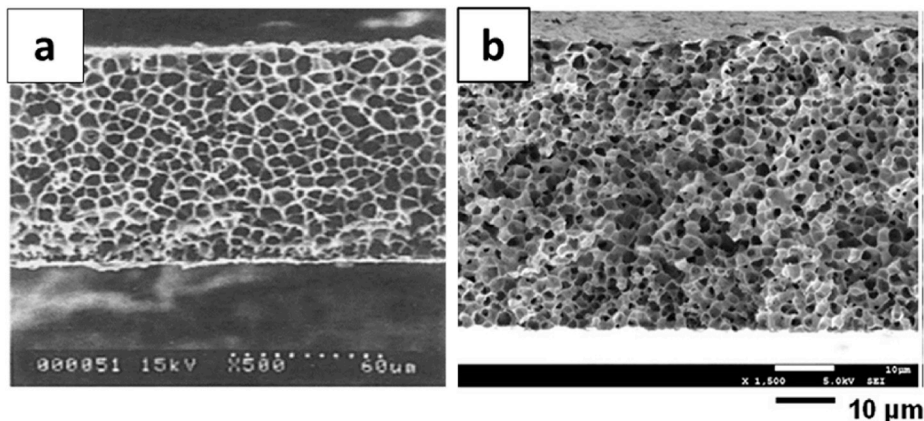


**Fig. 3.** The SEM images of the symmetric cellular structure of membrane prepared by VIPS a) Reproduced from Park et al. [59], b) Reproduced from Zhao et al. [60].
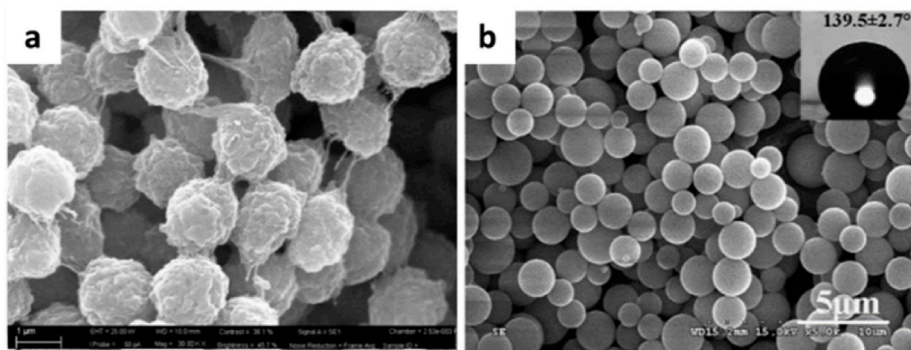
**Fig. 4.** The SEM images of the symmetric nodular structure of membrane prepared by VIPS a) Reproduced from Meringolo et al. [78], b) Reproduced from Zhao et al. [62].
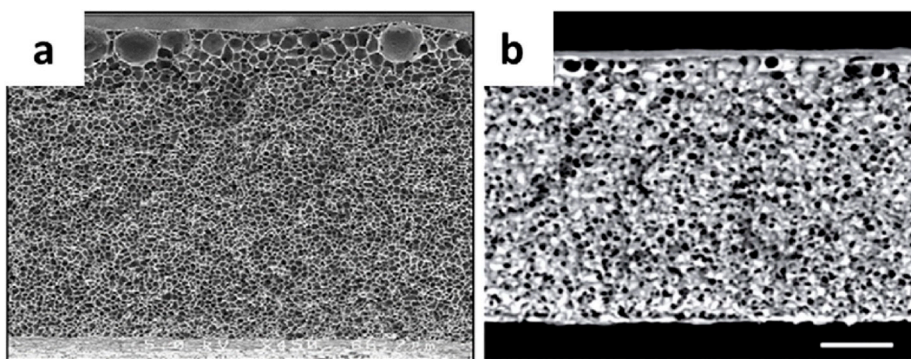


**Fig. 5.** The SEM images of the asymmetric cellular structure of membrane prepared by VIPS a) Reproduced from Menut et al. [61], b) Reproduced from Riu et al. [84].

compared to that of the deeper section of the polymer solution. Due to this phenomenon, the cell growth across the polymer solution section occurs at a different rate, eventually reducing the cellular size from the top layer to the bottom layer of the polymer solution. The delayed cell growth process of the near the top surface as compared to that in the bulk of the membrane significantly results in a cellular size gradient phenomenon across the membrane structure as reported previously [61, 79–83].

### 2.4. Sponge-like bi-continuous morphology

Another form of membrane structure that can be obtained via the VIPS fabrication approach is known as a sponge-like, bi-continuous structure (Fig. 6). Unlike the common sponge-like structure which is

dense and compact, this sponge-like, bi-continuous structure contains an open pore structure that can reduce the permeation resistance and thus, increase the permeability. This special structure can be obtained by controlling the rate of phase inversion. The moderately slow phase inversion rate will be fruitfully producing a membrane with this structure. Apart from the affinity of the solvent and non-solvent, the other parameters such as the viscosity of the polymer solution have also significantly affected the formation of this membrane structure [72, 85–87].

### 2.5. Asymmetric finger-like morphology

The asymmetric finger-like structure is commonly obtained by the NIPS technique (Fig. 7). In the VIPS fabrication, the exposure time to the
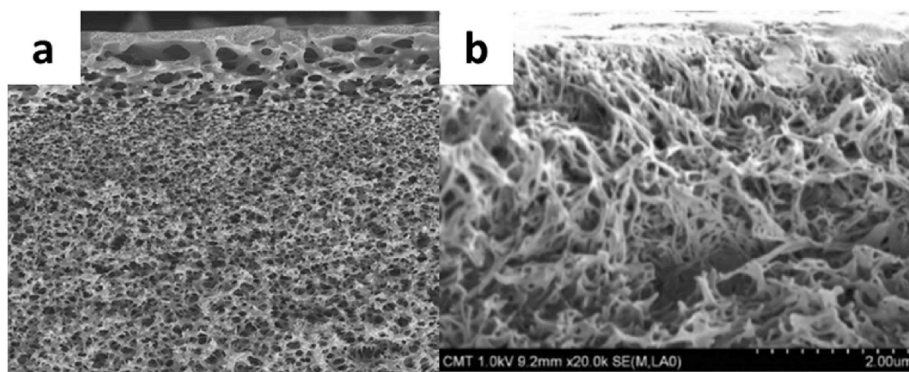


**Fig. 6.** The SEM images of the sponge-like bi-continuous structure of membrane prepared by VIPS a) Reproduced from Khare et al. [88], b) Reproduced from Tsai et al. [87].

vapor plays an important role in determining the structure of the fabricated membrane. A short exposure time prevents complete phase inversion throughout the cross-sectional layers of the polymer solution during the VIPS step, leaving the bottom layer to undergo the phase inversion by the coagulation bath via NIPS process. Additionally, it is worthwhile to mention here that this process has combined both VIPS and NIPS and is called V–NIPS [71,73,89]. The fabrication of membranes with finger-like structure has gained great attention of the researchers due to the high permeability of the obtained membranes [90].

### 2.6. Dense and porous morphology

The dense and porous structure can possibly be obtained using the VIPS technique. However, as mentioned earlier, the nature of the top-

$$\frac{\Delta G_m}{RT} = \sum_{i=1}^{4} n_i \ln(\varphi_i) + g_{12}n_1 \ln(\varphi_2) + g_{13}n_1 \ln(\varphi_3) + g_{14}n_1 \ln(\varphi_4) + g_{23}n_2 \ln(\varphi_3) + g_{24}n_2 \ln(\varphi_4) + g_{34}n_3 \ln(\varphi_4) \tag{1}$$

layer is affected by the polymer concentration as well as the growth of the polymer lean phase during the phase separation. The mechanism of the phase inversion that could conceivably drive into the formation of this dense structure is spinodal decomposition [88]. This issue will be discussed in more detail later in this manuscript.

### 3. VIPS process from the thermodynamic and kinetic perspective

To fabricate membrane by phase inversion an initial molecularly homogeneous polymer solution should be formed firstly. Then the thermodynamic equilibrium of the polymer solution can be broken up by different methods, accompanying the transformation of the solution from a single phase into two phases. Consequently, a polymer-lean phase and a polymer-rich phase will form. The former phase produces pores while the later phase forms the membrane matrix. Breaking the thermodynamic equilibrium can be initiated by one or a combination of the following driving forces: temperature (TIPS) [92–140], nonsolvent (NIPS) [44,141,142], evaporation (EIPS) [143–149], reaction [150], shear stress [151], and vapor (VIPS). Consequently, thermodynamic correlation along with mass and heat transfer should be considered simultaneously to have a better understanding of the phase inversion phenomena.

### 3.1. Thermodynamic in VIPS process

A thermodynamic model for the phase inversion is necessary to describe: 1) the multicomponent mass transfer; 2) to evaluate the driving force for mass transfer between the vapor and liquid phases which requires expressions for the activity coefficients for the transferring species, 3) to plot the phase diagram, for tracking the phase inversion path and anticipating the membrane morphology. The thermodynamic states of the polymer solution can be presented by a phase diagram (Fig. 8).

To date, many researchers used Flory-Huggins theory as a starting point for the thermodynamic analyzing and modeling in membrane science [80,88,143,152–159]. According to the Flory-Huggins theory, the Gibbs free-energy of mixing in a quaternary system (i.e. polymer, additive, solvent, and nonsolvent) is given by the following equation

where $n_i$, $\varphi_i$ and $g_{ij}$ are the number of moles of component $i$, the volume fraction of component $i$, and the interaction parameters of component $i$ and $j$, respectively. The subscripts 1, 2, 3, and 4 stand for the non-solvent, solvent, polymer, and additive, respectively. $T$ is the temperature and $R$ the constant of perfect gases. Table 1 presents the interaction parameters value in the different developed model for VIPS process.

The chemical potential of the component $i$ can be obtained from the expression of the Gibbs-free energy of mixing.

$$\frac{\Delta \mu_i}{RT} = \frac{\partial}{\partial n_i}\left(\frac{\Delta G_m}{RT}\right)\Bigg|_{P,T,\ n_{i\neq j}} \tag{2}$$

When equilibrium is established between two liquid phases (i.e. polymer-lean phase $\alpha$ and polymer-rich phase $\beta$) the chemical potential difference $\Delta \mu_i$ of component $i$ in these two phases are equal:

$$\Delta \mu_i^\alpha = \Delta \mu_i^\beta (i = 1,\ 2,\ 3,\ 4) \tag{3}$$

The cloud point curve for a ternary system can be calculated from the above equation by considering the following constraints ($\sum_i \varphi_i^{\alpha,\beta} = 1$).

The spinodal curve can be calculated by using the following equation and the mass balance equation

$$G_{22}G_{33} = (G_{23})^2 \tag{4}$$

Where

$$G_{ij} = \left\{ \partial^2 \Delta G_m^t \big/ \left(\partial \varphi_i \partial \varphi_j\right) \right\} v_1 \tag{5}$$
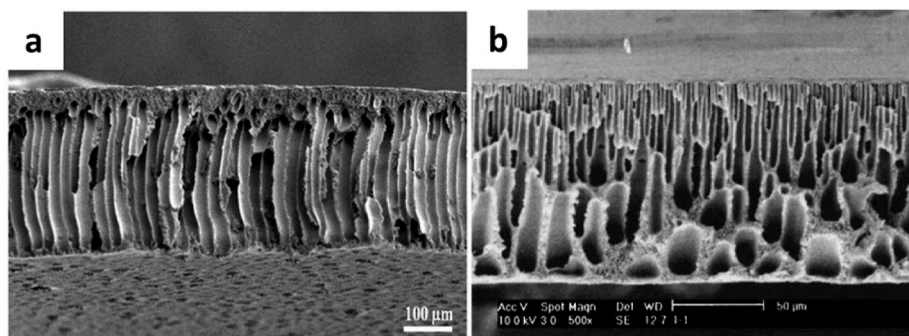


**Fig. 7.** The SEM images of the asymmetric finger-like structure of membrane prepared VIPS a) Reproduced from Harruddin et al. [90], b) Reproduced from Kim et al. [91].

*N. Ismail et al.*
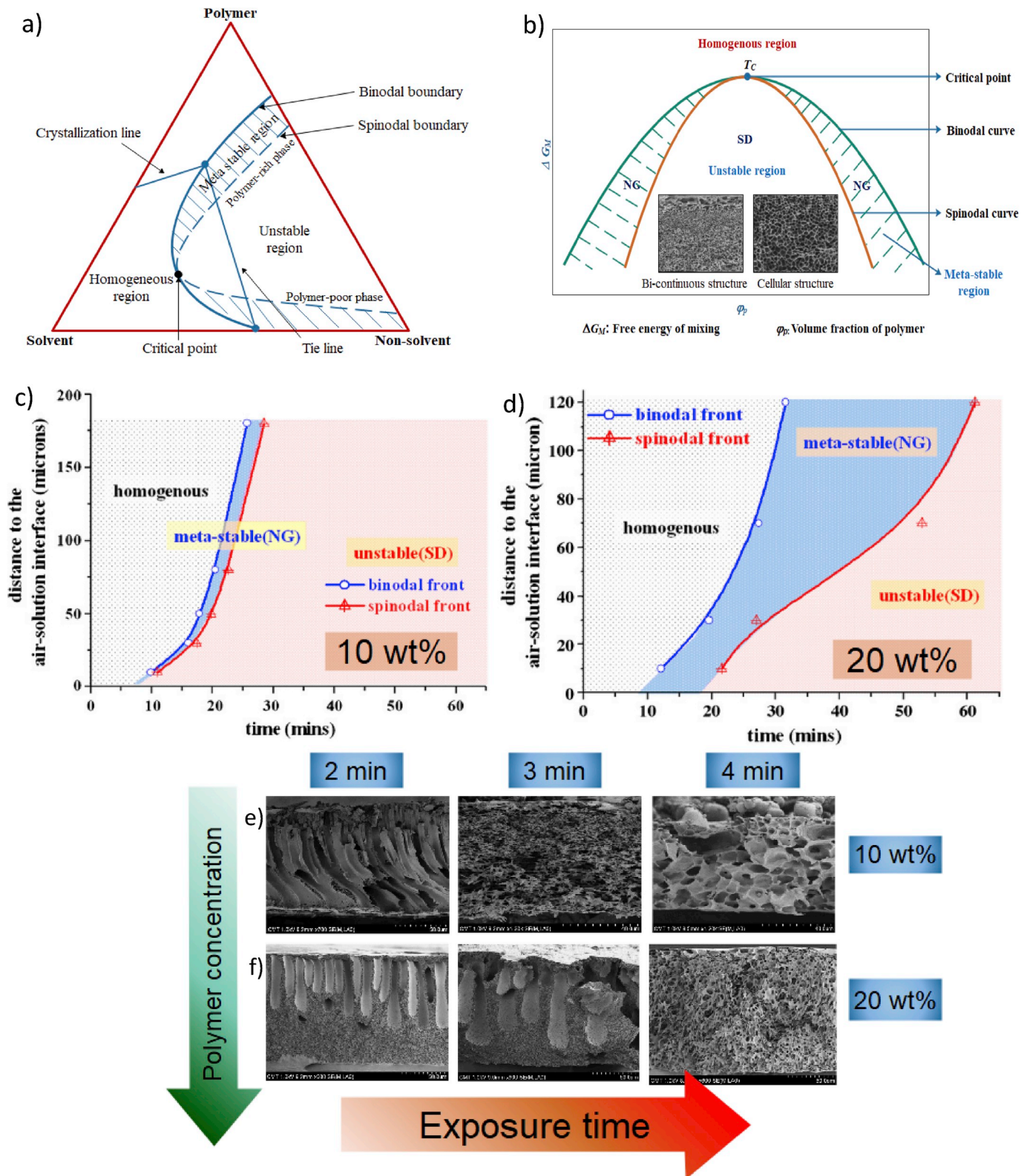
**Fig. 8.** a) Ternary phase diagram for VIPS process, b) The schematic representation of a phase diagram, c) Binodal and spinodal fronts for the 10 wt% (PSf/NMP/water, RH: 70%), d) binodal and spinodal fronts for the 20 wt%, e) SEM picture of the fabricated membranes by 10 wt% in 2, 3 and 4 min exposure time (PSf/NMP/water, RH: 70%), f) SEM picture of the fabricated membranes by 20 wt% in 2, 3 and 4 min exposure time (PSf/NMP/water, RH: 70%) reproduced from Ref. [89].

$\Delta G_m^t$ is the Gibbs free energy of mixing per unit volume and $v_1$ is the molar volume of component *i*. Consequently, a ternary phase diagram for polymer/solvent/nonsolvent can be obtained (Fig. 8a).

The crystallization line can also be obtained according to the theory

of melting point depression. The chemical potential of the polymer repeating unit in the crystalline state can be represented by

**Table 1**
The interaction parameters value in different developed models for VIPS.

| | $g_{12}$ | $g_{13}$ | $g_{23}$ | $g_{14}$ | $g_{24}$ | $g_{34}$ | Ref. |
|---|---|---|---|---|---|---|---|
| PES/PVP/NMP/water | 1.0 | 1.5 | 0.5 | 0.5 | 0.5 | −1.0 | [88] |
| PES/DMAC/water | $0.8923 - 0.5911 \times u^2 + 0.2821 \times u_u^2$ | 1.6 | 0.39 | – | – | – | [160] |
| PES/NMP/water | $0.785 + 0.665 \times u_2$ | 1.6 | 0.37 | – | – | – | [160] |
| PES/DMF/water | $0.5 + 0.04 \times u_2 + 0.8 \times u_2^2 - 1.2 \times u_2^3 + 0.8 \times u_2^4$ | 1.6 | 0.47 | – | – | – | [160–162] |
| PVDF/DMF/water | $0.5 + 0.04 \times u_2 + 0.8 \times u_2^2 - 1.2 \times u_2^3 + 0.8 \times u_2^4$ | 2.09 | 0.43 | – | – | – | [157,161] |
| PSf/2P/water | $0.32 + \dfrac{0.47}{1 - 0.5 \times u_2}$ | 2.5 | 0.5 | – | – | – | [87] |
| PSf/NMP/water | $0.785 + 0.665 \times u_2$ | 2.7 | 0.24 | – | – | – | [161] |
| PEI/NMP/water | $0.785 + 0.665 \times u_2$ | 2.1 | 0.507 | – | – | – | [88] |
| PEI/NMP/water | * | 2.1 | 0.507 | – | – | – | [80] |
| PEI/DMAC/water | $0.8923 - 0.5911 \times u^2 + 0.2821 \times u_u^2$ | 2.1 | 0.55 | – | – | – | [160–162] |
| PEI/DMF/water | $0.5 + 0.04 \times u_2 + 0.8 \times u_2^2 - 1.2 \times u_2^3 + 0.8 \times u_2^4$ | 2.1 | 0.59 | – | – | – | [161,162] |
| CA/acetone/water | 1.3 | 1.4 | 0.5 | – | – | – | [161] |

- (*) not reported.
- $u_2 = \dfrac{\varnothing_2}{\varnothing_1 + \varnothing_2}$.

$$\mu_u^c - \mu_u^0 = -\Delta H_u \left( 1 - T / T_m^0 \right) \tag{6}$$

Where $\mu_u^c$, $\mu_u^0$, $\Delta H_u$, and $T_m^0$ are refers to the chemical potential of polymer repeating unit, the chemical potential of polymer repeating unit in the standard state, the heat of fusion of the polymer repeating unit, and the melting point of pure polymer, respectively.

The chemical potential of the polymer repeating unit in the polymer solution is given by:

$$\mu_u - \mu_u^0 = (\partial \Delta G_m / \partial n_3)(v_u / v_3) \tag{7}$$

where $v_u$ is the molar volume per repeating unit in the polymer. Considering the equilibrium condition $\mu_u^c - \mu_u^0 = \mu_u - \mu_u^0$ the melting point depression can be obtained by using the following equation:

$$\left( \frac{1}{T_m} \right) - \left( \frac{1}{T_m^0} \right) = - \left( R / \Delta H_u \right) (v_u / v_1) \times \{ r \ln \varphi_3 + r(1 - \varphi_3) - \varphi_1 - s\varphi_2 + (g_{13}\varphi_1 + sg_{23}\varphi_2)(\varphi_1 + \varphi_2) - g_{12}\varphi_1\varphi_2 \} \tag{8}$$

here, r and s stand for $v_1/v_3$ and $v_1/v_2$, respectively.

In order to calculate the binary interaction parameter between non-solvent and solvent, first we need to assume that $g_{12}$ is only dependent on two components: (1) non-solvent and (2) solvent and not on the third component in the ternary system. It can be measured by considering excess Gibbs free energy ($G^E$) which can be obtained by vapor-liquid equilibrium experiments.

The $G^E$ is derived by:

$$G^E = \Delta G_m - RT \left( n_1 \ln(\varphi_1) + n_2 \ln(\varphi_2) \right) \tag{9}$$

Gibbs free energy for binary mixture can be expressed as below:

$$\frac{\Delta G_m}{RT} = n_1 \ln\varphi_1 + n_2 \ln\varphi_2 + g_{12}n_1\varphi_2 \tag{10}$$

As the $g_{12}$ is function of concentration, Tompa [163] suggested to apply the polynomial form:

$$g(\varphi_2) = a_0 + a_1\varphi_2 + a_1\varphi_2^2 + \tag{11}$$

thus, the non-solvent and solvent interaction can be obtained by this equation:

$$g_{12} = \frac{1}{x_1\varphi_2} \left[ x_1 \ln\left( \frac{x_1}{\varphi_2} \right) + x_2 \ln\left( \frac{x_2}{\varphi_2} \right) + \frac{G^E}{RT} \right] \tag{12}$$

For non-solvent/polymer interaction was determined by equilibrium swelling experiment by using this equation:

$$g_{13} = - \frac{\ln(1 - \varphi_3) + \varphi_3}{\varphi_3^2} \tag{13}$$

The phase separation in VIPS process is based on nucleation and growth (NG) mechanism and/or the spinodal decomposition (SD) mechanism. If the composition of the polymer solution locates in the meta-stable region, NG mechanism occurs, resulting in a closed and cellular pore (Fig. 8b). A bi-continuous or a droplet morphology (Fig. 8b) will form if the composition of the solution locates in the unstable region (SD mechanism) [68,89,164,165].

By adjusting the fabrication parameters, such as polymer solution parameters and/or fabrication process parameters the mechanism of the phase inversion can be tuned to NG and/or SD mechanism. For example, changing polymer concentration results in different areas of the meta-stable region, and changing exposure times lead to different duration time in this region (Fig. 8 **c-f**). Thus, the amount of the polymer solution that undergoes the NG or SD mechanism is variable resulting membrane with different structure [89,166,167]. The shorter the duration of stay in the meta-stable region, the higher the probability the solution phase separates via the SD mechanism [89].

Another critical factor needs to be considered is the formation of the skin due to the coarsening and shrinkage of the polymer-rich phase near the surface of the cast film. If the speed of SD is slow, the SD might not reach the bottom of the cast film when the skin forms. In this scenario, SD cannot propagate deeper into the cast film because in the deeper region water accumulation rate is retarded and the duration in the meta-stable region is prolonged [89]. On the other hand, for a system of the faster SD, the decomposition can reach the bottom of the cast film when the skin forms. Indeed, the formation of the skin is too slow to affect the phase separation and SD happens throughout the whole cast film [89].

### 3.2. Mass transfer in VIPS process

A typical geometry that has been used for analyzing mass transfer in VIPS process is presented in Fig. 9(a and b). Precipitation from the vapor phase is governed by a solvent and nonsolvent fluxes perpendicular to the film. Substituting of the solvent (solvent out-flow through evaporation) and non-solvent (inflow) occurs simultaneously.
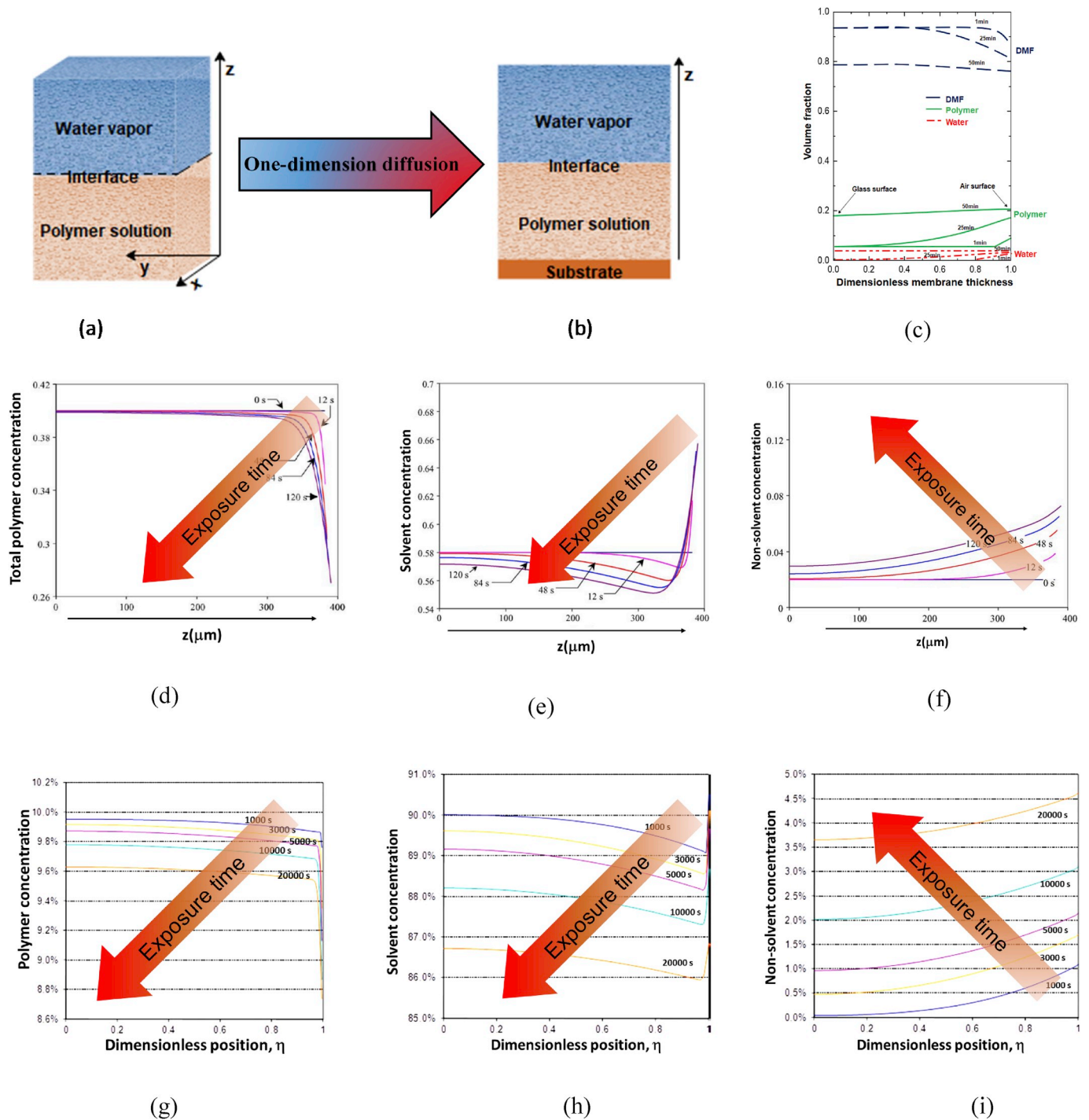
**Fig. 9.** a) Three dimensional schematic of a model for VIPS process. b) typical one dimensional model for mass transfer in VIPS process. c) Concentration profile of PVDF, DMF, and water. Initial polymer concentration: 10 wt%, RH: 20% [157]. d, e, and f) Model predictions for d)total polymer concentration e) solvent concentration and f) nonsolvent concentration profile for a film cast from a solution of 2/58/15/25 wt% (water/NMP/PES/PVP) with an initial film thickness of 381 μm [88]. g, h, i) concentration profile of g) polymer, h) solvent, and i) nonsolvent for 30 wt% PEI, NMP, water at RH: 75% and T = 45 °C [174].

The mathematical description of the VIPS process was considered more recently in literature comparing to other phase separation processes (TIPS, NIPS, and EIPS). It involves the mathematical description of:

- The thermodynamics of the ternary (polymer/solvent/non-solvent) or quaternary (polymer/solvent/non-solvent/additive) system
- The mass transport within the polymeric matrix (the diffusion of small species as solvent and non-solvent around the polymer chains),

- The mass transfer at the upper interface between the polymeric matrix and the environment (humid air in most cases),
- The heat transfer between the thin film and the environment, due to heat of vaporization and heat exchanges.

Moreover, some assumptions are usually done to simplify the mass transfer problem in VIPS process: i) ideal gas behavior at the air side, ii) gas liquid equilibrium at the air-film interface, iii) one dimensional diffusion, iv) constant partial specific volume, v) no polymer transfer to

air side, vi) no volume change on mixing [80,157,161].

The trickiest challenge obviously concerns the description of the diffusion within the polymeric matrix. Same as other phase inversion methods, Bearman statistical mechanical theory was used for analyzing mass transfer in VIPS process [168,169]. According to Bearman theory the frictional force in an n-components system is equal (but opposite in sign) to the chemical potential gradient:

$$\nabla\mu_i = -\sum_{j=1}^{n} c_j \varepsilon_{ij}(v_i - v_j) \tag{14}$$

Where $\nabla\mu_i$, $c_j$, $\varepsilon_{ij}$ and $v_i$ are the chemical potential gradient of component $i$, the molar concentration of $j$, and the friction coefficient between molecules $i$ and $j$, and the velocity of the ith component [168]. Based on the Bearman theory the self-diffusion coefficient $D_i$ derive from the friction factors as follow:

$$D_i = RT \Big/ \sum_{j=1}^{n} c_i \varepsilon_{ij} \tag{15}$$

Since the friction factor depends on both the composition and the temperature, determining this parameter is an obstacle. Furthermore, there is not enough experimental data to give an analytical expression for describing $\varepsilon_{ij}$. To address this challenge, some assumptions originated from the mutual diffusion coefficients for miscible fluids in the limit of quasi-binary diffusion should be taken into consideration [80, 88]. For example, Vrentas and Duda suggested to estimate $D_i$ according to the free volume theory [170]. Consequently, the mass transfer in the VIPS process can be formulated in two ways. First, the mass transfer model derived directly from the Bearman theory (such as model developed by Khare et al. [88]) and second the mass balance equation involving mutual diffusion coefficient (like model developed by Yip and McHugh [161], Matsuyama et al. [157]. and Bouyer et al. [80]). Starting from the Bearman theory and equation (9), a generalized expression was established by Price and Romdhane [171]:

$$D_{ik} = \left(1 - \rho_i V_i \left(1 - \frac{\alpha_i}{\alpha_3}\right)\right)\rho_i D_i \left(\frac{1}{RT}\frac{\partial\mu_i}{\partial\rho_k}\right) - \sum_{j=1\ j\neq i}^{2} \left(1 - \frac{\alpha_j}{\alpha_3}\right)\rho_j D_j \rho_i D_i \left(\frac{1}{RT}\frac{\partial\mu_j}{\partial\rho_k}\right) i, k = 1, 2 \tag{16}$$

Using this generalized friction-based approach, the diffusion model can be written depending on the expression of $\alpha_i$. Setting $\alpha_i = 1$ gives the theory of Alsoy and Duda [172]:

$$D_{ik} = \frac{\rho_i D_i}{RT}\left(\frac{\partial\mu_i}{\partial\rho_k}\right) i, k = 1, 2 \tag{17}$$

When $\alpha_i = 0$, the following expression can be written:

$$D_{ik} = (1 - \rho_i V_i)\rho_i D_i \left(\frac{1}{RT}\frac{\partial\mu_i}{\partial\rho_k}\right) - \sum_{j=1\ j\neq i}^{2} \rho_j D_j \rho_i D_i \left(\frac{1}{RT}\frac{\partial\mu_j}{\partial\rho_k}\right) i, k = 1, 2 \tag{18}$$

If $\alpha_i = 1/V_i$, Zielinski and Hanley [173] expressed the mutual-diffusion coefficient as follows:

$$D_{ik} = \left(1 - \rho_i V_i \left(1 - \frac{V_3}{V_i}\right)\right)\rho_i D_i \left(\frac{1}{RT}\frac{\partial\mu_i}{\partial\rho_k}\right) - \sum_{j=1\ j\neq i}^{2} \left(1 - \frac{V_3}{V_j}\right)\rho_j D_j \rho_i D_i \left(\frac{1}{RT}\frac{\partial\mu_j}{\partial\rho_k}\right) i, k = 1, 2 \tag{19}$$

And finally, taking $\alpha_i = 1/(V_i M_i D_i)$, Price and Romdhane found the following expression:

$$D_{ik} = \left(1 - \rho_i V_i \left(1 - \frac{V_3 M_3 D_3}{V_i M_i D_i}\right)\right)\rho_i D_i \left(\frac{1}{RT}\frac{\partial\mu_i}{\partial\rho_k}\right) - \sum_{j=1\ j\neq i}^{2} \left(1 - \frac{V_3 M_3 D_3}{V_j M_j D_j}\right)\rho_j D_j \rho_i D_i \left(\frac{1}{RT}\frac{\partial\mu_j}{\partial\rho_k}\right) i, k = 1, 2 \tag{20}$$

**Table 2**

Applied diffusion coefficient parameter for mass transfer modeling in VIPS.

| Ref. (Year) | Diffusion coefficient parameter | |
|---|---|---|
| Matsuyama et al. (1999) [157] | $D_{11} = -\frac{v_1}{N_A^2 E_0}\left(E_{22}\frac{\partial\mu_1}{\partial\varphi_1} - E_{12}\frac{\partial\mu_2}{\partial\varphi_1}\right)$ | (21) |
| | $D_{12} = -\frac{v_1}{N_A^2 E_0}\left(E_{22}\frac{\partial\mu_1}{\partial\varphi_2} - E_{12}\frac{\partial\mu_2}{\partial\varphi_2}\right)$ | (22) |
| | $D_{22} = D_2(1 - \varphi_2)^2(1 - 2g_{23}\varphi_2)$ | (23) |
| Yip and McHugh (2006) [161] | $D_{ik} = \frac{\rho_i}{RT}\sum_{j=1\ j\neq i}^{3}\varphi_j\left(D_i\frac{\partial\mu_i}{\partial\rho_k} - D_j\frac{\partial\mu_j}{\partial\rho_k}\right)i, k = 1, 2$ | (24) |
| Bouyer and Pochat-Bohatier (2012) [174] | $D_{ik} = (1 - \rho_i V_i)\rho_i D_i\left(\frac{1}{RT}\frac{\partial\mu_i}{\partial\rho_k}\right) - \sum_{j=1\ j\neq i}^{2}\rho_j D_j \rho_i D_j\left(\frac{1}{RT}\frac{\partial\mu_j}{\partial\rho_k}\right)i, k = 1, 2$ | (25) |

$D_i$: self-diffusion coefficient of $i$, $N_A$: Avogadro number, $E$: Energy required to overcome attractive forces from neighboring molecules (J/mol), $\varphi$: association factor.

In literature, some of the previous expressions were used to simulate the mass transfers during VIPS process and Table 2 presents the applied diffusion coefficient parameter for mass transfer modeling in VIPS process to date.

The concept of the evaporation process was first introduced by Tsay and McHugh [149]. For applying the equation below which referring to Fig. 8b, we should assume that, the system is one dimensional, isothermal, which followed Fickian diffusion (26), its polymer-solvent binary system (27); no change in volume during mixing (28); followed ideal gas behavior on air side (29); air-film interface (30):

$$\frac{\delta\rho_2}{\delta t} = \frac{\delta}{\delta z}\left(D\frac{\delta\rho_2}{\delta z}\right) \tag{26}$$

$$\rho_2 = \rho_{20} \tag{27}$$

$$\frac{\delta\rho_2}{\delta z} = 0 \ \ at \ z = 0 \tag{28}$$

$$\frac{d}{dt}\left(\int_0^{l(t)}\rho_2 dz\right) = -k(\rho_{2gt} - \rho_{2g\infty}) \ \ at \ z = l(t) \tag{29}$$

$$\int_0^{l(t)}\rho_3 dz = \int_0^{L}\rho_{30} dz \tag{30}$$

where $\rho$ is the mass density, t is the time and z represent the position of the component $i$

$$\rho_{2gt} = \frac{a_2 P_2^{sat}}{V_{2g}P} \tag{31}$$

where $P$, $P_2^{sat}$ and $V_{2g}$ are the total pressure, pure solvent vapor pressure and partial specific volume of the solvent in the gas phase, respectively. By Flory-Huggins theory, the activity can be evaluated by:

$$a_2 = \varnothing_3 exp\left[\varnothing_3\left(1 - \frac{v_2}{v_3} + \varnothing_3 g_{23} - \varnothing_2\varnothing_3\frac{dg_{23}}{d\varnothing_3}\right)\right] \tag{32}$$

Mass transfer coefficient is estimated by equation (33) since most of evaporation process is carried out under free convection condition. The equation for both free convection and forced convection conditions can be obtained from different empirical correlations. For example, Y. Yip and McHugh used the following correlation to obtain a mass transfer coefficient [161,175].

$$\frac{k_i L_c y_{air,lm}}{D_{ig}} = 0.27(GrSc_i)^{0.25} \ \ Free \ Convection \tag{33}$$

$$\frac{k_i L_c y_{air,lm}}{D_{ig}} = 0.27 \left( Re^{0.5} Sc_i^{0.33} \right) \quad Forced\ convection \tag{34}$$

$$Sc_i = \frac{\mu_g}{\rho_g D_{ig}} \tag{35}$$

$$Re = \frac{\rho_g u_\infty L_c}{\mu_g} \tag{36}$$

In another study, Matsuyama et al. [157] assumed mass transfer in the gas side is happening only by free convection condition and used the following equation to obtain the mass transfer coefficient.

$$\frac{k_i L_c y_{air,}}{D_{ig}} = 0.54 (GrSc)^{0.25} \tag{37}$$

$$Gr = L_c^3 \rho_g^2 g \left| \tau_i \left( y_{ig}^i - y_{ig}^\infty \right) \right| \tag{38}$$

Here, $L_c$ and $y_{air,lm}$ denote the characterisctic length of the cast film surface and the logarithm mean mole fraction difference of air. $D_{ig}$, $\rho_g$ and $\mu_g$ are the mutual diffusion coefficient of component $i$ in the gas phase, the total mass density of the gas phase and viscosity of the gas, respectively. $y_{ig}^i$ and $y_{ig}^\infty$ are the mole fraction of component $i$ at air-film interface and that in the gas bulk phase. $g$ is the gravity constant and coefficient $\tau_i$ is given by $-(1/\rho_g)\,(\partial \rho_g / \partial y_{ig})_{P,T}$.

Using the above mentioned mathematical models allows tracking the concentration profile in the interface and the bulk of the nascent membrane prior to phase inversion and during the phase inversion. Resulting in better understanding of final membrane morphology. For instance, Matsuyama et al. [157]. investigated mass transfer (PVDF/DMF/water, RH = 10%, 20%, and 40%) during the membrane formation and demonstrated the polymer volume fraction near the top surface increases at the initial stage, then the flat profile is formed and the whole polymer concentration increased with time. They attributed the formation of isotropic structure to the polymer concentration at the top surface. Based on their developed model the polymer concentration at the top surface is not so high compared with the initial concentration even at the initial stage. This theoretically finding was in agreement with the experimental data. The same trend in polymer concentration profile is observed by others [80,88,161] (Figure 9c and **9d-i**).

On the other hand, tracking the solvent concentration profile in phase inversion indicates a large gradient in the solvent mass fraction near the film/air interface. This trend is reported in all the developed mass transfer model for VIPS to date [80,88,157,161] (Fig. 9e and **h**). Similarly, concentration profile for non-solvent, which is water for all the developed model for VIPS process to date, shows a reduction across the nascent membrane (Z direction) during the phase inversion [80,88, 157,161] (Fig. 9f and **i**).

The following general trend can be concluded from the developed mathematical model for mass transfer: 1) Polymer concentration profile shows a reduction in the Z direction. Over a corresponding timeframe, the total polymer mass fraction decreases gradually in the Z direction 2) Solvent concentration profile displays a minimum at the location slightly below the top surface and increase significantly at the top surface. 3) non-solvent concentration profile shows an increment in the Z direction. 4) Changes in concentration profile are more significant at the beginning of the phase inversion in comparison with the later steps Fig. 9.

Exploring the above mentioned parameters one can change the effective parameters in mass transfer such as mass transfer coefficient or the polymer solution composition and obtain membrane with desire morphology.

### 3.3. Heat transfer in VIPS process

It is possible to solve the developed mass balance by assuming an isothermal condition for VIPS process. However, non-isothermal condition increases the accuracy of the developed model. In the VIPS process, the thickness of the casted film is low. Therefore, the heat transfer can be estimated by a lumped parameter approach [147,161,172] and the heat transfer resistance of the casted film can be neglected. Therefore, heat transfer in the gas phase is a rate controlling factor. By assuming the lumped parameter the external heat transfer occurs due to the heat exchange of casted polymer solution with ambient, water adsorption on the casted polymer solution surface and the cooling effect of solvent evaporation. The following equation can be used to determine the film temperature.

$$\frac{dT}{dt} = -\left[ \frac{h_{up}\left(T - T_g\right) + h_{down}\left(T - T_g\right) + \sum_i J_{ig} \Delta H_{vi}}{\rho_s C_{P_s} H + \rho_P C_{P_P} H_P} \right] \tag{39}$$

where $\rho$, $C_p$, $H$, $T$, $T_g$ $J_{ig}$, and $\Delta H_{vi}$ stand for density, heat capacity, thickness, solution temperature, the bulk temperature in the gas phase, the mass flux in the gas phase and the vaporization enthalpy, respectively. The subscript $p$ and $s$, refers to the polymer solution and the substrate, respectively. $h_{up}$ and $h_{down}$ are the heat transfer coefficient above and below of the system, respectively.

The free convection and forced convection heat transfer coefficient for solvent/nonsolvent can be obtained by using the following equations

$$\frac{h L_c}{K^G} = 0.27 (GrPr)^{0.25} \quad Free\ convection \tag{40}$$

$$\frac{h L_c}{K^G} = 0.664 Re^{0.5} Pr^{0.33} \quad Forced\ convection \tag{41}$$

Where $K^G$ is the air thermal conductivity and $Pr$, the Prandtl number.

$$Gr = \frac{L_c^3 \rho_g^2 g}{\mu_g^2} \left| \xi_h \left(T - T^G\right) + \xi_{m1} \left(y_{1gt} - y_{1g\infty}\right) + \xi_{m2} \left(y_{2gt} - y_{2g\infty}\right) \right| \tag{42}$$

Where $g$ is the gravitational constant and $T^G$, the air temperature.

Developing a predictive/simulative model for membrane fabrication is an important factor in membrane science. There is no doubt that analyzing the phase inversion by using the above-mentioned mathematical correlation gives the accurate trend in transport phenomenon. This fact is already demonstrated in several published papers [80,88, 157,161]. However, it is not possible to track the phase inversion phenomena in mesoscale. For example, polymer molecular weight distribution has an effect on membrane formation [33,176] but inserting these kinds of parameters in mass transfer equation is a bottleneck. Correlating the fabrication parameters to the final performance of the membrane based on the mathematical model with acceptable accuracy is challenging due to the complexity of the system. Therefore further investigation is required to understand better the phase separation
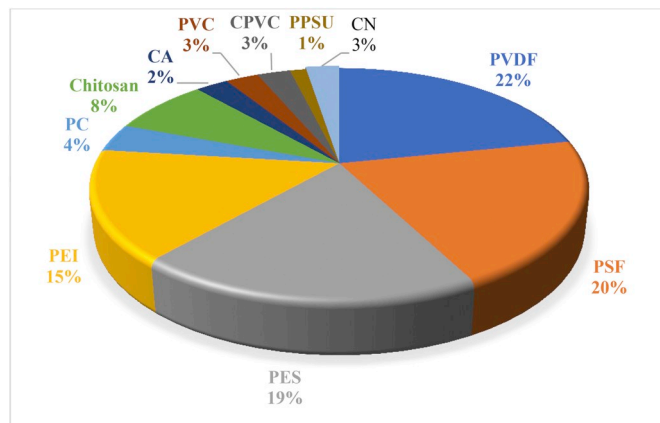


**Fig. 10.** Most common polymers used in VIPS method.

phenomena (see summary and outlook section).

## 4. The effective fabricating parameters in VIPS process

The parameters affecting the morphology of VIPS membranes and their arising performances can be categorized into two groups. The first group consists of polymer solution parameters such as polymer type and concentration, nature of the solvent, and additives. The second group consists of process paramete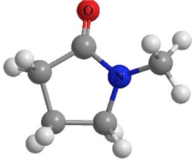rs including exposure time to non-solvent vapors, relative humidity (assuming that the non-solvent is water, which is a correct assumption in most cases), dissolution temperature, and vapor temperature.
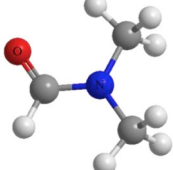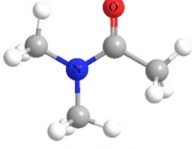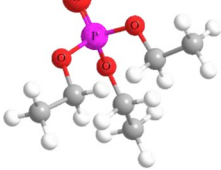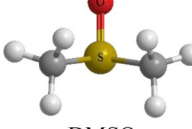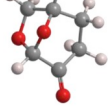
### 4.1. Polymer solution parameters

#### 4.1.1. Effect of the polymer

There are numerous types of polymers that are commonly used upon membrane fabrication such as polyvinylidene difluoride (PVDF),

**Table 3**
Solubility parameters and polymer-solvent affinity.

| Polymer | Dispersion Force, $\delta_d$ | Polar Force, $\delta_p$ | Hydrogen Bond Force, $\delta_H$ | Solubility Parameter, $\delta_{sp}$ | Polymer-Solvent Affinity, $\delta$ |
|---|---|---|---|---|---|
| [a]CA | 16.9 | 16.3 | 3.7 | 23.78 | – |
| [b]PVDF | 17.2 | 12.5 | 9.2 | 23.20 | – |
| [c]PSf | 19.7 | 8.3 | 8.3 | 22.94 | – |
| [d]PES | 18.7 | 10.3 | 7.7 | 22.70 | – |
| [e]PEI | 17.3 | 5.4 | 6.3 | 19.19 | – |
| **Solvents** | | | | | |
| NMP | 18.0 | 12.3 | 7.21 | 22.96 | [a]5.43 [b]2.15 [c]4.48 [d]2.17 [e]6.99 |
| DMF | 17.4 | 13.7 | 11.3 | 24.86 | [a]8.05 [b]2.43 [c]6.59 [d]2.16 [e]9.69 |
| DMAC | 16.8 | 11.5 | 10.2 | 22.77 | [a]8.08 [b]1.47 [c]4.71 [d]5.12 [e]7.25 |
| TEP | 16.8 | 11.5 | 9.2 | 22.34 | [a]7.30 [b]1.08 [c]4.41 [d]2.70 [e]6.77 |
| DMSO | 18.4 | 16.4 | 10.2 | 26.68 | [a]6.67 [b]4.20 [c]8.42 [d]6.59 [e]11.72 |
| Cyrene™ | 18.8 | 10.6 | 6.9 | 22.66 | [a]6.8 [b]3.39 [c]2.84 [d]0.86 [e]5.45 |

*N. Ismail et al.*

polysulfone (PSf), polyethersulfone (PES), polyetherimide (PEI) among many other. Each type of polymer has its own characteristics that fit the researcher's demand. A summary of polymers used in VIPS fabrication is illustrated in Fig. 10. We can see that PVDF attracted most of the researchers' attention, probably due to its hydrophobic behavior, as well as to its good chemical and thermal stability.

One can observe two major kinds of polymer concentration effects upon membrane formation. First, the change in volume fraction occupied by the polymer molecules which directly influences the pore size. Secondly, the change of viscosity which influences the mass transfer rates and the consequent membrane formation, mechanisms and membrane morphology. By increasing the polymer concentration, the viscosity of the solution increases which has a significant effect in terms of the kinetic aspect of phase inversion. Increasing the viscosity decreases the mobility of the polymer chain and the rate of non-solvent diffusion, resulting in higher resistance for coarsening of the polymer-lean phase [68,177–179]. Lee et al. [164] studied the effect of the PSf concentration in NMP of the prepared membrane by VIPS and demonstrated a strong correlation between the pore size and concentration. More precisely, as the polymer concentration increased from 15 wt% to 25 wt%, the viscosity obviously increased. Consequently, resulted in a delay of the solvent-nonsolvent demixing process and resulted in a decreasing membrane pore sizes from 8.28 μm to 3.51 μm.

In 2011, Park and his coworkers [68] investigated the effect of different polymer concentrations (15 and 30 wt% of the PSf membrane in NMP). Based on their findings, 30 wt% PSf membranes showed no flux due to the lack of interconnected pores whereas 15 wt% PSf solution permitted to prepare membranes with a 0.32–1.66 L/m$^2$.h permeability, depending also on the relative humidity (ranging from 70% to 100%). At this concentration level, more interconnected pores were formed during the late stage of coarsening. Similar findings have been observed by Bozdek and Bohdziewz [180] who proved that a lower polymer concentration permitted to enhance the pores interconnectivity by coarsening in polycarbonate membranes [180].

Matsuyama et al. [181] investigated the phase separation of PVDF/DMF solution by water vapors and found that by increasing polymeric concentration from 10 wt% to 20 wt% fewer pores were formed on the surfaces. The pore diameter increased by decreasing the PVDF content in the dope solution. As a consequence, the lower polymer concentration leads to a higher contact angle [182]. In other words, the polymer concentration has an important effect on VIPS membrane hydrophilicity, through the change in surface morphology, which can be explained by the importance of surface porosity/pore size on the wettability of the membrane (Cassie-Baxter effect) [183].

Another research work by Zhao et al. [60] studied the effect of PVDF concentration. They observed that by increasing the polymer concentration, the volume fraction of the polymer interface resulted in a lower porosity. Additionally, the mechanical properties of the membranes were also affected by polymer concentration. Higher PVDF content led to higher mechanical strength. This is due to the formation of the denser and thicker membrane.

### 4.1.2. Effect of solvent

The choice of solvent during phase inversion has a critical influence on the membrane morphology, its interfacial characteristics, mechanical properties, and separation performance. The solubility and compatibility of the solvent with the polymer is the most important factor to produce a homogenous dope solution [64,178,184–187]. Table 3
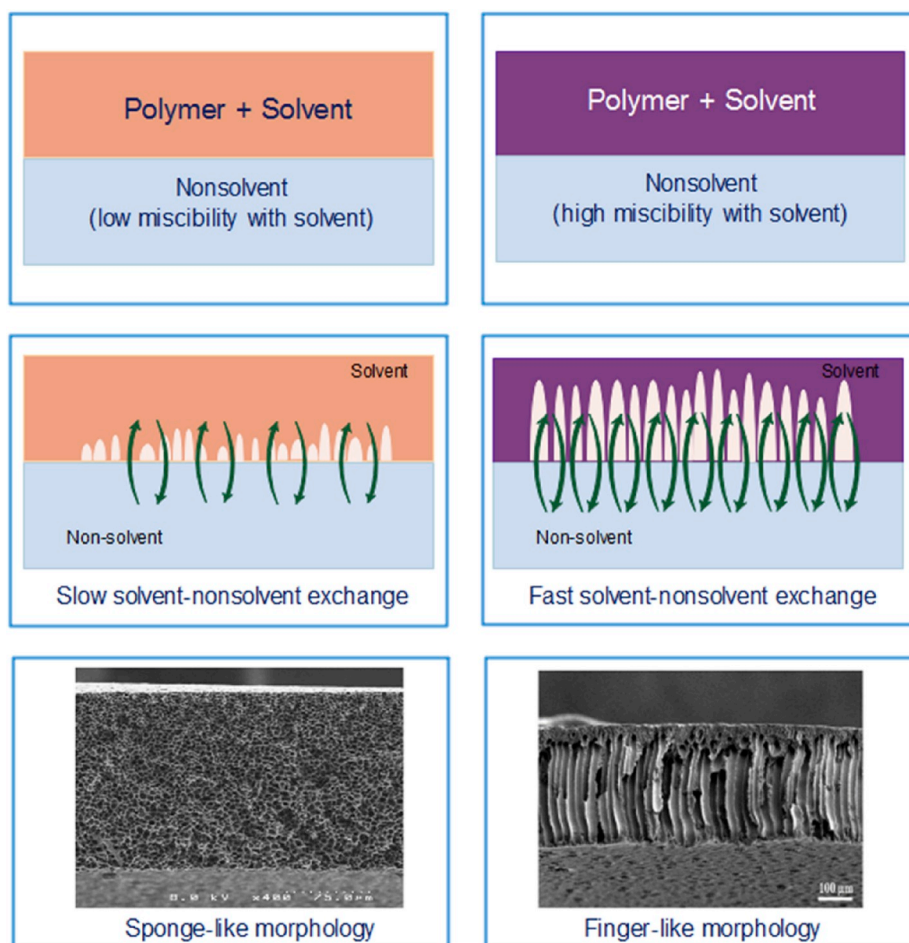


**Fig. 11.** Different types of demixing processes.

summarizes the solubility parameters of polymers and solvents. In addition, the polymer-solvent affinity is also presented in this table.

Based on the findings by Wang et al. [188], Strathmann et al. [189], Frommer and Lancet [190], the thermodynamic stability and membrane formation kinetics significantly control the membrane morphology. According to the membrane formation kinetics, when instantaneous demixing occurs, more pores form before the structure solidifies. When the delayed demixing process is dominated, the solvent-nonsolvent exchange will be slow and it will take a longer time for the membrane to form. Thus, a dense top layer and a sponge-like substructure will be obtained. This is complying with the equilibrium thermodynamic theory; the composition variation due to sufficient amount of non-solvent diffuses into the casting solution, its free energy decreases by separating two liquid phases of different composition. A similar trend has been observed by Wang and his co-worker [184]. Fig. 11 shows the structures of these two types of membranes.

In 2010, Tsai et al. [87] evaluated the effect of the type of solvent in PSf/NMP/water and PSf/2-pyrrolidone/water systems. The PSf membrane using 2-pyrrolidone (2P) solvent obtained a uniform bi-continuous structure throughout the whole cross-section. The combination of high viscoelasticity of the polymer-rich phase with the employment of 2P played an important role in retaining the nascent lacy structure. Meanwhile, for the PSf/NMP/water system, the morphology transformed into a cell-like structure with no pore connectivity. This is plausibly caused by the coarsening and coalesce of demixed domains, enforced by interfacial energy between the polymer-rich and polymer poor-phase.

The ability of the solvent to dissolve the polymer indicates the maximum polymer concentration at a certain temperature. Li et al. [191] investigated the influence of three different solvents (NMP, DMF, and DMAC) upon the formation of a homogenous PVDF solution. They pointed out that a poor solvent such as DMF needed a higher temperature to dissolve the same amount of PVDF. The solubility-parameter differences between PVDF and DMF gave rise to the highest differences as compared to DMAC and NMP. The smaller the difference of polymer-solvent solubility-parameter is the higher maximum concentration of PVDF can go to obtain a homogeneous clear solution.

One of the important criteria for choosing the appropriate solvent for membrane fabrication by VIPS is the impact of solvent on the environment and the solvent toxicity. Considering this factor has a significant effect on the sustainability in membrane fabrication. The necessity of utilizing non-toxic solvents in membrane fabrication is pointed out in a comprehensive review published in 2014 [2].

T. Marino et al. [192]. used Cyrene™ as a green solvent for fabricating PES and PVDF membranes. By changing the preparing condition membranes with different morphology obtained. The authors emphasized the potential of the Cyrene™ for sustainable membrane production. Following that Marino et al. [193] used TEP as another alternative and less-toxic solvent for PVDF membrane fabrication *via* VIPS process. The authors compared the effect of non-toxic solvents with conventional solvents such as DMF [194], DMAC [195], and NMP [196]. They claimed that TEP is a promising solvent for replacing commercially used hazardous solvents.

Another alternative green solvent is DMSO which introduced by Thuyavan et al. [197] and Arthanareeswaran and Stanov [198]. In both studies, PES/DMSO/water system was prepared with the same membrane concentration and experienced the same exposure time (0.5 min). Research on DMSO as a green solvent was followed by Marino et al. [199] by introducing a new grade version of DMSO solvent that is so called DMSO EVOL™. Surprisingly, the PWP result was at least 1000 times higher than reported by Thuyavan et al. [197] and Arthaneeswaran and Stanov [198]. Although the result of utilizing green solvent in VIPS process is promising, the investigation in this direction is limited to the few above-mentioned published papers. Considering the importance of the solvent toxicity, rules and regulation regarding the safe working environment and the importance role of solvents in the

phase inversion phenomena a comprehensive investigation in this direction is missing.

Remarkably, the volatility of the solvent is another important factor in membrane formation *via* VIPS. This parameter is more critical when a solvent with high partial pressure (high volatility) is used. In this case, the solvent evaporation is significant right after casting (or spinning) the polymer solution and has a significant effect in terms of the final membrane morphology [200]. Therefore, to avoid significant solvent outflow and have better control of phase inversion, low volatility solvents are preferred in VIPS processes [169].

### 4.1.3. Effect of additives

The addition of organic or inorganic and hydrophilic or hydrophobic, additives as another major component to a dope solution has been one of the important techniques used in membrane preparation *via* phase inversion. The goal of using an additive is to boost the performance of the polymeric membranes. The presence of another component in the polymer solution makes analyzing of solvent non-solvent system properties more complicated. Table 4 presents a list of used additives upon membrane fabrication *via* VIPS.
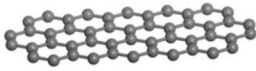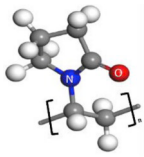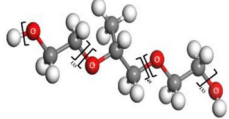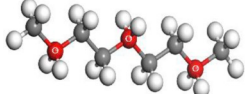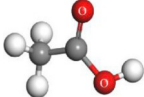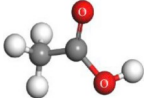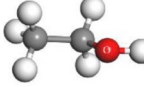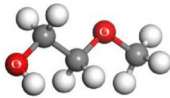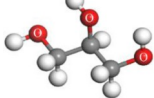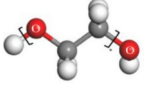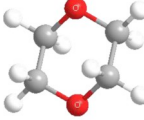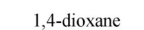
Increasing the membrane hydrophilicity is one of the main goals of using additives upon fabrication of a membrane *via* VIPS. When aiming at improving membrane hydrophilicity, two groups of responses are observed namely the physical impacts (structure modification) and chemical impacts (membrane interface modification). For instance, a study conducted by Venault et al. [201] pointed out that a solution containing 22 wt% PVDF and 3 wt% Pluronic F127 is less viscous than a solution containing 25 wt% PVDF. When the viscosity is low, it will create two opposite effects 1) facilitate the growth of crystals as there are less viscous forces, 2) reduced the crystal to grow since the crystallization is slower than L/L phase separation. For this case, the employment of F127 into the polymer solution increases the mass transfer rates and helps to enhance non-solvent (water) diffusion rate due to its high affinity towards water (chemical effect).

Polyvinylpyrrolidone (PVP) is one of the most common additives used upon membrane fabrication *via* VIPS and NIPS methods [71,85,86, 88,185,186,202–207]. Madaeni et al. [208] modeled and optimized the PES and PSf membrane fabrication by NIPS. In their research, they also investigated the effect of PVP content in the dope solution. It was found that by increasing the PVP content, at low concentrations, the interaction between the S=O groups of PSf and N–C=O groups existed since PVP encourages the flux enhancement. Susanto et al. [71] have also reported a similar finding. This may be due to the formation of a thin top layer with small pores and large pores as a sublayer. Meanwhile, at higher concentrations of PVP, the formation of a dense top layer reduced the membrane performance [209].

The trend as discussed above is also in general agreement with another case of VIPS membrane. There exists a trade-off between the thermodynamic instability of the dope solution and viscosity of the solution (kinetic effect). At low PVP concentrations, the viscosity of the solution does not change significantly with the PVP content. Therefore, the thermodynamic instability plays a role and the phase separation occurs faster resulting in a finger-like structure. While at higher PVP content, the viscosity of the dope solution is changing (increasing) and phase separation will be delayed by a diffusive hindrance, resulting in a cellular-like structure. Girones et al. reported shrinkage, tearing or similar defects in membrane formation when PVP content exceeds an optimum level [185].

Kang et al. [86] supported that the mean pore size of the membrane increased and pore size distribution becomes broader using PVP in the fabrication of microporous chlorinated poly (vinyl chloride). They attribute this result to the hydrophilicity of PVP. They explained that using hydrophilic PVP increases the absorption of water from the chamber environment, which in turn increases the surface pore size. Similar results were obtained by Han et al. [203]. They observed that by increasing the PVP content in the dope solution, the formation of

**Table 4**
Additive types and their advantages upon VIPS fabrication.

| Additive | Goal | Dope solution | Fabrication condition | Ref. |
|---|---|---|---|---|
| Graphene | ● To increase hydrophobicity, chemical stability, and mechanical strength | PES/NMP/Water | $T_{coagulation} = 50\,°C$ time = 30s RH = 80% | [90] |
| PVP | ● Pore-forming agent ● To increase hydrophilicity | PSf/NMP/Water | $T_{coagulation} = 25\,°C$ time = 0–20 min RH = 65% | [203] |
| Pluronic F108 | ● Generate hydrophobic interactions ● Increase hydration capacity | PVDF/NMP/Water | $T_{coagulation} = 30\,°C$ time = 20 min RH = 70% | [74] |
| Diethylene glycol dimethyl ether (DGDE) | ● Weak non-solvent additive | PEI/NMP/Water | $T_{coagulation} = 25\,°C$ time = 30 s RH = 65% ± 5% | [220] |
| Acetic acid (AA) | ● Strong non-solvent additive | | | |
| AA | ● Strong non-solvent additive | PS/Cyclohexane or toluene/Water | $T_{coagulation} = 28\,°C, 31\,°C$ time = 30 s – 1 h RH: 15–95% | [221] |
| Ethanol | ● Non-solvent additive | PVDF/DMAC/Water | $T_{coagulation} = 50\,°C$ time = 24 h RH = 80% | [202] |
| 2-ME | ● Hydrophilic additive ● Non-solvents with reverse thermal gelation properties | PES/NMP/Water | $T_{coagulation} = 50\,°C$ time = 2 s–20 s RH: 74% | [222] |
| Glycerol | ● To increases membrane porosity ● To increases membrane pure water flux | CN/Acetone/Water | $T_{coagulation} = 25\,°C$ time = 0.5–20 min RH: 70%, 80%, 90% | [223] |
| PEG-400 | ● Pore-forming agent ● Increase hydrophilicity | BPPO + TEOA, Chlorobenzene & NMP, Water | $T_{coagulation} = 25\,°C$ time = 0–10 min RH: 20%–90% | [179] |
| 1,4-dioxane | • Volatile additive • Significant decrease of flux and porosity | PI/DMF/Water | $T_{coagulation} = 25\,°C$ time = 0–4000 s RH: 40%–90% | [224] |

macropores was enhanced. However, a decreasing trend was observed when the PVP content approached 20 wt%. This phenomenon is caused by two factors, namely the thermodynamic and kinetic effects, as discussed above.

Other common additives that attracted attention among researchers working on the VIPS process is Polyethylene Glycol (PEG) [74,179, 210–212]. It is generally believed that PEG acts as a pore-forming agent and it enhances membrane hydrophilicity. In addition, it also affects the thermodynamics and kinetics of the phase inversion processes. A study carried out by Kim and Lee [213], on the effect of PEG on PSf/NMP membrane formation, revealed that by increasing the PEG/NMP ratio, the casting solution becomes thermodynamically unstable. Shieh et al. [214] also mentioned that the hydrophilic character of PEG can help to improve the membrane permeability [214]. Further, Kim and Lee [91] continued the investigation in terms of the effect of PEG for different molecular weight PEI membranes. Interestingly, they reported that PEG with a low molecular weight (PEG 200) works as a pore-reducing agent in PEI membranes and not as a pore-forming agent [91]. They attributed their results to the PEG solubility, viscosity and mass-transfer rate. In the case of low molecular weight PEG (PEG 200), the high rate of PEG outflow results in a membrane morphology with small cells without macrovoids. However, with increasing PEG molecular weight (PEG 600) the viscosity increases and the rate of PEG outflow in the coagulation bath retards. Consequently, open pores (i.e. macrovoids) are formed.

Besides including solvent additives as a third component in the casting solution, also a non-solvent additive can be used to enhance the membrane performance. For example, Mousavi and Zadhoush [215] were investigating the effect of a strong non-solvent (water) to the PSf/2P solution. Consequently, the interaction between the mixed solvent molecules (an amino group of 2P) with PSf chains (sulfonyl and ether groups) and water molecules resulted in an increase in the solution viscosity *via* hydrogen bonding. This phenomenon resulted in the retarded macro-void formation in the membrane sublayer [216–219].

The volatility of the used additive in the VIPS process should be considered as well. For instance a co-solvent additive with low boiling point evaporates from the casting solution resulting in a more concentrated layer at the top of the casted polymer solution. The formation of a concentrated layer in the top layer of the casting solution was analyzed by Soroko et al. [224]. They demonstrated that the evaporating of 1, 4-dioxane in PI/1,4-dioxane/DMF system prior to coagulation form a concentrated skin layer. Soroko et al. [224]. explained experimentally and theoretically the low diffusion coefficient within the evaporating PI film lead to 1–4,-dioxane depletion from the very top film layer. Consequently, polymer concentration increase. As evaporation time increases, the thickness of that layer increases. It is worthwhile to note that the mentioned concentrated layer acts as an extra barrier between the bulk of the polymer solution and the nonsolvent, thus slowing down the rate of nonsolvent inflow. Demixing will thus be delayed and membranes with a more selective layer can be expected [225]. This expectation were confirmed for a PSf system before coagulation [226, 227] but also contradicted for a PI system [224].

Ye et al. [202] investigated the effect of volatile additive (ethanol, bp = 89 °C) into PVDF/DMAC solution. The larger porosity was obtained due to the hydrophilicity behavior of ethanol which enhanced the thermodynamic driving force for the phase separation which simultaneously increased the surface adsorption of water in the vapor. Besides that, the low boiling point of ethanol (89 °C) triggered the polymer solution to evaporate at the beginning of the phase inversion process. This phenomenon increased the polymer concentration, mainly on the top layer of the vapor-film interface. As predicted, the dense skin layer and smaller pore size were obtained in consequence of the formation of polymer-rich surface concentration by the ethanol evaporation. Another study on the effect of the volatile additive by Shin et al. [222]. 2-methoxyethanol (2-ME) has been used as an additive upon PES/NMP membrane fabrication for microfiltration application. Based on their observations, this volatile additive was responsible to delay the kinetics of liquid-liquid demixing. Other believe that the delay in liquid-liquid demixing is a dominant effect as this method is typically used to produce dense films [228].

The impact of a particular additive on the structure and performance of the membrane is highly dependent on its affinity with dope solution, interaction with a nonsolvent, volatility, and its concentration in the casting solution, as well as on the specific polymer/solvent system. A multicomponent polymer dope solution creates a highly complex thermodynamic/kinetic situation that can hardly be rationalized and surely be predicted.

### 4.2. Effect of the process parameters

#### 4.2.1. Exposure time

During the VIPS process, the exposure time is one of the major factors that influence the membrane morphology and as a result, the performance of the resulting membrane. The exposure time has a significant influence on the coarsening effect and on the droplet size of the polymer-lean phases [59].

There exists a synergetic effect in fabricating parameters such as polymer solution parameters as well as operating parameters with exposure time. Therefore, it is challenging to extrapolate and generalize the effect of exposure time for all possible polymer/solvent systems. For example, a short exposure time for a polymer in a non-volatile solvent could be a very long exposure time for the same polymer in the same operating parameter with a volatile solvent. To analyze the effect of exposure time in detail, the exposure time is categorized into three groups: short, moderate and long time. However, the readers should note that this parameter is not identical for each system. Depending on other fabrication parameters, the exposure time could be in the range of seconds [229], minutes [60] or hours [202].

If the exposure time is too short, the membrane structure may not change significantly during the VIPS step and phase inversion occurs mainly by NIPS when the casted solution is immersed in a non-solvent. The resulting morphology is similar to typical morphologies obtained by the wet-immersion process, (i.e. dense layer and finger-like macrovoids) [179].

If the exposure time is moderate, the mechanism of the phase inversion will be a combination of VIPS and NIPS (i.e. N-VIPS). The structures of membranes change from the asymmetrical structure (a combination of dense layer and finger-like macrovoids) to symmetrical structure with sponge-like pores [223,230].

If the exposure time is long, the mechanism of membrane formation is based on the pure VIPS process. Depending on the type of polymer solution, the obtained structure could be an isolated cellular-like structure [230]. However, like in another case, especially for semi-crystalline PVDF membranes, the longer exposure time will give rise to spherulitic microstructures [78] or dense sponge-like structure [231]. Nevertheless, it is important to consider other parameters such as polymer concentration and polymer crystallinity in this case. Critical evaluation for the effect of exposure time on membrane morphology, pore size, porosity, permeability, and mechanical properties is presented in the following section.

#### 4.2.1.1. Effect of exposure time on membrane morphology. One study conducted by Sun et al. [223] on the effect of exposure time on CN/acetone membrane structure has been carried out. They figured out that when the exposure time increased from zero to 20 min, the structure of the membrane changed from an asymmetrical structure to a symmetrical structure attached on the cellular structure. This happens due to coarsening of the polymer lean phase at the late stage of phase separation. In addition, this phenomenon happens because of two factors affected by evaporation which are 1) evaporation of solvent increased the polymer concentration at the membrane surface 2) inhalation of non-solvent decreased the polymer concentration [223].

*N. Ismail et al.*
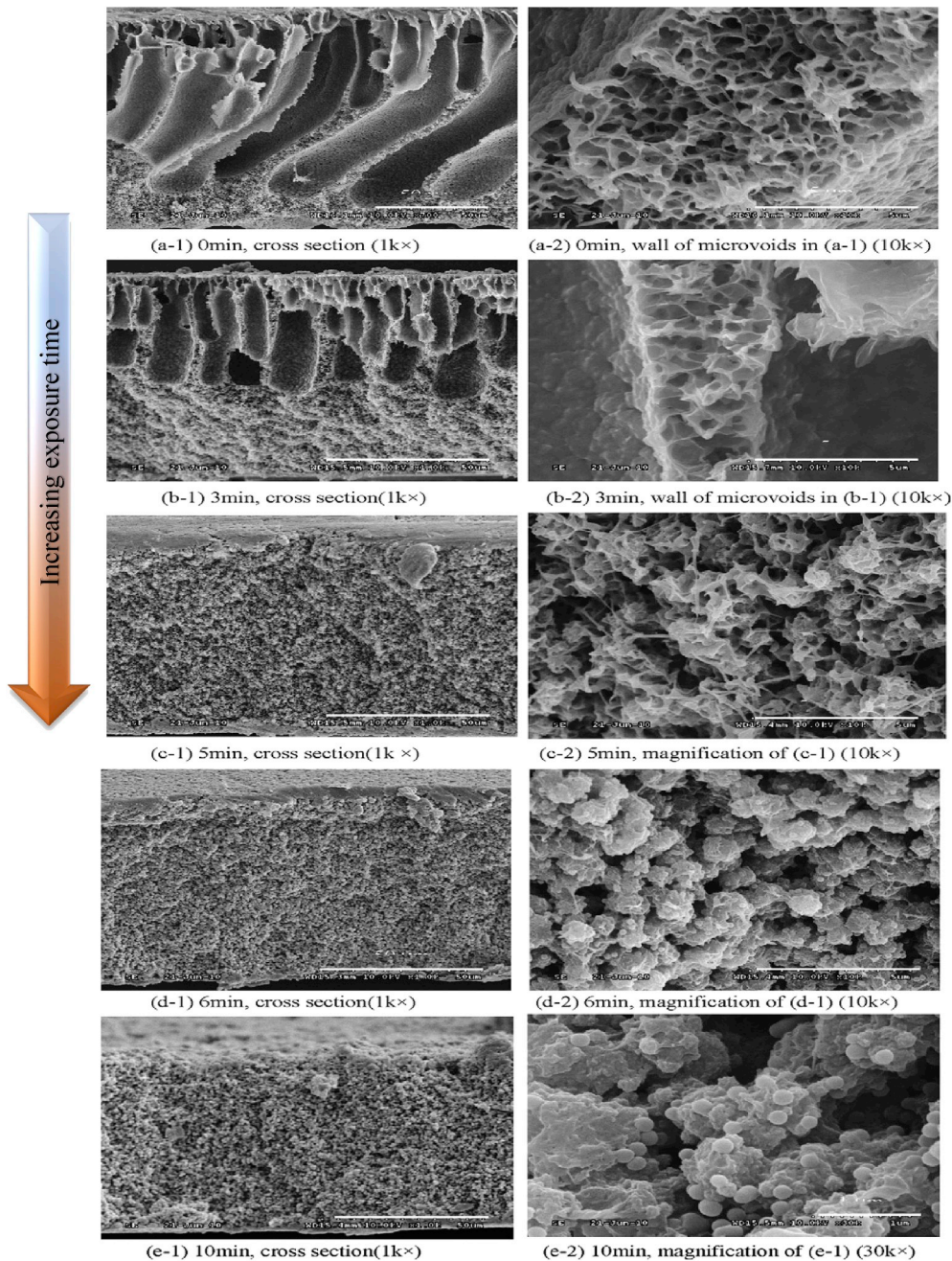
**Fig. 12.** SEM images of PVDF membrane with different exposure time a) 0 min, b) 3 min c) 5 min, d) 6 min e) 10 min operated at room temperature and 100% RH (Peng et al. [73]).

Peng and coworkers [73] studied the effect of exposure time on 15 wt % PVDF membrane *via* VIPS. They showed that the typically large and digitate macrovoids were formed when the exposure time was close to 0 min. Images depicted by SEM (Fig. 12) illustrate that there were no micropores but instead, a dense and smooth top surface topology similar to morphology obtained by NIPS membrane can be seen. The digitate macrovoid structures become shorter when the exposure time increases to 3 min. No digitate macrovoids were formed and spherulitic morphology appeared at 5 min exposure time. Next, at 10 min exposure time, no cellular structures appeared [73]. Similar findings were observed by Chen et al. [230] on their study on the influence of the exposure time of CA/PEI blend microfiltration membranes to water vapor. The casting solution was allowed to evaporate from 0 to 30 s and after that, the membrane was exposed to water vapor (RH > 95% at T = 50 °C) from 0.5 to 30 min and subsequently immersed in deionized

water (DI). For short exposure times (0.5–2 min), a morphology similar to the morphology of a membrane prepared by NIPS method was obtained [230]. This result is in agreement with previous research papers [89,222]. When the exposure time was further increased (>2–30 min), a cellular structure was formed by the coarsening of the polymer-lean phase, at the late stage of phase separation.

Another study concerning the of the exposure time was carried out by Zhao et al. [60]. They observed that at an exposure time of 0.5 min, a critical membrane structure lying between the typical NIPS structure and typical VIPS structure was obtained. They investigated the exposure time from 0 to 20 min and observed a combination of the interlaced mesh structure near the membrane surface and cellular structure throughout the cross-section of the membrane. As the water vapor contacts the near surface of the wet film, it results in the formation of interlaced polymer-lean phase and polymer-rich phase near the surface.

However, the exposure time of 0.5 min was insufficient for the coarsening process in this system, thus interlaced polymer lean phase and the polymer-rich phase generates the mesh structure after the solidification process.

*4.2.1.2. Effect of exposure time on membrane pore size and porosity.*
Membrane porosity is influenced by several factors such as the number of pores, pore size, and tortuosity [232]. A study on *in situ* cross-linking PSf/PPEGMA to fabricate PEGylated PSf membranes done by Zhu et al. [233] revealed that by increasing the exposure time from 0 to 5 min, the pore sizes increased from 9.3 to 10.8 nm. With the prolongation of the exposure time, more PPEGMA chains spontaneously segregated onto the membrane/water interface, resulting in a larger coverage of PEG chains, consequently increasing the membrane hydrophilicity and resulting in larger pore sizes.

Another study involving the *in-situ* cross-linking process of acrylic acid into PSf solution to fabricate PSf/PAA membrane revealed the opposite result: the pore sizes decreased from 81.9 to 40.7 nm with increasing exposure time from 0 to 60 s [234]. Wormlike networks were formed and the network diameter increased as the exposure time increased. This can be attributed to the delayed phase separation of the films.

Harruddin et al. [90] mentioned in their study of PES/DMAC system that the porosity of the membrane increased along with the exposure time due to the increasing interconnection of the cellular pores. The reason is that the polymer solution has sufficient time to crystallize and produce a porous membrane. This is also supported by the findings of other researchers [235].

Fig. 13 presents experimental data from different research groups and interpolation of the obtained data when all other parameters are held constant except relative humidity (RH) and exposure time. Considering the influence of the exposure time on the PVDF/DMAC system, three research groups have conducted investigations concerning these parameters (Table 5). Surprisingly, Peng et al. [73] observed no changes in the mean pore size of the membrane by increasing the exposure time from 0 to 6 min in a PVDF/DMAC solution, at 100% RH but the porosity greatly increased. Nevertheless, they provided no further explanation of why similar mean pore size was obtained. Fan et al. [236] used a similar polymer system as Peng et al. with same 100% RH and observed an increment in the pore size from 0.34 to 1.02 μm by increasing the exposure time from 0 to 5 min. They explained that the

**Table 5**
Comparison between different exposure time of PVDF membrane via NIPS-VIPS

| Solvent type | RH % | Exposure time (min) | Mean pore diameter (mm) | Ref. |
|---|---|---|---|---|
| DMAC | 60 | 2 | 0.06 | [237] |
|  |  | 5 | 0.06 |  |
|  |  | 10 | 0.14 |  |
| DMAC | 80 | 2 | 0.07 | [237] |
|  |  | 5 | 0.13 |  |
|  |  | 10 | 0.14 |  |
| DMAC | 100 | 0 | 0.34 | [236] |
|  |  | 1 | 0.62 |  |
|  |  | 2 | 0.8 |  |
|  |  | 5 | 1.02 |  |
| DMAC | 100 | 0 | 0.11 | [73] |
|  |  | 3 | 0.11 |  |
|  |  | 5 | 0.11 |  |
|  |  | 6 | 0.11 |  |
| TEP | 55 | 0 | 0.14 | [231] |
|  |  | 2.5 | 0.43 |  |
|  |  | 5 | 0.42 |  |
|  |  | 7.5 | 0.45 |  |
| DMSO | 50 | 0 | 0.07 | [78] |
|  |  | 1 | 0.08 |  |
|  |  | 5 | 0.37 |  |
|  |  | 10 | 0.22 |  |
|  |  | 20 | 0.22 |  |

solvent/non-solvent exchange rate was slow in the presence of water vapor. When the exposure time is increasing, there will be enough time for the lean phase to grow and the mean pore size is increasing. Almarzooqi et al. [237] detected that the pore size increased as the exposure time increased. The presence of droplet-like pore mouths on membrane surfaces increased which leads to the formation of larger pore sizes. This is more obvious when higher RH is implemented. Based on the obtained result it can be concluded that by increasing RH from 60 to 100% for a PVDF/DMAC system, the mean pore size is increased and the effect of exposure time in higher RH is more obvious. The further explanations on this aspect of RH are discussed in detail in section 3.2.2.

In the work of Meringolo et al. [78], considering on the effect of the exposure time on PVDF/DMSO systems have clarified the pointed that the membrane pore size increases with the exposure time to vapors shorter than 5 min, but then dropped when ranging between 10 and 20 min. At 5 min exposure time, the more porous and rough surface was induced. Consequently, the formation of interconnected pores was
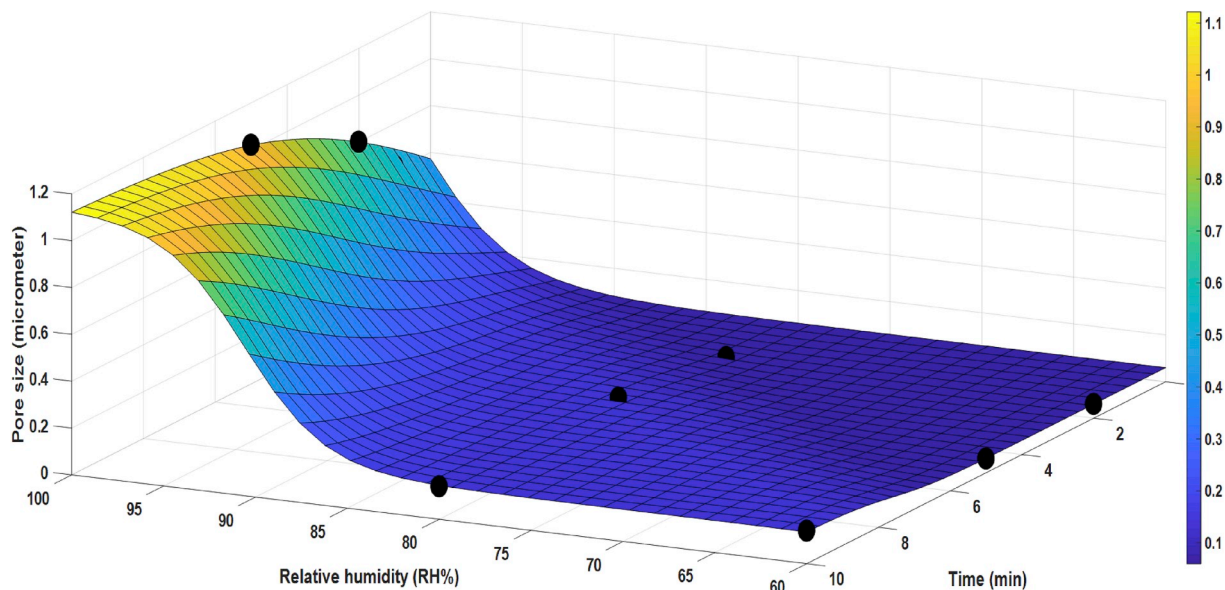


**Fig. 13.** Synergetic observations of exposure time and relative humidity on PVDF membrane pore size (experimental data are taken from Refs. [236,237]).

completed by the solvent/non-solvent exchange. The longer exposure time gives longer water condensation process on the cast film. Thus, denser regions on the membrane surface were formed which leads to pore size suppression.

On the PVDF/TEP system studied by Marino et al. [231] focused on the formation of PVDF/TEP membrane reported that by increasing the exposure time from 0 to 7.5 min, the pore size increased. Similar explanation as Fan et al. [236] have reported, the longer exposure time resulted in more time for the lean phase to grow, thus increasing the pore size.

*4.2.1.3. Effect of exposure time on membrane permeability.* Chen et al. [230] reported on their study of CA/PEI blended membranes that as the exposure time is increased, the growth of the polymer-lean phase increases the sizes of the voids (pores) but is, at the same time, associated with the coalescence of the polymer-rich phase. This phenomenon decreases the interconnectivity of pores. Note that even though larger pores were formed, they were not inter-connected. As a result, the structure is no longer an open porous structure but a cellular-like one. Consequently, a drastic decrease in membrane permeability occurs. This is in agreement with the findings of other research groups [89,222].

In contrary to the aforementioned statement, Sun and co-workers observed in their study of a CN/acetone solution that the permeability increased by increasing the exposure time from 0.5 to 1 min [223]. When the exposure time increased, the membrane structure changed from asymmetrical to the symmetrical and cellular structure by the coarsening of the polymer lean phase, at the late stage of phase inversion. Therefore, the size of the cell increased resulting in a pore size enlargement. Thus, higher membrane permeability could be recorded.

Zhao et al. [60] observed on their study of PVDF/NMP system that by increasing the exposure time from 0 to 20 min, the water permeability increases from 88 L/m$^2$h·bar to 8590 L/m$^2$h·bar [60]. As the induced time increases, the more enlarged pores are generated which results in higher flux. Meanwhile, for a short exposure time (<0.5 min), the coarsening of polymer lean is limited, resulting in dense membrane structure formation with no connected pores.

In another study on PSf/DMF membrane prepared by VIPS, Han and Bhattacharyya [238] carried out the experiment with 3 different exposure time namely 0 min, 3 min and 3 days. From the experimental result on water permeability, the permeate water flux decreased as the exposure time increased from 0 to 3 min. When the membrane underwent complete evaporation for 3 days without immersion in a coagulation bath, no permeation was observed. This result was attributed to the resistance from closed cell-like structures [238].

*4.2.1.4. Effect of exposure time on mechanical strength.* Since the

exposure time plays an important role in membrane morphology, adjusting this parameter enables to tune the mechanical stability of the membrane. Peng et al. [73] observed the morphology of the PVDF membrane changed from cellular structure to granular structure when the exposure time increased from 0 to 8 min in PVDF/DMAC system. Consequently, they reported by increasing the exposure time, the tensile strength of the membrane decreases sharply. However, Zhao et al. [60] revealed that the PVDF membranes prepared at exposure times longer than 0.5 min resulted in a very high mechanical strength as compared to zero exposure time in a PVDF/NMP system. This is due to the formation of symmetric cellular structures that are mechanically stronger than the asymmetric structure of the dense skin layer with finger-like macrovoids obtained from the NIPS process (zero exposure time).

Considering the synergetic effect of exposure time on morphology, skin layer, and degree of crystallinity, it is difficult to have a general rule for the optimum exposure time. Several thermodynamic and kinetic obstacle variables prevent generalizing the influence of exposure time. Indeed, finding an optimum exposure time to obtain maximum mechanical properties based on the nature of polymer and solvent is an interesting topic that could be investigated further in the future.

*4.2.2. Relative humidity*

Relative humidity implicit water molecules exist in the vapor phase and promote the raise of the partial pressure of the water vapor. This parameter has an impact on the membrane morphology and properties as stated by several researchers [59,79,85,86,177,181,223,239]. Matsuyama et al. studied the effect of RH on the membrane structure by modeling [181] and experimental works [177]. They studied the effect of RH (10%, 20%, and 40%) on the PVDF/DMF system while all the other parameters were constant. Based on the experimental results, it is evident that a dense, cellular and lacy-like structure was obtained by increasing of RH. They clarified that with 10% RH, no porous structure is forming although a few pores could be found on the membrane surface. The pores form due to polymer crystallization. The porous structure formed when the RH increased to 20%. When the RH increased to 40%, a lace-like structure and spherical bead structure obtained from crystallinity of PVDF were observed. To have a better understanding, the structures obtained are depicted in Fig. 14.

Ye et al. [202] studied the effect of RH in PVDF/DMAC/PVP casting solution and found that the membrane formed at RH 30% exhibited a finger-like structure and numerous micro-pores were formed on the top surface [202]. A similar structure was obtained when the RH increased to 60% and 90%. On the other hand, the membrane porosity was slightly increased at 90% of RH. They also explained that there was a rivalry between different phenomena when RH was further increased: i) the hygroscopicity (absorbing moisture from the air) of DMAC occurs when
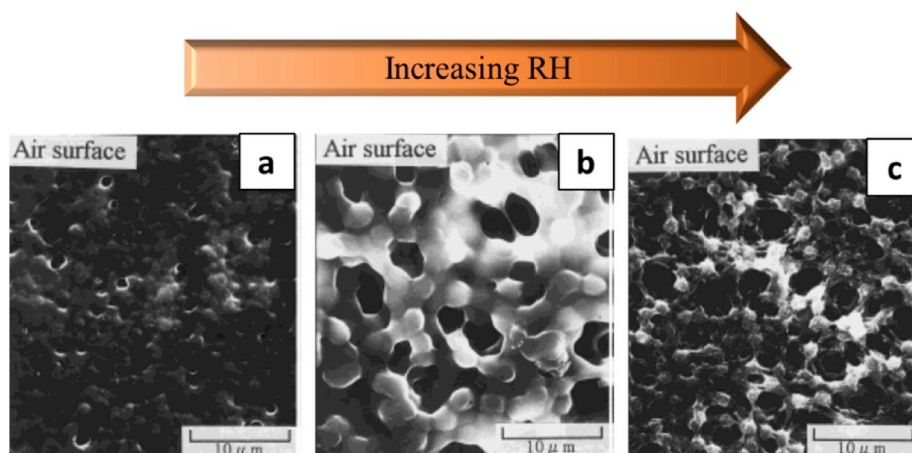


**Fig. 14.** Effect of RH in PVDF/DMF system at a) 10%, b) 20% and c) 40% RH (Reproduced from Matsuyama et al. [177]).

the water inflow to the film and ii) evaporation by the outflow of volatile molecules occurs from the film [66].

Kang et al. have likewise conducted another study on the effects of RH to CPVC/PVP membrane properties [86]. In this study, tetrahydrofuran (THF) was used as a solvent and n-butyl alcohol (n-BA) as a co-solvent. The pore size of the membrane surface increased and the pore size distribution broadened with an increase in RH of CPVC polymer solution. The mean pore sizes were limited to a narrow range of 0.15–0.22 μm when the RH increased to 45, 60 and 80%, respectively. However, the CVPC polymer solution embedded with PVP gave rise to larger pore sizes in the range of 0.8, 1.2 and 1.4 μm, respectively. In this case, the high volatility of n-BA and THF solvents played an important role in the initiation of the phase separation and generation of pores on the membrane surface.

On the one hand, Park et al. [59] explained in their study effect of RH into PSf/NMP system explained that, for this system, the phase separation did not occur at RH below 65%. The reason for this is that water vapor activity was too low to cause phase separation. They also justified that by increasing the RH from 70% to 100%, the pore size of the membrane decreased from 16.4 μm to 6.9 μm. This is due to the fact that phase separation will proceed more slowly and longer and, therefore, more time is allocated for the coarsening process at lower RH (70%). As a result, larger cellules structure were formed.

Caquineau et al. [240] studied the influence of RH on the PEI/NMP membrane. They observed a cell-like structure from RH 27%–70% emerges. The size of the cells became smaller as the RH increased. The cell size was getting smaller from top to bottom, resulting in anisotropy in the membrane structure. These results are in agreement with Park et al. [59] and explained that for a high amount of RH, a significant amount of water was penetrating into the system fast and, subsequently caused the formation of a large number of nuclei. This resulted in an increase in the polymer concentration in the polymer-rich phase. Simultaneously, the viscosity of this phase was increased and causing reduction of the cell-growth and hindering the coarsening phenomena. In both cases, it can be concluded that a higher RH favored nucleation to the detriment of the cell growth rate and coalescence.

A number of studies above have reported how RH affects membrane morphology and properties. However, as the wide range of RH were proposed with different polymer systems approached, the results vary.

At lower RH, there is a possibility to form a dense, cell-like or even a finger-like structure. At higher RH, spherulitic, bi-continuous or cell-like structures tend to form. It is important to note that the optimum RH will depend upon other parameters such as the type of polymer, polymer concentration, and many other factors.

### 4.2.3. Dissolution temperature

Dissolution temperature, $T_d$ is the temperature at which a polymer is dissolved to form the casting solution. This parameter is found to heavily affect the membrane morphology as proven by several researchers [241–243]. In their investigation on the effect of $T_d$ in PVDF/DMF solution, Lin et al. [241] pointed out that by increasing the $T_d$, the obtained membranes were composed of PVDF nodules (spheroids) along with an increase in the size of the nodules. This is attributed to the polymer crystallization of solid-liquid demixing process. In addition, higher $T_d$ also renders lower connectivity of polymer domains in PVDF membranes [241]. Besides that, an increase in $T_d$ results in a rougher film surface. This has also been reported by Benz et al. [244] in their study on spin-coating of PVDF solutions.

Another investigation on the effect of $T_d$ on PVDF/NMP solution was conducted by Li et al. [72]. They demonstrated that the morphology of the PVDF membrane is changing together with $T_d$ while keeping the other parameters constant. They observed a membrane morphology composed of polymer nodules when the $T_d$ was higher than 40 °C. By increasing the $T_d$ from 45 °C to 150 °C, the nodule size increased. Furthermore, the connectivity among the nodules increased when the $T_d$ is decreased. By further lowering the $T_d$ to 32 °C, the morphology changed to a bi-continuous structure. This phenomenon existed because of the limited growth of crystallites triggered by the competition of more growing sites in the solutions. Therefore, the PVDF membrane with smaller nodules was obtained.

According to Zhao et al. [60], the polymeric chain interactions decreased with the increasing of $T_d$ from 25 to 65 °C. It can be explained that the $T_d$ affected the crystalline behavior of PVDF polymeric chain and has a significant impact on the microstructure of the membranes. The FESEM images shown in Fig. 15 justified that by increasing the $T_d$, the membrane microstructure tends to gradually change from a spherulitic structure to a cellular structure. This could be attributed to the dissolution states of PVDF polymer chains interactions in the casting
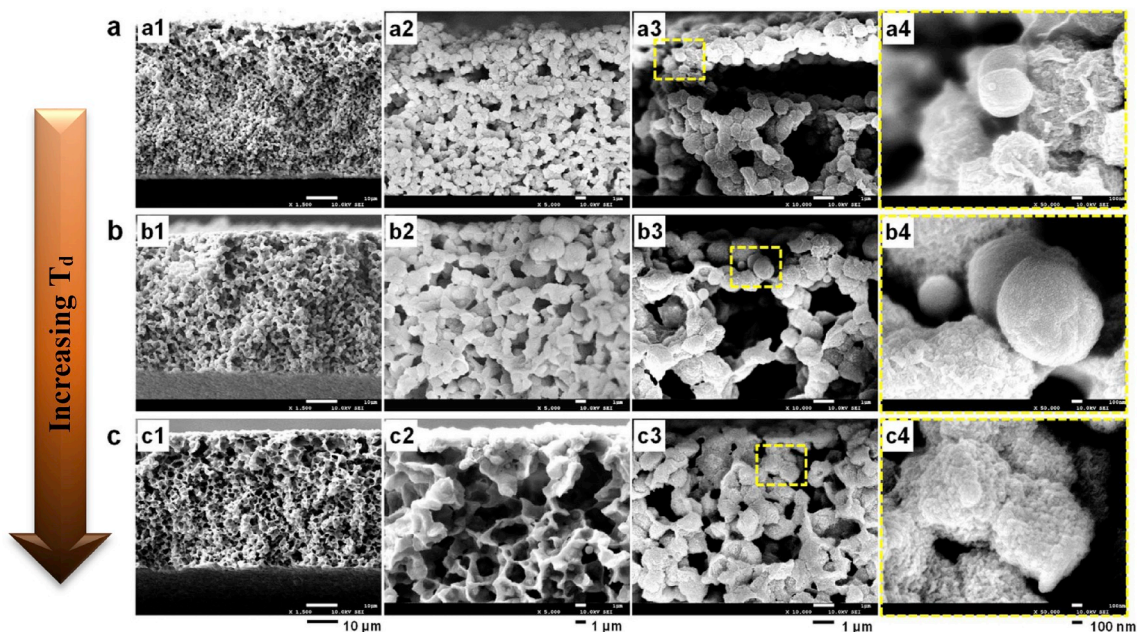


**Fig. 15.** FESEM images of cross-section of 15 wt% PVDF prepared membranes with different $T_d$: (a) 25 °C, (b) 45 °C (c) 65 °C at $T_v = 25$ °C and 70% RH. Reproduced from Zhao et al. [60].

solution. At low $T_d$, the entangled PVDF polymeric chains act as crystal nuclei which provokes the liquid-liquid phase separation to occur thus resulting in the spherulitic structure of the membrane. Meanwhile, a high $T_d$ enhanced the liquid-liquid phase separation and formation of the cellular structure.

Based on the findings above, it is clear to conclude that an increase in the $T_d$ value can have a strong effect on the membrane morphology and crystalline polymorphs, especially in case of semi-crystalline PVDF membranes. Higher $T_d$ values reign over spherulitic structures along with increasing the size of nodules whereas lower $T_d$ is favorable to obtain bi-continuous structures accompanied by well-connected pores.

### 4.2.4. Vapor temperature

Only limited research can be found about the influence of vapor temperature ($T_v$) on the resulting membrane morphology formed via the VIPS strategy. A study by Girones et al. [185] concerning the formation of microsieves by phase separation (VIPS and NIPS) micro molding pointed out that the contribution of $T_v$ is minor in terms of the perforation level of the microsieverts [185]. A similar finding has been observed by Bouyer et al. [80]. They revealed that the cell size gradients of the cellular-like structure were slightly reduced when the temperature was decreasing from 40 °C to 25 °C. Hence, the cells near the upper layer morphology (under skin layer) appearing at 40 °C were bigger than those formed at 25 °C [80]. This can be explained by simulation results, which proved that lower temperatures should result in retarded mass transfer rate and consequently, in an increase in the demixing time. This trend is also in agreement with Zhao et al. [60]. The thermodynamic instability of the system increases at higher $T_v$ and, thus the liquid-liquid demixing process was preferred over solid-liquid demixing. Hence, in this manner, the spherulitic structure was surpressed and the cellular structure of the membranes was promoted.

On the other hand, Peng et al. [182] investigated the influence of the chamber temperature on the morphology of PVDF membrane with very low polymer concentration (4 wt%). They observed that a bi-continuous structure was replaced by a dense structure in the skin layer simply by increasing the chamber temperature. They attributed this phenomenon to the spinodal decomposition.

### 4.3. Combination of phase inversion

As stated earlier breaking the thermodynamic equilibrium and having the phase inversion can be initiated by a combination of driving forces. For instance, the combination of NIPS and TIPS which is so-called N-TIPS [35,245–247]. In the case of VIPS process, there are two possible scenarios: 1) the combination of VIPS and NIPS process (V–NIPS process [231]) and 2) the combination of VIPS and TIPS process (V-TIPS process).

V–NIPS process is a well-known procedure for membrane fabrication and often authors pointed out the VIPS step by different names such as evaporation step [248], dry phase inversion step [141,249–254], etc. in casting flat sheet membrane and spinning hollow fiber membranes. Indeed, evaporation before coagulation is a popular technique to fabricate membrane via NIPS. By advancing membrane science the importance of the VIPS became more obvious and recently researchers are analyzing this step separately [231,255]. The readers should consider that all the above mentioned factors for the phase inversion by VIPS process are applicable in the V–NIPS process as well. The only difference between VIPS process and V–NIPS process is in the later process before completing the phase separation by VIPS process the nascent membrane will move to the coagulation bath and the phase separation will be continued by NIPS process. Therefore, to analyze the morphology of the fabricated membranes both phase inversion should be considered. VIPS process before coagulation and NIPS process after coagulation. This issue is discussed in detail in 4.2.

Typically the solvent/diluent in the TIPS process is not water soluble [92–140]. Therefore, evaporation of the solvent and changing the temperature effect the phase inversion rather than substitution of solvent and non-solvent. However, using a water soluble solvent in the TIPS process is expanding (N-TIPS) [34,35,245,246]. The effect of VIPS process in the N-TIPS process has not been investigated to date. We anticipate a complicated phase separation process in this scenario. The tricky question is: is it necessary to have such a complicated phase separation procedure to fabricate membrane?

## 5. Design of fouling-resistant membranes *via* the VIPS process

### 5.1. Basic concepts for preparing antifouling membranes

Recent developments of antifouling or low-fouling membranes are mostly based on the design criteria for protein resistant interfaces established in the group of Whiteside some 20 years ago [256]. The rationale behind is that major compounds responsible for membrane fouling in common wastewater treatment or biomedical applications of porous membranes are biological systems including proteins, bacteria or human cells. Among these biofoulants, proteins are the smallest entities, that is, they can readily diffuse between polymeric chains forming the membrane matrix and interact with the polymer. Once they adhere to surfaces, they can then mediate biofouling by larger biological systems. So, if a membrane efficiently resists non-specific protein adsorption, it is likely to be resilient towards the adhesion of larger biofoulants [257]. As the development of fouling-resistant membranes has similarities with the development of biofouling-resistant materials, membranologists worldwide have been developing filters able to maintain a high level of hydration at the interface between the membrane and the medium, an essential design criterion [256,258]. This can be achieved using antifouling brushes which possess hydrogen-bond acceptor groups but no hydrogen-bond donor groups [256]. Besides, as most biofoulants are charged, it is important to ensure that the membrane surface is neutral [256]. Consequently, the use of poly (ethylene glycol) (PEG) derivatives and zwitterionic systems have been widely applied to membrane systems [259]. Furthermore, there are three main routes to incorporate antifouling materials in a membrane system, namely coating, grafting or *in-situ* modification, each one presenting a number of advantages and disadvantages. The purpose of this review is to focus on VIPS membranes, and thus, we will only concentrate on the latter method. The *in-situ* modification consists of blending the main polymer forming matrix with an antifouling polymer prior to the membrane casting. The major advantage of this technique is that it is a one-step process as the membrane is formed and modified in a one single unit operation. Therefore, if one can find a common solvent to the main polymer (most often very hydrophobic) and the antifouling material (amphiphilic or hydrophilic), then it is possible to design antifouling membranes by phase inversion, using common wet-immersion process or VIPS for example. It leads to the formation of matrices in which antifouling moieties are distributed along with the entire thickness of the membrane. Although very limited evidence can be found, a gradient of antifouling polymer concentration is expected to propagate from the bottom (substrate/polymeric solution interface) to the top (polymeric solution/non-solvent interface) due to thermodynamic reasons, this being referred as surface segregation. In some way, surface segregation would play a similar role to the coating density (coating processes) or the grafting density (grafting processes) on the final membrane protection against biofoulants.

### 5.2. Why is VIPS workable?

VIPS can be an ideal process to prepare antifouling membranes for the following reasons: First, slower phase separation gives better control of the membrane structure, as mentioned earlier in this review. The more compounds there reside in a polymeric casting solution, the harder it is to control the membrane formation. By slowing down the mass-transfer exchange, it is easier to reach a better understanding of and

control of important parameters responsible for membrane formation. However, more importantly, the VIPS approach promotes surface segregation. It is indeed difficult to directly measure the surface segregation as one would need to determine the concentration of the antifouling agent, at various film thicknesses, of approximately 100–200 μm. A technique based on FT-IR measurements exists to determine the composition of a polymeric system during phase inversion but it relies on a number of assumptions related to the length and time scales and has never been tested in quaternary (polymer/copolymer/solvent/non-solvent) systems [89]. So, unless one would be able to cut the membrane into thin layers and measure the surface chemical composition of each and every one of these layers, it will remain challenging to explain and characterize the surface segregation. What we do know, however, is that the mobility of polymer chains in the system decreases as the phase separation occurs, which must reflect on the diffusion of the antifouling agent. Once the polymer chains are fixed in the polymer-rich domains, the antifouling moieties can no longer diffuse towards the polymeric system/non-solvent interface. So, if one wants to maximize the concentration of antifouling moieties at the membrane surface, it is better to aim at slower mass transfer. In other words, VIPS is a much better option than wet-immersion.

Another reason that renders VIPS (and all in-situ modification processes) a viable technique for the design of fouling-resistant membranes is that the water permeability is not sacrificed once the antifouling material is incorporated in the system. On the contrary, one can expect that the thin layer of an antifouling polymeric material deposited at the surface of the membrane during the surface modification (coating, grafting), will affect the pore size and surface porosity of the resulting material. As a result, decrease its permeability, given the importance of structure parameters in terms of mass transfer through porous membrane systems. Playing with the casting solution preparation and VIPS parameters, it is possible not just to maintain water permeability, but

also to increase it because the pore size/porosity is maintained. The addition of hydrophilic moieties further enhances water wetting and promotes the water transfer [233,260].

Finally, an ideal structure for porous membranes is the so-called bi-continuous structure. With common commercial polymers widely applied upon the formation of porous membranes for large scale applications, such as polysulfone (PSf) and poly (vinylidene fluoride) (PVDF), wet-immersion using water as a non-solvent leads to the formation of finger-like structures with a skin top-layer with small pores. These common structures cannot compete with bi-continuous structures in terms of both mechanical stability and permeability because unlike in finger-like structures, bi-continuous structures are composed of two perfectly interconnected polymer phases (polymer-rich ensuring the mechanical stability of the system and polymer-poor enabling permeability). As discussed earlier in this review, it was shown that PSf and PVDF bi-continuous structures could be obtained *via* the VIPS process, by simply changing the solvent in the case of PSf [87] or the temperature of dissolution of the casting solution in the case of PVDF [72]. These studies could then be extended to the formation of bi-continuous and fouling-resistant membranes, as can be seen in the next sections, by adding an antifouling copolymer in the casting solution.

### 5.3. Polymers used as antifouling materials in VIPS membranes

Herein we focus on the antifouling materials used to mitigate fouling of VIPS membranes. It is implied that the main polymer used to prepare the membrane is hydrophobic and prone to fouling as in most cases (PVDF, PSf, etc.) and thus, that a copolymer had to be added to the casting solution. However, one should note that the VIPS method has been applied to casting solutions containing a hydrophilic polymer, poly (phenyl sulfone) and a solvent [229]. As a result, the intrinsic hydrophilicity of the film did not require the use of any copolymer specifically



**Fig. 16.** Timeline of recent developments of fouling-resistant membranes by VIPS process and tentative summary of the advantages/drawbacks of the proposed polymers/copolymers used.

used to promote the formation of a hydration layer and mitigating fouling.

The most widely used polymers in a blend with common membrane polymers are derivatives of poly (ethylene glycol) (PEG). The reason for their widespread application is besides the low price that they can easily be solubilized with the main polymer in the casting solution prior to phase inversion. As represented in Fig. 16, typical examples of such derivatives used to design antifouling membranes by VIPS are Pluronic® polymers or poloxamers, which are triblock copolymers made of two side-blocks of poly (ethylene oxide) (PEO) and one central block of poly (propylene oxide) (PPO). Attempts have been made to blend PSf and PVDF with Pluronic® F108 or F127 thus enabling the construction of membranes by the VIPS approach [74,201,210,211]. The surface hydrophilicity of the membranes could be greatly improved. For example, the initial water contact angle (WCA) was decreased from 85° to 60° in the case of PSf VIPS membranes [210], and from 130° to 40° in the case of PVDF VIPS membranes [74]. In the case of PVDF/F108 VIPS membranes, dynamic measurements showed that after 11 s, complete spreading of water on the membrane surface could be reached [74]. Given the high surface roughness and large pore size/porosity of these membranes, all promoting air entrapment, a 0 WCA dictates a large density of the copolymer at the surface of the membranes, although no evidence related to surface segregation of the copolymer was presented. As a consequence, the antifouling properties of the membranes were drastically improved using a large span of biofoulants including proteins and bacteria. Nevertheless, in some particular cases, little or no improvement occurred. Hence, using fibrinogen, a very sticky protein, at best a 30% reduction in the adsorption on the PVDF/F108 membrane was obtained, compared to the virgin PVDF membrane [74]. The large molecular weight of the protein (compared to smaller bovine serum albumin (BSA) or lysozyme with which antifouling performances were better) can be the explanation as it correlates with the number of hydrophobic domains able to interact with the hydrophobic domains of the membrane. The water solubility of the copolymer is another possible explanation. Fibrinogen adsorption is commonly tested using enzyme-linked immunosorbent assay (ELISA) which is a lengthy procedure that involves numerous incubation steps in aqueous media and washings of the samples with aqueous solvents. So, the membrane system must be stable in an aqueous media. As Pluronic® polymers are water-soluble, membrane systems containing these poloxamers may lack stability, which leads to a decreased performance.

To address this challenge, other PEGylated materials were synthesized, made of polystyrene and poly (ethylene glycol) methacrylate. At some particular compositions, these copolymers can be solubilized in water-insoluble N-methyl-2-pyrrolidone, a common solvent for PVDF or PSf. They were first introduced by Prof. Chang's lab and later on used for the surface modification of membrane systems applied to the treatment of wastewaters [261,262]. In their work, Lin et al. synthesized a series of diblock copolymers of PS and PEGMA and coated them on commercial PVDF membranes [262]. Unlike in VIPS or NIPS in which chain entanglement is at focus, only surface hydrophobic interactions were achieved after coating. Yet, the authors stated that they achieved ultra-stable biofouling resistance, which implies that hydrophobic interactions between the PVDF and PS-*b*-PEGMA were stable as supported by experimental results. It was observed that over 95% of the polymer remained anchored after 6 h of washing in acidic, basic and saline solutions and that the antifouling properties were maintained. Besides, tested in a membrane bioreactor used to treat wastewater from Tokyo municipality, the results indicated that after 12 days of treatment, very low biofouling occurred on the PS-*b*-PEGMA-coated membrane (low increase in TMP, about 10–12 kPa) while important fouling was measured on the virgin membrane (TMP increased to 80 kPa). Based on these results one can conclude not only that the copolymer worked well to limit biofouling thanks to the PEGMA units but also that it remained at the surface of the membranes over that period of time. Therefore, the stability of the design was achieved. Because of this, PS-*b*-PEGMA could

replace Pluronic® systems which failed at providing stable antifouling VIPS membranes. Diblock (PS-*b*-PEGMA) [263,264] and triblock (PEGMA-*b*-PS-*b*-PEGMA) [265] copolymers were successfully incorporated in VIPS membranes. Importantly, bi-continuous and antifouling VIPS PVDF-based membranes could be obtained by carefully tuning the temperature of dissolution of the casting solution [263,265], as we can learn from an earlier study of Li et al. [72]. The results indicated that the membranes could resist a variety of biofoulants including model proteins such as bovine serum albumin or lysozyme [264], proteins from blood (fibrinogen, globulin, human serum albumin) and blood cells [263], bacteria (*Escherichia coli, Streptococcus mutans*) [263–265] but also microalgae [264] (in static (adsorption tests) but also in dynamic operations (filtration tests). The versatility of antifouling performances was demonstrated by these various studies suggesting a wide range of potential applications (wastewater treatment, blood-contacting -devices).

Stability concerns met with Pluronic® systems were addressed using derivatives of polystyrene and PEGMA. Nonetheless, there is still room for improvement. PEG-derivatives are known to self-oxidize and fail in complex media while zwitterionic materials provide more stable antifouling properties. While surface modification of membranes with zwitterionic polymers is easily achievable and has been reported [259], the *in-situ* modification of VIPS membranes using zwitterionic copolymers is tricky. Problems are met either during the polymer synthesis stage or during the casting solution preparation step. For example, while the synthesis of copolymers made of polystyrene and poly (sulfobetaine methacrylate) (PSBMA) is doable, we noticed that it was extremely difficult to re-solubilize the product of the polymerization reaction (possibly PS-*r*-PSBMA) due to large differences in polarity between the hydrophobic units and the hydrophilic units. A strategy then proposed by Dizon consisted of incorporating PEGMA units in the random copolymer, where PEGMA would be used as a solubility enhancer [266]. The resulting random copolymer then consisted of three units, PS-*r*-PEGMA-*r*-PSBMA, each of which had a well-defined function: (i) polystyrene units interacting with PVDF and providing stability; (ii) PEGMA units aiming at tuning the solubility of the copolymer with the hydrophobic membrane polymer; (iii) SBMA units providing the antifouling properties. The solubility of the copolymer with PVDF in NMP was proven from dynamic light scattering measurements: the particle sizes increased with the content of SBMA in the copolymer, with a limit of about 9 nm obtained with a PEGMA/SBMA molar ratio of 2-to-1. Above this value, much larger particles were obtained and the solution turned cloudy indicating lack of solubility of the polymers in the casting solution. Bi-continuous membranes formed by VIPS then showed excellent antifouling properties even in complex media such as humic acids. Besides, while PEGMA was used as a solubility enhancing unit, it also possesses very good antifouling properties, as stated above. Yet, membranes formed with control random copolymer PS-*r*-PEGMA showed poorer performances than those designed with PS-*r*-PEGMA-*r*-PSBMA, highlighting the improvement brought by the zwitterionic units. Finally, another recent strategy was to use a copolymer made of 2-methacryloyloxyethyl phosphorylcholine and methacryloyloxyethyl butyl urethane group referred to as PMBU [267]. This copolymer was synthesized and characterized in Prof. Ishihara's lab in the mid-'90s [268]. While the units of 2-methacryloyloxyethyl phosphorylcholine (MPC) deliver the antifouling property, the urethane groups provide flexibility to the copolymer, hence promoting its solubility in hydrophobic polymers. Yet, this compound was never tested in membrane preparation *via* VIPS until recently. It was again shown that solubility was achievable and that bi-continuous antifouling membranes could be prepared.

Finally, a recent original approach to modify VIPS membranes was presented by Zhu in a series of articles in which VIPS membranes were *in-situ* modified using various hydrophilic polymers including poly (ethylene glycol) methacrylate (PEGMA) [233], poly (N-isopropylacrylamide) (PNIPAm) [260], and poly (acrylic acid) (PAA) [234]

that were cross-linked in the casting solution. This original method comprises the addition of a cross-linker and an initiator to the casting solution. As a result, the polymerization and cross-linking of PEGMA, PNIPAm or PAA occurs around the main membrane polymer chains (PSf in all cases) during the preparation of the casting solution. Then membranes were formed *via* the VIPS approach. The arrangement of polymeric chains is referred to as a wormlike morphology by the authors.

From the thermodynamic perspective of incorporating hydrophilic polymers into the polymer system, Zhu et al. [234] discovered an enlargement of wormlike diameter by increasing the concentration of the copolymer (PAA). This is attributed to the delayed phase separation of the films. Typical macroporous were formed at lower AA concentration, while membranes with wormlike networks were formed at higher concentration [234]. In the case of PSf/PNIPAm study copolymer concentration together with exposure time are playing a crucial role in membrane formation [260]. The hydrophilic copolymer is responsible to enhance the driving force for the growth of the polymer-lean phase. In terms of exposure time, the longer exposure time permits the polymer-lean phase to expand, thus more hydrophilic copolymer (PNIPAm) chains move to the film/water vapor interface as the low surface energy. When the phase inversion happens, the surface covered with high PNIPAm content with large network pores. As the exposure time is longer, the droplets' mobility of aqueous phase is decreased. Consequently, suppress the wormlike structure to grow [260].

In general, adding a hydrophilic polymer or copolymer will not only modify the thermodynamic of the system but also kinetic of mass transfer rates. This is not specific to the VIPS process, but also common to the wet-immersion process which requires the use of a non-solvent as well. From a thermodynamic aspect, a shift of the binodal line towards the polymer-solvent axis is expected because of the presence of the hydrophilic units of the added polymer/copolymer. It means that a smaller mass fraction of nonsolvent is needed to induce phase separation. From a kinetic aspect, affinity of the additive with water tends to promote water transfer in the polymer/additive/solvent system, which results in faster phase separation. However, one should note that adding a hydrophilic polymer/copolymer to the casting solution may also lead to an increase in the initial casting solution viscosity, compared to the solution without additive (in the case where a part of the solvent is changed to the additive and the main polymer weight fraction kept constant). The change in casting solution viscosity may also significantly affect exchange rates of solvent/non-solvent. Besides, for PVDF systems, increasing the system viscosity is not favorable to membrane formation by crystallization. In other words, bi-continuous structures, arising from spinodal decomposition, are quite readily obtained upon the addition of a copolymer to the initial polymer/solvent system [263,267].

A major advantage of this technique is the availability of the monomers used. Besides and although further dedicated studies are necessary, it probably leads to a more stable modification than using Pluronic® and despite the absence of hydrophobic units, cross-linking around the main polymer chains occurs. As PEGMA is one of the most important antifouling materials, PEGylated PSf membranes designed with this technique showed improved permeability and antifouling performances (tested using BSA) [233]. Using PNIPAm [260], improved water flux and fouling-resistance can be obtained in a certain range of temperature because PNIPAm has a lower-critical solution temperature. Hence, it undergoes conformational changes, turning the system from hydrophilic to hydrophobic. Finally, PAA is a pH-responsive polymer and thus, does not fit in the criteria of fouling-resistant materials but is worth mentioning in this study considering the similar approach used (polymerization of the hydrophilic monomer in the casting solution).

## 6. Applications

To date, a number of articles have reported the various application fields of the membranes prepared by the VIPS method including microfiltration (MF), ultrafiltration (UF), membrane distillation, water and wastewater treatment, gas separation, medical and biomedical applications as well as for secondary batteries application.

### 6.1. VIPS applications in water and wastewater treatment

In 2019, Benhabiles and coworkers studied the $TiO_2$-PVDF/PMMA materials prepared *via* the VIPS approach in UF/MF and photocatalytic applications. They observed that by increasing the evaporation time from 0 to 5 min, the porosity, pore size, and pure water flux increased. Based on their results, the photocatalytic membranes exhibited more than 99% of methylene blue (MB) degradation, which manifests that this membrane has a high potential in the treatment and purification of wastewater [269].

Superhydrophobic membranes prepared by VIPS, which is favorable for the direct contact membrane distillation (DCMD) application, has caught some researchers attention. Fan and coworkers [270] have fabricated thin PVDF flat-sheet membranes for desalination by the DCMD process. The membrane was capable to remove 99.7% of NaCl with a high flux ($18.9 \, kg/m^2 \cdot h$). The rejection value was maintained for 6 h test thus indicating that the wetting during the DCMD process is hardly occurring. Another research group [271] also worked on the PVDF membrane for MD applications. The membrane gave rise to $9-32 \, L/m^2 \cdot h$ flux and higher than 99% degree of salt rejection was achieved. These obtained fluxes are within the range of MD flux reported for other studies performed with PVDF membranes [272–274].

The structure of VIPS membranes can be controlled to yield highly porous materials. Nodular or bi-continuous structures typically have a pore size in the higher range of the UF domain or in the MF domain, and a porosity higher than 70%. This combination of structure parameters renders VIPS membranes suitable for ultra-low pressure or gravity-driven separation of oil and water. Table 6 summarizes the applications and performance of the membranes fabricated *via* VIPS for water treatment.

Upon utilizing the fabricated membrane obtained *via* VIPS for oil/water separation, the main parameters that need to be considered are related to the nature of the rich phase forming the emulsion. Starting with oil-rich emulsions, the membrane material has to be oleophilic, and hydrophobic in oil. It was reported that PVDF VIPS membranes had a water contact angle in toluene, hexane, heptane or hexadecane higher than 140°, while the oil almost instantaneously wetted the membrane material under water [275]. The high hydrophobicity of PVDF VIPS membranes arises both from structural parameters (pore size, porosity, roughness) promoting air trapping, and from the intrinsic chemical nature of the materials used. Further, according to the Cassie-Baxter theory [183], high water contact angles are easily obtained with these membranes. Nodular structures, in which air is easily trapped, are particularly attractive for gravity-driven separation of oil-rich emulsions. Although weaker than bi-continuous structures, nodular PVDF membranes can be handled without breaking, and because there exists no extra-mechanical transmembrane pressure in a gravity-driven oil/water separation, nodular membranes remain mechanically stable. The first study, to our knowledge, that reported the use of an air exposure step to form nodular PVDF membranes applied to the gravity-driven breaking of W/O emulsions was that of Zhang et al. although VIPS was not directly mentioned [276]. The authors explained that the use of ammonia in the casting solution was responsible for the formation of clusters that later on led to the growth of spherical particles (or nodules). However, they also exposed the solutions to air "for several minutes" before immersion in a non-solvent bath. It is unclear how long time this "several minutes" is, but it is well established that even short exposure times to humid air can drastically affect a membrane structure. Therefore, it can also be suspected that the exposure to air is a VIPS step that was decisive in the final membrane structuring, resulting in efficient and fast separation of oil-rich emulsions. Separation kinetics can be tuned by playing with the membrane structure or its composition, but even in the simplest case, gravity-driven membrane separation is going to

**Table 6**

Application in water treatment and performances of the membrane by VIPS method.

| Main polymer | Co-polymer Additive/ | Application | Configuration | Remarks | Performance | Ref. |
|---|---|---|---|---|---|---|
| PVDF | | DCMD | Flat sheet | 1) Combination of VIPS method and co-casting<br>2) Super hydrophobic surface | 99.8% NaCl rejection | [270] |
| PVDF | | DCMD | Flat sheet | 1) High contact angle<br>2) Low bubble point pore size by adjusting casting thickness | >99% Salt rejection | [271] |
| PVDF | PMMA | UF/MF | Flat sheet | By increasing evaporation time from 0 to 5 min<br>1) Pure water flux increase<br>2) Porosity and pore size increase<br>3) Mechanical strength decrease | Flux = 226 L/m$^2$.h | [269] |
| PVDF | PMMA/TiO$_2$ | Photocatalytic | Flat sheet | 1) Membrane pore size increase<br>2) Improving hydrophilic nature<br>3) Mechanical strength increase | >99% of MB degradation | [269] |
| PEI | DGDE/AA | NF | Flat sheet | 1) Ideal membrane morphology was obtained<br>2) Integrally skinned NF membranes exhibit appropriate NF performance | Flux = 635 L/m$^2$.h<br>Rejection (PEG 600) = 83% | [220] |
| PEEK-WC | | UF | Hollow fiber | 1) Without PVP, high flux was obtained but low rejection | Flux = 412 L/m$^2$.h.bar<br>Dextran rejection = 75% | [279] |
| PEEKWC | PVP | UF | Hollow fiber | 1) By adding PVP results in a very steep increase of dextran rejection | Flux = 354 L/m$^2$.h.bar<br>Dextran rejection = 82% | [279] |
| CN | Glycerol | UF | Flat sheet | 1) At 1 min exposure time, 20 wt% glycerol shows the best performance | BSA absorption capacity, q$_m$ = 110 µg cm$^{-2}$ | [223] |
| BPPO | | UF | Flat sheet | 1) At exposure time 2 min, highest BSA rejection obtained | Flux = 1236 L/m$^2$.h<br>BSA rejection = 90% | [179] |
| PES | Pluronic | UF | Flat sheet | 1) Addition of Pluronic results in the highest hydraulic permeability | Flux = 75 L/m$^2$.h at 450 kPa<br>70% Rate of recovery | [212] |
| PES | Pluronic, TEG as nonsolvent | MF | Flat sheet | 1) Higher fluxes obtained with membranes prepared from the casting solution having a composition of PES/NMP/TEG/Pluronic = 10/30/55/5 (wt. %), with 3 min exposure time to humid air, at 50–60% RH. | Flux = 94,960 L/m$^2$.h.bar<br>Protein rejection (initial) = 31%<br>Protein rejection final = 43% | [71] |

significantly increase the separation times, compared to gravity separators. For example, while separating 50 mL of a 1 wt% emulsion of water/toluene emulsion, the process can take 4 h when using a gravity separator. This time can be significantly reduced to 60 min with a 0.1 µm-pore size PVDF VIPS membrane or 8–10 min with a modified PVDF VIPS membrane in a gravity-driven membrane filtration process [277]. Typically, the separation efficiency can reach values of 99.9% or higher.

The second case is the breaking of water-rich emulsions. Using this kind of emulsion, the membrane should be hydrophilic and oleophobic under water. With common membrane materials, it is not achievable because they are usually hydrophobic. In a recent study, surface modification was applied to VIPS membranes, aiming at depositing zwitterionic moieties on their surface [278]. This process led to the formation of superhydrophilic PVDF-based membranes, which were applied in a low-pressure driven separation (0.5 bar TMP) of oil and water from water-rich emulsions. The process was not gravity driven, possibly because of the tight hydration layer forming thanks to the zwitterionic units, thus preventing large water fluxes. In another attempt, however, the gravity-driven separation of oil and water from water-rich emulsions was achieved using VIPS PVDF membrane modified with graphene oxide (GO) [277]. The GO particles are amphiphilic and possess numerous hydrophilic functional groups that promote wetting by water. Provided that a pre-wetting step by aqueous solvent was performed, gravity-driven filtration of water-rich emulsions was made possible for a large variety of emulsions (toluene/water, hexane/water, diesel/water, soybean oil/water). The hydrophilic functional groups of GO facilitate air replacement by water during the pre-wetting step which, in turn, explains significantly faster separation kinetics/higher separation efficiency than obtained with a pristine membrane. Besides, as GO is an amphiphilic material, it was found that switchable separation was possible, that is, the separation of oil-rich emulsions was achieved after pre-wetting of the material with pure oil [277].

In general, one limitation of these gravity-driven separation membranes (prepared by VIPS or other processes), is linked to the viscosity of

some oils. For instance, vegetable oils are significantly more viscous than model synthetic oils or diesel, which slows down the separation [277,278]. Besides, it has been proven with synthetic emulsions that the smaller the droplet size, the slower the separation [278]. Both the emulsion size and the emulsion viscosity definitely need to be taken into account to orientate the choice of the membrane filtration process (gravity-driven or with a supplementary transmembrane pressure).

## 6.2. VIPS applications in gas separation

Polymer membranes prepared via VIPS can also be used in gas separation. A dense membrane is preferable in case of gas separation because it relies on kinetic diameters of specific air components which are totally different from the properties of the membrane for water applications. Wu et al. [280] applied the VIPS method in their study on oxygen enrichment. They prepared PSf/PDMS composite membranes to produce isolongifolenone from the isolongifolene oxidation process. In their work, they figured out that at 5 min pre-evaporation time, the maximum oxygen concentration was obtained. It can be explained that by increasing the pre-evaporation time, the skin layer became thicker and denser thus resulting in high selectivity and low permeability [280].

In the case of hollow fiber membrane air gap, it is not only defining the polymer chain entanglement but also it is indicating the duration of nascent fiber exposure. Widjojo et al., following their dual-layer hollow fibers study on Ultem/P84 system, explained that water vapor exposure (air gap) could induce phase separation; therefore, more closed-cell structures in the outer layer were obtained at the longer air-gap length (i.e., 5 or 10 cm). Meanwhile, shorter air gap (i.e., 0 or 1 cm) resulted in a sponge-like microporous structure. Consequently, as the thickness of closed-cell cellular structure increases with the increasing of air-gap or evaporation time, the selectivity of the membranes is enhanced [187].

## 6.3. VIPS for medical and biological applications

Membranes prepared via VIPS were also used in wound dressings

[281–287], cell cultures [221], drug release [288] and the separation of antibodies [223] applications. Organic materials such as chitin and chitosan have been chosen for dressing applications due to their biocompatibility, bioresorbability and bioactive behavior. The natural biopolymer of chitin is mostly made by the extraction of shells of

(a)

(b)

(c)

(d)

**Fig. 17.** a) The schematic design of flow battery. b) The 1 kW VFB cell stack prototype, and its operating performance and the cell stack performance at current densities ranging from 80 to 120 mA cm$^{-2}$. c) cycle performance of the cell stack 120 mA cm$^{-2}$ (Reproduce from Yuan et al. [299]). d) Correlating the VIPS phase separation and ion permeability of the resulting membranes. $\eta$ is the solution viscosity, and P is the vanadium ion permeability [300].

crustaceans, which form N-acetylglucosamine. The deacetylation of chitin will produce chitosan. It is important that these materials are created through VIPS-like gelation processes to have better control of hydrogels structuring and therefore, obtain the desired structural properties. Gels offered a porous structure fit for optimal drainage of discharge. Therefore, extensive work has been carried out on the formation of hydrogels by the VIPS process for wound-dressing applications [281,282,285–287,289].

A study on the application of drug release using membrane prepared via VIPS has been performed by Ma et al. [288]. The effects of naproxen (a lipophilic drug) on the CA/acetone/water system was the main objective of this study. Based on the findings, one can summarize that naproxen can inhibit locking-in of the CA membrane structure due to the combinatorial effects associated with a) reduction in transition glass temperature, b) the crystallization rate of drug and c) the mass transfer path of the casting solution. Furthermore, they also emphasized that by controlling the interplay of phase inversion, drug crystallization and membrane formation will allow higher drug loads without bursting.

### 6.4. VIPS potential in electrochemical applications

One of the most attractive and promising technologies for large-scale energy storage is flow batteries due to their intriguing characteristics of high safety, long cycle life, high efficiency, low cost, and flexible modular design [166,290,291]. The most common approach for improving the performance of a flow battery is optimizing its key components. Fig. 17a shows the schematic design of a flow battery. Among the different flow battery components (i.e. anode, cathode, electrolyte, and membrane), the membrane is a key component, serving as a separator to isolate the anode and cathode to prevent the occurrence of a short circuit. Simultaneously, the membrane must also allow the transport of charge carriers to achieve a complete circuit. One of the most popular flow batteries is a vanadium flow battery (VFB) [292–297].

There is a trade-off between high ion selectivity and proton conductivity in VFB. The combination of the sponge-like porous structure and charged groups is in favor of the realization of better performance for porous membranes in VFB. By optimizing the fabrication condition during the VIPS process the pore structure can be tailored and a uniformly distributed porous structure can be obtained. For example, a porous polybenzimidazole (PBI) membrane of sponge-like cross sectional morphology was fabricated directly from a PBI polymer solution by VIPS (PBI/NMP system under 80% RH, 50 °C vapor temperature and 50 min exposure time) for VFB application in 2016 [298]. The produced PBI membrane demonstrated good proton conductivity of 16.6 mS cm$^{-1}$, low VO$^{2+}$ permeability ($4.5 \times 10^{-8}$ cm$^2$ min$^{-1}$), and 98% Coulombic efficiency (which is 10% higher energy efficiency than VFB operated with Nafion 112 at applied current densities of 20–40 mA cm$^{-2}$).

In the same year, a novel PBI polymer containing positively charged N groups adopted as the membrane material [299]. The porous membranes prepared by the VIPS method (PBI/DMAC system, under 100% RH condition at temperature 50 °C for 10 min exposure time) also had spongy porous structures and positively charged groups. High ion selectivity was obtained due to the unique spongy pore structures composed of thousands of micron-sized cells, uniformly distributed and disconnected porous structures produced in the VIPS process, and multiple barriers for vanadium ions due to the positively charged pore walls of all disconnected cells. On the other hand, the acids doped in PBI pores resulted in high proton conductivity, owing to the fact that nitrogen in the PBI ring could be easily protonated under acidic conditions. Consequently, the fabricated PBI *via* VIPS method demonstrated 98.9% Coulumbic efficiency, 91.1% voltage efficiency, and 90.1% energy efficiency which were overall much higher than that of commercial Nafion 115 [299]. The most notable result in this pioneering research was its extremely high chemical stability. The fabricated PBI membrane
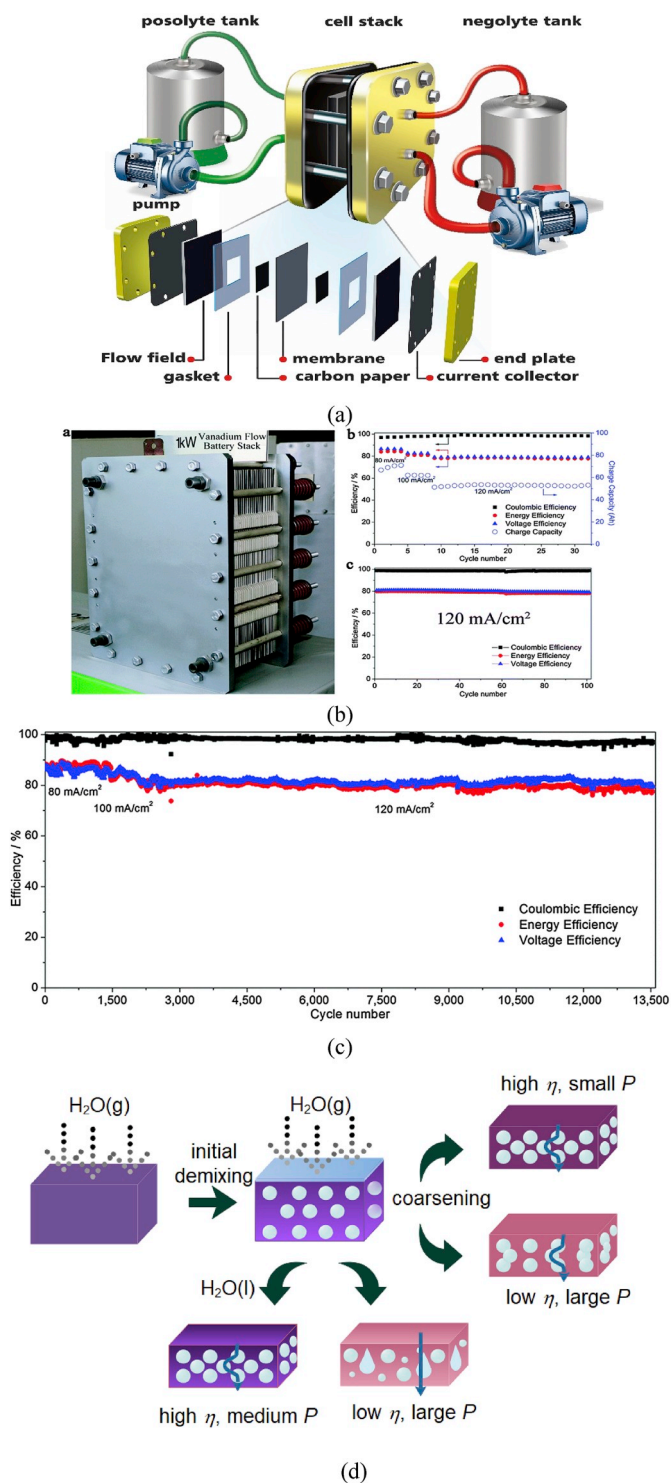
by VIPS could run for more than 13 000 cycles, with no obvious efficiency decay. This was the first time that a non-perfluorinated porous membrane had been fabricated with stability over 10 000 cycles. One should consider that such excellent performance is the combination of introducing the novel hydrophilic membrane material, introducing positively charged amine groups and optimizing preparation parameters during the VIPS process [299]. Fig. 17b and c shows the performance and prototype of VFB assembled with the PBI-68 membrane.

Luo et al. [300] studied the influence of the material properties of poly (2,5-benzimidazole) (ABPBI) on the membrane structure formation and ion transport characteristics. They critically analyzed the correlation between membrane fabrication parameters in the VIPS process and ion selectivity in ABPBI/NMP system and pointed out the role of the surface liquid layer on membrane selectivity [300]. Fig. 17d represents their proposed phase separation mechanisms in VIPS process and ion permeability of the resulting membranes.

One of the major barriers in the way of broad deployment and deep market penetration of flow batteries is the use of expensive metals as the active species in the electrolytes [301]. The use of organic redox couples in aqueous or non-aqueous electrolytes is a promising approach to reduce the overall cost in long-term since these materials can be low-cost and abundant [301–303]. In recent years, significant developments in organic redox flow batteries have taken place, with the introduction of new groups of highly soluble organic molecules, capable of providing a cell voltage and charge capacity comparable to the conventional metal-based system [301]. However, to our best knowledge, there is not any report of fabricating membrane via VIPS for this kind of a flow battery.

Another class of secondary batteries is a Lithium-ion battery. It consists of four fundamental components: the negative electrode (anode), the positive electrode (cathode), the electrolyte, and the separator as shown schematically in Fig. 18. Although separator does not participate in the electrochemical reactions in a Li-ion battery, they perform the critical functions of physically separating the positive and negative electrodes while permitting the free flow of lithium ions through the liquid electrolyte that fills in their open porous structure [304]. Porous membranes are the most commonly used material as separator due to their relatively low processing cost and good

mechanical properties [304]. Fabrication of membrane via VIPS process for Li-ion battery is pointed out in some papers [166,304] and patent [305]. However, a critical investigation about the potential of VIPS process for fabricating membrane for Li-ion battery is missing.

Supercapacitors with, high power density, fast charging−discharging ability and excellent cycling stability have been widely employed as powerful substitutions to back-up power devices and some other renewable energy systems [306,307]. Electrodes in supercapacitors usually are constructed by a slurry coating method, where the active materials, conductive agent, and binder are coated together onto the metallic current collector, and as result, the active materials are easily detached from the current collector during the electrochemical reaction [308]. In addition, conventional supercapacitors are not bendable in shape thereby restricting the development of wearable electronic devices [309]. Using PES, nickel hydroxide, DMAC, and water as polymer, active material, solvent, and nonsolvent, respectively, Dong et al. [309] used VIPS process to fabricate a flexible membrane electrode for the supercapacitor. They analyzed the effects of relative humidity (60%, 70%, 80%, and 90%), exposure time (5, 20, and 40 min), and temperatures (25, 30, and 35 °C) of the phase inversion on the electrochemical performance and structure of VIPS membrane. They reported the VIPS process as a robust, simple and easy method for fabricating foldable, symmetric membrane structure with long cycle life. Based on their report, the slow phase inversion process provides a symmetric morphology without any micropores, macropores, and finger holes [309]. The prepared morphology with a short path of electrolyte ions during the electrochemical reaction process effectively improved the cycle stability of the membrane electrode [309]. Using the fabricated membrane as positive electrode a high specific capacitance of $96.03 \, \mathrm{F \, g^{-1}}$ at $1 \, \mathrm{A \, g^{-1}}$, a maximum energy density of $30.01 \, \mathrm{W \, h \, kg^{-1}}$, and maximum power density of $3750.95 \, \mathrm{W \, kg^{-1}}$ with the energy density of $16.4 \, \mathrm{W \, h \, kg^{-1}}$.

## 7. Summary and outlook

In this review, a comprehensive analysis concerning membrane preparation via VIPS, in terms of effective parameters in membrane formation, membrane morphology, physicochemical properties as well
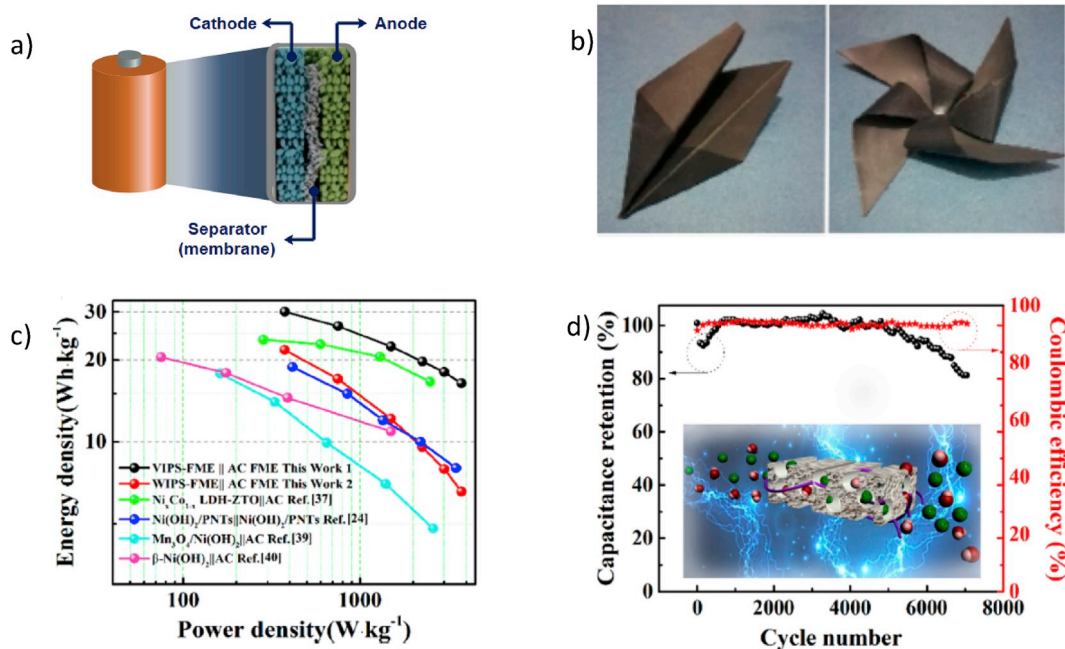


**Fig. 18.** a) Schematic design of a supercapacitor b) Flexible membrane electrodes fabricated by VIPS c) Ragone plot and d) Cycle life of the fabricated membrane reproduced from Dong et. al. [309].

as modeling and applications are presented. In a nutshell,

1) Among four common membrane morphologies obtained via the VIPS method, bi-continuous or sponge-like structures are the most favorable ones for liquid phase separation in order to achieve high membrane permeability. The dissolution temperature and polymer solution viscosity are also important parameters to be controlled when aiming at such structures.

2) Polymer concentration was shown to be strongly influenced by the system viscosity and, hence, process demixing rate. Polymer-solvent affinity is also of major importance upon the formation of homogenous solutions and phase inversion. It is good to emphasize that solvents with low volatility are commonly employed in the VIPS process in order to avoid fast solvent outflow.

3) To have sustainability in membrane production there is an urgent need to substitute the toxic solvents with environmentally friendly solvents. Research in this direction is in the primary steps and a more comprehensive investigation is required.

4) Developing a predictive/simulative model for membrane fabrication is an important factor in membrane science. There is no doubt that analyzing the phase inversion by using mathematical correlation gives the accurate trend in transport phenomenon. This fact is already demonstrated in several published papers [80,88,157,161]. However, there are several obstacles for developing mathematical models for VIPS process. Due to the complexity of the system, all the developed models are based on one-dimensional transport. However, the phase inversion is a three dimensional phenomena. As stated earlier some theoretical parameters cannot be determined and require some assumptions. Furthermore, additional assumptions need to be considered for solving the developed equations. Inserting the above-mentioned assumptions to the developed model deviate the model prediction from the real condition and decrease the accuracy of the model. Moreover, it is not possible to track the phase inversion phenomena in mesoscale. For example, polymer molecular weight distribution has an effect on membrane formation [33,176] but inserting these kinds of parameters in mass transfer equation is a bottleneck. To address this issue, the researcher used successfully three dimensional model based on Dissipative Particle Dynamic simulation (DPD) to study the phase inversion phenomena both in TIPS [176,310–312] and NIPS [46] method. However, there is not such an investigation in the VIPS process.

5) Correlating the fabrication parameters to the final performance of the membrane based on mathematical with acceptable accuracy is challenging due to the complexity of the system. One approach for understanding the effect of fabricating parameters on the final performance of the produced membranes and determine the optimum preparation condition is using artificial intelligence methods. For example, Madaeni et al. [208]. used an artificial neural network and genetic algorithm for modeling and optimizing the PES membranes for milk ultrafiltration.

6) The influence of the process parameters, exposure time, relative humidity, dissolution temperature, vapor temperature were also discussed.

   - It is difficult to generalize the effect of the exposure time due to the wide array of thermodynamic and kinetic obstacle variables. Indeed, finding an optimum exposure time to have good mechanical properties based on the nature of polymer and solvent is an interesting topic that necessitates further research in the future.

   - Different trends and morphologies have been observed which requires a deep investigation mainly focusing on the influence of RH in a variety of polymer/solvent systems. At lower RH, there is a possibility that dense, cell-like or even finger-like structures are formed. At higher RH, spherulitic, bi-continuous or cell-like structures tend to form. It is important to note that, the optimum RH will depend upon other parameters such as type of polymer, polymer concentration among many other.

   - Dissolution temperature is found to give dramatic improvements in terms of membrane properties. Based on this review, lower $T_d$ is suggested for membrane preparation in order to obtain bi-continuous structures with good interconnectivity of pores.

   - Only limited studies have been conducted in terms of the effect of vapor temperature to the membrane formation. Further investigation is required to understand the effect of vapor temperature.

7) The VIPS method has a high potential to be applied in water and wastewater treatment applications (MF, UF, NF, DCMD), gas separation, medical and biological applications as well as for secondary batteries application. Membrane applications are expanding in the new arena, including applications such as membrane condenser, membrane crystallizer, etc. The potential of the membrane fabricated *via* VIPS in the new area is an interesting research direction.

Even though the application of the VIPS process enables better ability to control the membrane morphology than other methods, it has only been tested in lab-scale. It is worthwhile to consider the possibility of any defects such as polymer aggregation during the scale-up process. Hence, the continuous effort will be a need for controlling the membrane structure without neglecting the conditions during larger scale manufacturing.

On the other hand, the viewpoint of antifouling VIPS membranes design should be emphasized. We hope to have demonstrated that VIPS definitely is a viable option to prepare bi-continuous antifouling membranes, either PEG-based or zwitterionic-based. Nonetheless, a number of improvements can be made concerning our understanding of membrane formation as well as material design, as listed below:

- The tricky question is how the antifouling copolymer migrates during the membrane formation, Until today, this remains unexplored and unanswered, to the best of our knowledge. No in-depth study presenting with accuracy the concentration distribution of the polymer/copolymer forming an antifouling membrane has yet been presented. Membranologists rely on surface segregation since this phenomenon was reported and proven that the concentration of antifouling moieties of a membrane formed by NIPS was much larger at the surface than in the initial casting solution [313]. So, there is clearly room for more investigations on the formation mechanisms of antifouling membranes by VIPS.

- Other than the zwitterionic systems and pseudo-zwitterionic materials, introduced about 10 years ago by Prof. Jiang and his group [314], which are materials formed of an equal amount of positively-charged moieties and negatively-charged moieties, have not been incorporated in VIPS membranes. The major advantage of these material systems is the control of the charge bias from the molar composition of each charged brush. Surely, if one wants to design antifouling membranes resisting any type of biofoulant, then a zero charge is better and they might as well use PEG-based or zwitterionic-based copolymer. But one can also play with the surface charge to achieve controlled biofouling of membranes. Leukodepletion relying on controlled chemical interactions with white blood cells could be a potential application of such membranes, but it has only been achieved with surface-modified membranes [315] and never with *in-situ* modified membranes. So, work could be done with these pseudo-zwitterionic materials, starting with putting effort on the improvement of the solubility of mixed-charge polymers with hydrophobic membrane polymers.

### Declaration of competing interest

The authors declare that they have no known competing financial interests or personal relationships that could have appeared to influence the work reported in this paper.

**Abbreviations**

| | |
|---|---|
| AA | acetic acid |
| ABPBI | poly(2,5-benzimidazole) |
| BPPO | brominated polyphenylene oxide |
| BSA | bovine serum albumin |
| CN | cellulose nitrate |
| CPVC | chlorinated poly(vinyl chloride) |
| DCMD | direct contact membrane distillation |
| DGDE | diethylene glycol dimethyl ether |
| DI | deionized water |
| DMAC | dimethylacetamide |
| DMF | dimethylformamide |
| EIPS | evaporation induced phase separation |
| ELISA | enzyme-linked immunosorbent assay |
| GO | graphene oxide |
| L-L | liquid-liquid |
| LIPS | liquid induced phase separation |
| MD | membrane distillation |
| MF | microfiltration |
| MPC | 2-methacryloyloxyethyl phosphorylcholine |
| n-BA | N-bromoacetamide |
| NF | nanofiltration |
| NIPS | nonsolvent induced phase separation |
| NMP | N-methyl-2-pyrrolidone |
| PAA | poly(acrylic acid) |
| PBI | polybenzimidazole |
| PDMS | polydimethylsiloxane |
| PEEKWC | modified poly(ether ether ketone) |
| PEG | poly(ethylene glycol) |
| PEGMA | poly(ethylene glycol) methacrylate |
| PEGMA-*b*-PS-*b*-PEGMA | poly(ethylene glycol) methacrylate-*block*-polystyerene-*block*-poly(ethylene glycol) methacrylate |
| PEI | polyetherimide |
| PEO | poly(ethylene oxide) |
| PEO-*b*-PPO-*b*-PEO | poly(ethylene oxide)-*block*-poly(propylene oxide)-*block*-poly(ethylene oxide) |
| PES | polyethersulfone |
| Plu | pluronic |
| PMBU | poly(2-methacryloyloxyethyl phosphorylcholine-*co*-methacryloyloxyethyl butylurethane) |
| PMMA | poly(methyl methacrylate) |
| PNIPAm | poly(N-isopropylacrylamide) |
| PPO | poly(propylene oxide) |
| PSBMA | poly(sulfobetaine methacrylate) |
| PS-*b*-PEGMA | polystyerene-*block*-poly (ethylene glycol) methacrylate |
| PSf | polysulfone |
| PS | polystyrene |
| PS-*r*-PEGMA | polystyerene-*random*-poly(ethylene glycol) methacrylate |
| PS-*r*-PEGMA-*r*-PSBMA | polystyerene-*random*-poly(ethylene glycol) methacrylate *random*-poly(sulfobetaine methacrylate) |
| PVC | polyvinylchloride |
| PVDF | poly (vinylidene fluoride) |
| PVP | polyvinylpyrrolidone |
| RH | relative humidity |
| SEM | scanning electron microscopy |
| TEG | triethylene glycol |
| TEP | triethylene phosphate |
| THF | tetrahydrofuran |
| $TiO_2$ | titanium dioxide |
| TIPS | thermal induced phase separation |
| TMP | transmembrane pressure |
| UF | ultrafiltration |
| VFB | vanadium flow batteries |

| | |
|---|---|
| VIPS | vapor induced phase separation |
| VNIPS | vapor nonsolvent induced phase separation |
| WCA | water contact angle |
| 2P | 2-pyrrolidinone |
| 2-ME | 2-methoxyethanol |

*Nomenclature*

| | |
|---|---|
| $n_i$ | moles of component i |
| $\varphi_i$ | volume fraction of component i |
| $g_{ij}$ | the interaction parameters of component i and j |
| T | temperature |
| R | constant of perfect gases |
| $\Delta\mu_i$ | chemical potential difference of component i |
| $\Delta G_m^t$ | Gibbs free energy of mixing per unit volume |
| $v_1$ | molar volume of component |
| $\mu_u^c$ | chemical potential of polymer repeating unit |
| $\mu_u^0$ | chemical potential of polymer repeating unit in the standard state |
| $\Delta H_u$ | heat of fusion of the polymer repeating unit |
| $T_m^0$ | melting point of pure polymer |
| $v_u$ | molar volume per repeating unit in the polymer |
| r | $v_1/v_3$ |
| s | $v_1/v_2$ |
| $\nabla\mu_i$ | chemical potential gradient of component i |
| $c_j$ | molar concentration of j |
| $\varepsilon_{ij}$ | friction coefficient between molecules i and j |
| $v_i$ | velocity of the ith component |
| Di | self-diffusion coefficient of i |
| NA | Avogadro number |
| E | Energy required to overcome attractive forces from neighboring molecules (J/mol) |
| $\Phi$ | association factor |
| Lc | characterisctic length of the cast film surface |
| yair,lm | logarithm mean mole fraction difference of air |
| Dig | mutual diffusion coefficient of component i in the gas phase |
| ρg | total mass density of the gas phase |
| μg | viscosity of the gas |
| g | gravity constant |
| τi | $-(1/\rho g)(\partial\rho g/\partial yig)P,T$ |
| ρ | density |
| $C_p$ | heat capacity |
| H | thickness |
| T | solution temperature |
| $T_g$ | bulk temperature in the gas phase |
| $J_{ig}$ | mass flux in the gas phase |
| $\Delta H_{vi}$ | vaporization enthalpy |
| $h_{up}$ | heat transfer coefficient above of the system |
| $h_{down}$ | heat transfer coefficient below of the system |
| $K^G$ | air thermal conductivity |
| Pr | Prandtl number |
| $T^G$ | air temperature |
| δ | Polymer-solvent affinity |
| δsp | Solubility parameter |
| δd | Dispersion force |
| δp | Polar force |
| $\delta_H$ | Hydrogen bond force |

## References

[1] Jimmy L. Humphrey, G.E. Keller, Separation Process Technology (Builder's Guide, McGraw-Hill, 1997.

[2] A. Figoli, T. Marino, S. Simone, E. Di Nicolò, X.M. Li, T. He, S. Tornaghi, E. Drioli, Towards non-toxic solvents for membrane preparation: a review, Green Chem. 16 (2014) 4034–4059.

[3] J.F. Kim, G. Székely, I.B. Valtcheva, A.G. Livingston, Increasing the sustainability of membrane processes through cascade approach and solvent recovery—pharmaceutical purification case study, Green Chem. 16 (2014) 133–145.

[4] S. Mansur, M.H.D. Othman, A.F. Ismail, S.H.S.A. Kadir, P.S. Goh, H. Hasbullah, B. C. Ng, M.S. Abdullah, F. Kamal, M.N.Z. Abidin, R.A. Lusiana, Synthesis and characterisation of composite sulphonated polyurethane/polyethersulphone membrane for blood purification application, Mater. Sci. Eng. C 99 (2019) 491–504.

[5] D.F. Stamatialis, B.J. Papenburg, M. Gironés, S. Saiful, S.N.M. Bettahalli, S. Schmitmeier, M. Wessling, Medical applications of membranes: drug delivery, artificial organs and tissue engineering, J. Membr. Sci. 308 (2008) 1–34.

[6] P.S. Goh, T. Matsuura, A.F. Ismail, N. Hilal, Recent trends in membranes and membrane processes for desalination, Desalination 391 (2016) 43–60.

[7] Z. Yang, X.-H. Ma, C.Y. Tang, Recent development of novel membranes for desalination, Desalination 434 (2018) 37–59.

[8] G. G, A. G, I. Af, Perspective of renewable desalination by using membrane distillation, Chem. Eng. Res. Des. 144 (2019) 520–537.

[9] W. Pronk, A. Ding, E. Morgenroth, N. Derlon, P. Desmond, M. Burkhardt, B. Wu, A.G. Fane, Gravity-driven membrane filtration for water and wastewater treatment: a review, Water Res. 149 (2019) 553–565.

[10] M. Gündoğdu, Y.A. Jarma, N. Kabay, T.Ö. Pek, M. Yüksel, Integration of MBR with NF/RO processes for industrial wastewater reclamation and water reuse-effect of membrane type on product water quality, J. Water Process Eng. 29 (2019) 100574.

[11] S. Kim, K.H. Chu, Y.A.J. Al-Hamadani, C.M. Park, M. Jang, D.-H. Kim, M. Yu, J. Heo, Y. Yoon, Removal of contaminants of emerging concern by membranes in water and wastewater: a review, Chem. Eng. J. 335 (2018) 896–914.

[12] J. Ma, R. Dai, M. Chen, S.J. Khan, Z. Wang, Applications of membrane bioreactors for water reclamation: micropollutant removal, mechanisms and perspectives, Bioresour. Technol. 269 (2018) 532–543.

[13] D. Im, N. Nakada, Y. Fukuma, Y. Kato, H. Tanaka, Performance of combined ozonation, coagulation and ceramic membrane process for water reclamation: effects and mechanism of ozonation on virus coagulation, Separ. Purif. Technol. 192 (2018) 429–434.

[14] Q. Li, L.-J. Beier, J. Tan, C. Brown, B. Lian, W. Zhong, Y. Wang, C. Ji, P. Dai, T. Li, P. Le Clech, H. Tyagi, X. Liu, G. Leslie, R.A. Taylor, An integrated, solar-driven membrane distillation system for water purification and energy generation, Appl. Energy 237 (2019) 534–548.

[15] L. Zhang, Y. Ding, C. Zhang, Y. Zhou, X. Zhou, Z. Liu, G. Yu, Enabling graphene-oxide-based membranes for large-scale energy storage by controlling hydrophilic microstructures, Chem 4 (2018) 1035–1046.

[16] D. Wang, Z. Liu, S. Zhang, X. Tian, Y. Li, Investigation of heat and mass transfer characteristics during energy discharge in an energy storage unit using hollow fiber membranes, Int. J. Heat Mass Transf. 117 (2018) 559–570.

[17] Y.A. Hugo, W. Kout, F. Sikkema, Z. Borneman, K. Nijmeijer, Performance mapping of cation exchange membranes for hydrogen-bromine flow batteries for energy storage, J. Membr. Sci. 566 (2018) 406–414.

[18] J. Xu, H. Wu, Z. Wang, Z. Qiao, S. Zhao, J. Wang, Recent advances on the membrane processes for CO2 separation, Chin. J. Chem. Eng. 26 (2018) 2280–2291.

[19] Y. Han, W.S.W. Ho, Recent advances in polymeric membranes for CO2 capture, Chin. J. Chem. Eng. 26 (2018) 2238–2254.

[20] U.W.R. Siagian, A. Raksajati, N.F. Himma, K. Khoiruddin, I.G. Wenten, Membrane-based carbon capture technologies: membrane gas separation vs. Membrane contactor, J. Nat. Gas Sci. Eng. 67 (2019) 172–195.

[21] A. Huang, L.-H. Chen, C.-H. Chen, H.-Y. Tsai, K.-L. Tung, Carbon dioxide capture using an omniphobic membrane for a gas-liquid contacting process, J. Membr. Sci. 556 (2018) 227–237.

[22] Y. Wu, D. Zhao, J. Ren, Y. Qiu, M. Deng, A novel Pebax-C60(OH)24/PAN thin film composite membrane for carbon dioxide capture, Separ. Purif. Technol. 215 (2019) 480–489.

[23] K.K. Sirkar, A.G. Fane, R. Wang, S.R. Wickramasinghe, Process intensification with selected membrane processes, Chem. Eng. Process: Process Intensif. 87 (2015) 16–25.

[24] P. Pal, R. Kumar, A.K. Ghosh, Analysis of process intensification and performance assessment for fermentative continuous production of bioethanol in a multi-staged membrane-integrated bioreactor system, Energy Convers. Manag. 171 (2018) 371–383.

[25] S. Shukla, J.P. Méricq, M.P. Belleville, N. Hengl, N.E. Benes, I. Vankelecom, J. Sanchez Marcano, Process intensification by coupling the Joule effect with pervaporation and sweeping gas membrane distillation, J. Membr. Sci. 545 (2018) 150–157.

[26] O. Iglesias, M.J. Rivero, A.M. Urtiaga, I. Ortiz, Membrane-based photocatalytic systems for process intensification, Chem. Eng. J. 305 (2016) 136–148.

[27] K.J. Lu, Z.L. Cheng, J. Chang, L. Luo, T.-S. Chung, Design of zero liquid discharge desalination (ZLDD) systems consisting of freeze desalination, membrane distillation, and crystallization powered by green energies, Desalination 458 (2019) 66–75.

[28] R. Schwantes, K. Chavan, D. Winter, C. Felsmann, J. Pfafferott, Techno-economic comparison of membrane distillation and MVC in a zero liquid discharge application, Desalination 428 (2018) 50–68.

[29] S.G.J. Heijman, H. Guo, S. Li, J.C. van Dijk, L.P. Wessels, Zero liquid discharge: heading for 99% recovery in nanofiltration and reverse osmosis, Desalination 236 (2009) 357–362.

[30] M. Ulbricht, Advanced functional polymer membranes, Polymer 47 (2006) 2217–2262.

[31] H.A. Tsai, C.Y. Kuo, J.H. Lin, D.M. Wang, A. Deratani, C. Pochat-Bohatier, K. R. Lee, J.Y. Lai, Morphology control of polysulfone hollow fiber membranes via water vapor induced phase separation, J. Membr. Sci. 278 (2006) 390–400.

[32] Z. Cui, N.T. Hassankiadeh, S.Y. Lee, J.M. Lee, K.T. Woo, A. Sanguineti, V. Arcella, Y.M. Lee, E. Drioli, Poly(vinylidene fluoride) membrane preparation with an environmental diluent via thermally induced phase separation, J. Membr. Sci. 444 (2013) 223–236.

[33] N.T. Hassankiadeh, Z. Cui, J.H. Kim, D.W. Shin, A. Sanguineti, V. Arcella, Y. M. Lee, E. Drioli, PVDF hollow fiber membranes prepared from green diluent via thermally induced phase separation: effect of PVDF molecular weight, J. Membr. Sci. 471 (2014) 237–246.

[34] Z. Cui, N.T. Hassankiadeh, S.Y. Lee, K.T. Woo, J.M. Lee, A. Sanguineti, V. Arcella, Y.M. Lee, E. Drioli, Tailoring novel fibrillar morphologies in poly(vinylidene

[35] N.T. Hassankiadeh, Z. Cui, J.H. Kim, D.W. Shin, S.Y. Lee, A. Sanguineti, V. Arcella, Y.M. Lee, E. Drioli, Microporous poly(vinylidene fluoride) hollow fiber membranes fabricated with polar clean as water-soluble green diluent and additives, J. Membr. Sci. 479 (2015) 204–212.

[36] K. Xu, Y. Cai, N.T. Hassankiadeh, Y. Cheng, X. Li, X. Wang, Z. Wang, E. Drioli, Z. Cui, ECTFE membrane fabrication via TIPS method using ATBC diluent for vacuum membrane distillation, Desalination 456 (2019) 13–22.

[37] M.C. Nayak, A.M. Isloor, A. Moslehyani, N. Ismail, A.F. Ismail, Fabrication of novel PPSU/ZSM-5 ultrafiltration hollow fiber membranes for separation of proteins and hazardous reactive dyes, J. Taiwan Inst. Chem. Eng. 82 (2018) 342–350.

[38] M.C. Nayak, A.M. Isloor, Inamuddin, B. Prabhu, N.A.F. Ismail, A.M. Asiri, Novel PPSU/nano Tin Oxide Mixed Matrix Ultrafiltration Hollow Fiber Membranes: Fabrication, Characterization and Toxic Dyes Removal from Aqueous Solutions, Reactive and Functional Polymers, 2019.

[39] M. Kumar, S. RaoT, A.M. Isloor, G.P.S. Ibrahim, Inamuddin, N. Ismail, A.F. Ismail, A.M. Asiri, Use of cellulose acetate/polyphenylsulfone derivatives to fabricate ultrafiltration hollow fiber membranes for the removal of arsenic from drinking water, Int. J. Biol. Macromol. 129 (2019) 715–727.

[40] L. Zheng, Z. Ma, Z. Li, Q. Yan, Rapid nanostructuration of polymer colloid surfaces by nonsolvent induced phase separation, J. Colloid Interface Sci. 441 (2015) 39–45.

[41] T. Zha, L. Song, P. Chen, W. Nie, Y. Zhou, Nonsolvent/solvent-induced phase separation to multi-porous sulfonated polystyrene/chitosan/silver particles and their application in adsorbing chromium ion(III) and reduction of methylene blue, Colloid. Surf. Physicochem. Eng. Asp. 481 (2015) 423–430.

[42] C. Yen, H. He, L.J. Lee, W.S.W. Ho, Synthesis and characterization of nanoporous polycaprolactone membranes via thermally- and nonsolvent-induced phase separations for biomedical device application, J. Membr. Sci. 343 (2009) 180–188.

[43] H.H. Wang, J.T. Jung, J.F. Kim, S. Kim, E. Drioli, Y.M. Lee, A novel green solvent alternative for polymeric membrane preparation via nonsolvent-induced phase separation (NIPS), J. Membr. Sci. 574 (2019) 44–54.

[44] D.-M. Wang, J.-Y. Lai, Recent advances in preparation and morphology control of polymeric membranes formed by nonsolvent induced phase separation, Curr. Opin. Chem. Eng. 2 (2013) 229–237.

[45] H. Minbu, A. Ochiai, T. Kawase, M. Taniguchi, D.R. Lloyd, T. Tanaka, Preparation of poly(L-lactic acid) microfiltration membranes by a nonsolvent-induced phase separation method with the aid of surfactants, J. Membr. Sci. 479 (2015) 85–94.

[46] H.-h. Lin, Y.-h. Tang, H. Matsuyama, X.-l. Wang, Dissipative particle dynamics simulation on the membrane formation of polymer–solvent system via nonsolvent induced phase separation, J. Membr. Sci. 548 (2018) 288–297.

[47] Y.H. Cho, S.D. Kim, J.F. Kim, H.-g. Choi, Y. Kim, S.-E. Nam, Y.-I. Park, H. Park, Tailoring the porous structure of hollow fiber membranes for osmotic power generation applications via thermally assisted nonsolvent induced phase separation, J. Membr. Sci. 579 (2019) 329–341.

[48] L. Brockway, L. Berryman, H. Taylor, Nonsolvent-induced phase separation synthesis of superhydrophobic coatings composed of polyvinylidene difluoride microspheres with tunable size and roughness, Prog. Org. Coat. 119 (2018) 230–238.

[49] T.V. Plisko, A.V. Penkova, K.S. Burts, A.V. Bildyukevich, M.E. Dmitrenko, G. B. Melnikova, R.R. Atta, A.S. Mazur, A.A. Zolotarev, A.B. Missyul, Effect of Pluronic F127 on porous and dense membrane structure formation via non-solvent induced and evaporation induced phase separation, J. Membr. Sci. 580 (2019) 336–349.

[50] A.A.S. Gonçalves, M. Jaroniec, Evaporation-induced self-assembly synthesis of nanostructured alumina-based mixed metal oxides with tailored porosity, J. Colloid Interface Sci. 537 (2019) 725–735.

[51] D. Pan, W. Chen, X. Huang, J. Zhang, Y. Yang, F. Yu, S. Chen, B. Fan, X. Shi, X. Cui, R. Li, C. Yu, Solvothermal-assisted evaporation-induced self-assembly of ordered mesoporous alumina with improved performance, J. Colloid Interface Sci. 529 (2018) 432–443.

[52] A.Z. Samuel, A. Umapathy, S. Ramakrishnan, Functionalized and postfunctionalizable porous polymeric films through evaporation-induced phase separation using mixed solvents, ACS Appl. Mater. Interfaces 3 (2011) 3293–3299.

[53] M. Yamamura, T. Nishio, T. Kajiwara, K. Adachi, Evaporation-induced pattern formation in polymer films via secondary phase separation, Chem. Eng. Sci. 57 (2002) 2901–2905.

[54] Q. Zhang, M. Xu, X. Liu, W. Zhao, C. Zong, Y. Yu, Q. Wang, H. Gai, Fabrication of Janus droplets by evaporation driven liquid–liquid phase separation, Chem. Commun. 52 (2016) 5015–5018.

[55] X. Wang, D. Liu, W. Li, Q. Tian, X. Zhou, Microencapsulation of cholesteric liquid crystal by combined method of solvent evaporation and photopolymerization, Mol. Cryst. Liq. Cryst. 571 (2013) 57–66.

[56] C. Stegelmeier, A. Exner, S. Hauschild, V. Filiz, J. Perlich, S.V. Roth, V. Abetz, S. Förster, Evaporation-induced block copolymer self-assembly into membranes studied by in situ synchrotron SAXS, Macromolecules 48 (2015) 1524–1530.

[57] R. Zsigmondy, W.Z. Bachmann, Uber neue filter, Anorg. U. Allgem. Chem 103 (1918) 119–128.

[58] W.J. Elford, Principles governing the preparation of membranes having graded porosities. The properties of "GRADOCOL" membranes as ultrafilters, Trans. Faraday Soc. 33 (1937) 1094–1104.

[59] H.C. Park, Y.P. Kim, H.Y. Kim, Y.S. Kang, Membrane formation by water vapor induced phase inversion, J. Membr. Sci. 156 (1999) 169–178.

[60] Q. Zhao, R. Xie, F. Luo, Y. Faraj, Z. Liu, X.-J. Ju, W. Wang, L.-Y. Chu, Preparation of high strength poly(vinylidene fluoride) porous membranes with cellular structure via vapor-induced phase separation, J. Membr. Sci. 549 (2018) 151–164.

[61] P. Menut, Y.S. Su, W. Chinpa, C. Pochat-Bohatier, A. Deratani, D.M. Wang, P. Huguet, C.Y. Kuo, J.Y. Lai, C. Dupuy, A top surface liquid layer during membrane formation using vapor-induced phase separation (VIPS)—evidence and mechanism of formation, J. Membr. Sci. 310 (2008) 278–288.

[62] N. Zhao, Q. Xie, L. Weng, S. Wang, X. Zhang, J. Xu, Superhydrophobic surface from vapor-induced phase separation of copolymer micellar solution, Macromolecules 38 (2005) 8996–8999.

[63] Y. Peng, Y. Dong, H. Fan, P. Chen, Z. Li, Q. Jiang, Preparation of polysulfone membranes via vapor-induced phase separation and simulation of direct-contact membrane distillation by measuring hydrophobic layer thickness, Desalination 316 (2013) 53–66.

[64] W. Albrecht, K. Kneifel, T. Weigel, R. Hilke, R. Just, M. Schossig, K. Ebert, A. Lendlein, Preparation of highly asymmetric hollow fiber membranes from poly (ether imide) by a modified dry–wet phase inversion technique using a triple spinneret, J. Membr. Sci. 262 (2005) 69–80.

[65] H.J. Lee, B. Jung, Y.S. Kang, H. Lee, Phase separation of polymer casting solution by nonsolvent vapor, J. Membr. Sci. 245 (2004) 103–112.

[66] A. Ripoche, P. Menut, C. Dupuy, H. Caquineau, A. Deratani, Poly(ether imide) membrnae formation by water vapour induced phase inversion, Macromol. Symp. 188 (2002) 37–48.

[67] P.v.d. Witte, P.J. Dijkstra, J.W.A.v.d. Berg, J. Feijen, Phase separation processes in polymer solutions in relation to membrane formation, J. Membr. Sci. 117 (1996) 1–31.

[68] H. Chae Park, Y. Po Kim, H. Yong Kim, Y. Soo Kang, Membrane formation by water vapor induced phase inversion, J. Membr. Sci. 156 (1999) 169–178.

[69] T.-H. Young, Y.-H. Huang, Y.-S. Huang, The formation mechanism of EVAL membranes prepared with or without the nonsolvent absorption process, J. Membr. Sci. 171 (2000) 197–206.

[70] N. Zhao, J. Xu, Q. Xie, L. Weng, X. Guo, X. Zhang, L. Shi, Fabrication of biomimetic superhydrophobic coating with a micro-nano-binary structure, Macromol. Rapid Commun. 26 (2005) 1075–1080.

[71] H. Susanto, N. Stahra, M. Ulbricht, High performance polyethersulfone microfiltration membranes having high flux and stable hydrophilic property, J. Membr. Sci. 342 (2009) 153–164.

[72] C.-L. Li, D.-M. Wang, A. Deratani, D. Quémener, D. Bouyere, J.-Y. Lai, Insight into the preparation of poly(vinylidene fluoride) membranes by vapor-induced phase separation, J. Membr. Sci. 361 (2010) 154–166.

[73] Y. Peng, H. Fan, Y. Dong, Y. Song, H. Han, Effects of exposure time on variations in the structure and hydrophobicity of polyvinylidene fluoride membranes prepared via vapor-induced phase separation, Appl. Surf. Sci. 258 (2012) 7872–7881.

[74] A. Venault, Y. Chang, D.-M. Wang, J.-Y. Lai, Surface anti-biofouling control of PEGylated poly(vinylidene fluoride) membranes via vapor-induced phase separation processing, J. Membr. Sci. 423–424 (2012) 53–64.

[75] N. Zhao, Q. Xie, L. Weng, S. Wang, X. Zhang, J. Xu, Superhydrophobic surface from vapor-induced phase separation of copolymer micellar solution, Macromolecules 38 (2005) 8996–8999.

[76] Y. Peng, H. Fan, Y. Dong, Y. Song, H. Han, Effects of exposure time on variations in the structure and hydrophobicity of polyvinylidene fluoride membranes prepared via vapor-induced phase separation, Appl. Surf. Sci. 258 (2012) 7872–7881.

[77] A. Venault, YungChang, Da-MingWang, Juin-YihLai, Surface anti-biofouling control of PEGylated poly(vinylidenefluoride) membranes via vapor-induced phase separation processing, J. Membr. Sci. 423 (2012) 53–64.

[78] C. Meringolo, T.F. Mastropietro, T. Poerio, E. Fontananova, G. De Filpo, E. Curcio, G. Di Profio, Tailoring PVDF membranes surface topography and hydrophobicity by a sustainable two-steps phase separation process, ACS Sustain. Chem. Eng. 6 (2018) 10069–10077.

[79] H. Caquineau, P. Menut, A. Deratan, C. Dupuy, Influence of the relative humidity on film formation by vapor induced phase separation, Polym. Eng. Sci. 43 (2003) 798–808.

[80] D. Bouyer, W. Werapun, C. Pochat-Bohatier, A. Deratani, Morphological properties of membranes fabricated by VIPS process using PEI/NMP/water system: SEM analysis and mass transfer modelling, J. Membr. Sci. 349 (2010) 97–112.

[81] P. Menut, Y.S. Su, W. Chinpa, C. Pochat-Bohatier, A. Deratani, D.M. Wang, P. Huguet, C.Y. Kuo, J.Y. Lai, C. Dupuy, A top surface liquid layer during membrane formation using vapor-induced phase separation (VIPS)—evidence and mechanism of formation, J. Membr. Sci. 310 (2008) 278–288.

[82] D. Bouyer, W. Werapun, C. Pochat-Bohatier, A. Deratani, Morphological properties of membranes fabricated by VIPS process using PEI/NMP/water system: SEM analysis and mass transfer modelling, J. Membr. Sci. 349 (2010) 97–112.

[83] Y.S. Su, C.Y. Kuo, D.M. Wang, J.Y. Lai, A. Deratanid, C. Pochate, D. Bouyere, Interplay of mass transfer, phase separation, and membrane morphology in vapor-induced phase separation, J. Membr. Sci. 338 (2009) 17–28.

[84] X. Rui, L. Feng, Z. Lei, G. Shi-Fei, L. Zhuang, J. Xiao-Jie, W. Wei, C. Liang-Yin, A novel thermoresponsive catalytic membrane with multiscale pores prepared via vapor-induced phase separation, Small 14 (2018) 1703650.

[85] J.S. Kang, S.H. Lee, H. Huh, J.K. Shim, Y.M. Lee, Preparation of chlorinated poly (vinyl chloride)-g-Poly(Nvinyl-2-pyrrolidinone) membranes and their water permeation properties, J. Appl. Polym. Sci. 88 (2003) 3188–3195.

[86] J.S. Kang, K.Y. Kim, Y.M. Lee, Preparation of microporous chlorinated poly(vinyl chloride) membrane in fabric and the characterization of their pore sizes and pore-size distributions, J. Appl. Polym. Sci. 86 (2002) 1195–1202.

[87] J.T. Tsai, Y.S. Su, D.M. Wang, J.L. Kuo, J.Y. Lai, A. Deratani, Retainment of pore connectivity in membranes prepared with vapor-induced phase separation, J. Membr. Sci. 362 (2010) 360–373.

[88] V.P. Khare, A.R. Greenberg, W.B. Krantz, Vapor-induced phase separation—effect of the humid air exposure step on membrane morphology: Part I. Insights from mathematical modeling, J. Membr. Sci. 258 (2005) 140–156.

[89] Y.S. Su, C.Y. Kuo, D.M. Wang, J.Y. Lai, A. Deratani, C. Pochat, D. Bouyer, Interplay of mass transfer, phase separation, and membrane morphology in vapor-induced phase separation, J. Membr. Sci. 338 (2009) 17–28.

[90] N. Harruddin, S.M. Saufi, C.K.M. Faizal, A.W. Mohammad, Effect of VIPS fabrication parameters on the removal of acetic acid by supported liquid membrane using a PES–graphene membrane support, RSC Adv. 8 (2018) 25396–25408.

[91] I.-C. Kim, K.-H. Lee, Effect of poly(ethylene glycol) 200 on the formation of a polyetherimide asymmetric membrane and its performance in aqueous solvent mixture permeation, J. Membr. Sci. 230 (2004) 183–188.

[92] D.R. Lloyd, K.E. Kinzer, H. Tseng, Microporous membrane formation via thermally induced phase separation. I. Solid-liquid phase separation, J. Membr. Sci. 52 (1990) 239–261.

[93] D.R. Lloyd, S.S. Kim, K.E. Kinzer, Microporous membrane formation via thermally-induced phase separation. II. Liquid—liquid phase separation, J. Membr. Sci. 64 (1991) 1–11.

[94] S.S. Kim, D.R. Lloyd, Microporous membrane formation via thermally-induced phase separation. III. Effect of thermodynamic interactions on the structure of isotactic polypropylene membranes, J. Membr. Sci. 64 (1991) 13–29.

[95] G.B. Lim, S.S. Kim, Q. Ye, Y.F. Wang, D.R. Lloyd, Microporous membrane formation via thermally-induced phase separation. IV. Effect of isotactic polypropylene crystallization kinetics on membrane structure, J. Membr. Sci. 64 (1991) 31–40.

[96] S.S. Kim, G.B.A. Lim, A.A. Alwattari, Y.F. Wang, D.R. Lloyd, Microporous membrane formation via thermally-induced phase separation. V. Effect of diluent mobility and crystallization on the structure of isotactic polypropylene membranes, J. Membr. Sci. 64 (1991) 41–53.

[97] A.A. Alwattari, D.R. Lloyd, Microporous membrane formation via thermally-induced phase separation. VI. Effect of diluent morphology and relative crystallization kinetics on polypropylene membrane structure, J. Membr. Sci. 64 (1991) 55–67.

[98] K.s. McGuire, D.R. Lloyd, G.B.A. Lim, Microporous membrane formation via thermally-induced phase separation. VII. Effect of dilution, cooling rate, and nucleating agent addition on morphology, J. Membr. Sci. 79 (1993) 27–34.

[99] A. Laxminarayan, K.S. McGuire, S.S. Kim, D.R. Lloyd, Effect of initial composition, phase separation temperature and polymer crystallization on the formation of microcellular structures via thermally induced phase separation, Polymer 35 (1994) 3060–3068.

[100] K.S. McGuire, A. Laxminarayan, D.R. Lloyd, A simple method of extrapolating the coexistence curve and predicting the melting point depression curve from cloud point data for polymer-diluent systems, Polymer 35 (1994) 4404–4407.

[101] S.-W. Song, J.M. Torkelson, Coarsening effects on microstructure formation in isopycnic polymer solutions and membranes produced via thermally induced phase separation, Macromolecules 27 (1994) 6389–6397.

[102] B.J. Cha, K. Char, J.J. Kim, S.S. Kim, C.K. Kim, The effects of diluent molecular weight on the structure of thermally-induced phase separation membrane, J. Membr. Sci. 108 (1995) 219–229.

[103] S.-W. Song, J.M. Torkelson, Coarsening effects on the formation of microporous membranes produced via thermally induced phase separation of polystyrene-cyclohexanol solutions, J. Membr. Sci. 98 (1995) 209–222.

[104] S. Berghmans, H. Berghmans, H.E.H. Meijer, Spinning of hollow porous fibres via the TIPS mechanism, J. Membr. Sci. 116 (1996) 171–189.

[105] K.S. McGuire, A. Laxminarayan, D.S. Martula, D.R. Lloyd, Kinetics of droplet growth in liquid–liquid phase separation of polymer–diluent systems: model development, J. Colloid Interface Sci. 182 (1996) 46–58.

[106] M.R. Caplan, C.-Y. Chiang, D.R. Lloyd, L.Y. Yen, Formation of microporous Teflon® PFA membranes via thermally induced phase separation, J. Membr. Sci. 130 (1997) 219–237.

[107] H. Matsuyama, M. Yuasa, Y. Kitamura, M. Teramoto, D.R. Lloyd, Structure control of anisotropic and asymmetric polypropylene membrane prepared by thermally induced phase separation, J. Membr. Sci. 179 (2000) 91–100.

[108] H. Sun, K.B. Rhee, T. Kitano, S.I. Mah, HDPE hollow-fiber membrane via thermally induced phase separation. II. Factors affecting the water permeability of the membrane, J. Appl. Polym. Sci. 75 (2000) 1235–1242.

[109] H. Matsuyama, T. Maki, M. Teramoto, K. Asano, Effect of polypropylene molecular weight on porous membrane formation by thermally induced phase separation, J. Membr. Sci. 204 (2002) 323–328.

[110] M. Shang, H. Matsuyama, M. Teramoto, D.R. Lloyd, N. Kubota, Preparation and membrane performance of poly(ethylene-co-vinyl alcohol) hollow fiber membrane via thermally induced phase separation, Polymer 44 (2003) 7441–7447.

[111] H. Matsuyama, H. Okafuji, T. Maki, M. Teramoto, N. Kubota, Preparation of polyethylene hollow fiber membrane via thermally induced phase separation, J. Membr. Sci. 223 (2003) 119–126.

[112] W. Yave, R. Quijada, M. Ulbricht, R. Benavente, Syndiotactic polypropylene as potential material for the preparation of porous membranes via thermally induced phase separation (TIPS) process, Polymer 46 (2005) 11582–11590.

[113] W. Yave, R. Quijada, D. Serafini, D.R. Lloyd, Effect of the polypropylene type on polymer–diluent phase diagrams and membrane structure in membranes formed via the TIPS process: Part II. Syndiotactic and isotactic polypropylenes produced using metallocene catalysts, J. Membr. Sci. 263 (2005) 154–159.

[114] X. Fu, H. Matsuyama, M. Teramoto, H. Nagai, Preparation of hydrophilic poly (vinyl butyral) hollow fiber membrane via thermally induced phase separation, Separ. Purif. Technol. 45 (2005) 200–207.

[115] Z. Yang, P. Li, L. Xie, Z. Wang, S.-C. Wang, Preparation of iPP hollow-fiber microporous membranes via thermally induced phase separation with co-solvents of DBP and DOP, Desalination 192 (2006) 168–181.

[116] Z. Yang, P. Li, H. Chang, S. Wang, Effect of diluent on the morphology and performance of IPP hollow fiber microporous membrane via thermally induced phase Separation 1 1 Supported by the national natural science foundation of China (No.20236030), Chin. J. Chem. Eng. 14 (2006) 394–397.

[117] X. Fu, H. Matsuyama, M. Teramoto, H. Nagai, Preparation of polymer blend hollow fiber membrane via thermally induced phase separation, Separ. Purif. Technol. 52 (2006) 363–371.

[118] M. Gu, J. Zhang, X. Wang, W. Ma, Crystallization behavior of PVDF in PVDF-DMP system via thermally induced phase separation, J. Appl. Polym. Sci. 102 (2006) 3714–3719.

[119] Y. Su, C. Chen, Y. Li, J. Li, Preparation of PVDF membranes via TIPS method: the effect of mixed diluents on membrane structure and mechanical property, J. Macromol. Sci., Part A 44 (2007) 305–313.

[120] Y. Su, C. Chen, Y. Li, J. Li, PVDF membrane formation via thermally induced phase separation, J. Macromol. Sci., Part A 44 (2007) 99–104.

[121] B. Luo, Z. Li, J. Zhang, X. Wang, Formation of anisotropic microporous isotactic polypropylene (iPP) membrane via thermally induced phase separation, Desalination 233 (2008) 19–31.

[122] G.-l. Ji, L.-p. Zhu, B.-k. Zhu, Y.-y. Xu, Effect of diluents on crystallization of poly (vinylidene fluoride) and phase separated structure in a ternary system via thermally induced phase separation, Chin. J. Polym. Sci. 26 (2008) 291–298.

[123] G.-L. Ji, L.-P. Zhu, B.-K. Zhu, C.-F. Zhang, Y.-Y. Xu, Structure formation and characterization of PVDF hollow fiber membrane prepared via TIPS with diluent mixture, J. Membr. Sci. 319 (2008) 264–270.

[124] S. Rajabzadeh, T. Maruyama, T. Sotani, H. Matsuyama, Preparation of PVDF hollow fiber membrane from a ternary polymer/solvent/nonsolvent system via thermally induced phase separation (TIPS) method, Separ. Purif. Technol. 63 (2008) 415–423.

[125] J. Yang, D.W. Li, Y.K. Lin, X.L. Wang, F. Tian, Z. Wang, Formation of a bicontinuous structure membrane of polyvinylidene fluoride in diphenyl ketone diluent via thermally induced phase separation, J. Appl. Polym. Sci. 110 (2008) 341–347.

[126] X. Han, H. Ding, L. Wang, C. Xiao, Effects of nucleating agents on the porous structure of polyphenylene sulfide via thermally induced phase separation, J. Appl. Polym. Sci. 107 (2008) 2475–2479.

[127] X. Li, Y. Wang, X. Lu, C. Xiao, Morphology changes of polyvinylidene fluoride membrane under different phase separation mechanisms, J. Membr. Sci. 320 (2008) 477–482.

[128] Y.-R. Qiu, N.A. Rahman, H. Matsuyama, Preparation of hydrophilic poly(vinyl butyral)/Pluronic F127 blend hollow fiber membrane via thermally induced phase separation, Separ. Purif. Technol. 61 (2008) 1–8.

[129] X. Lu, X. Li, Preparation of polyvinylidene fluoride membrane via a thermally induced phase separation using a mixed diluent, J. Appl. Polym. Sci. 114 (2009) 1213–1219.

[130] S. Rajabzadeh, T. Maruyama, Y. Ohmukai, T. Sotani, H. Matsuyama, Preparation of PVDF/PMMA blend hollow fiber membrane via thermally induced phase separation (TIPS) method, Separ. Purif. Technol. 66 (2009) 76–83.

[131] Y.-H. Lin, P.-C. Lee, T.-P. Chang, Practical expert diagnosis model based on the grey relational analysis technique, Expert Syst. Appl. 36 (2009) 1523–1528.

[132] Y.K. Lin, G. Chen, J. Yang, X.L. Wang, Formation of isotactic polypropylene membranes with bicontinuous structure and good strength via thermally induced phase separation method, Desalination 236 (2009) 8–15.

[133] Y.-R. Qiu, H. Matsuyama, G.-Y. Gao, Y.-W. Ou, C. Miao, Effects of diluent molecular weight on the performance of hydrophilic poly(vinyl butyral)/Pluronic F127 blend hollow fiber membrane via thermally induced phase separation, J. Membr. Sci. 338 (2009) 128–134.

[134] Y. Tang, Y. Lin, W. Ma, Y. Tian, J. Yang, X. Wang, Preparation of microporous PVDF membrane via tips method using binary diluent of DPK and PG, J. Appl. Polym. Sci. 118 (2010) 3518–3523.

[135] Y.-R. Qiu, H. Matsuyama, Preparation and characterization of poly(vinyl butyral) hollow fiber membrane via thermally induced phase separation with diluent polyethylene glycol 200, Desalination 257 (2010) 117–123.

[136] W. Ma, S. Chen, J. Zhang, X. Wang, Kinetics of thermally induced phase separation in the PVDF blend/methyl salicylate system and its effect on membrane structures, J. Macromol. Sci., Part B 50 (2010) 1–15.

[137] N. Li, C. Xiao, S. Mei, S. Zhang, The multi-pore-structure of polymer–silicon hollow fiber membranes fabricated via thermally induced phase separation combining with stretching, Desalination 274 (2011) 284–291.

[138] N. Ghasem, M. Al-Marzouqi, A. Duaidar, Effect of quenching temperature on the performance of poly(vinylidene fluoride) microporous hollow fiber membranes fabricated via thermally induced phase separation technique on the removal of CO2 from CO2-gas mixture, Int. J. Greenhouse Gas Contr. 5 (2011) 1550–1558.

[139] N. Ghasem, M. Al-Marzouqi, N. Abdul Rahim, Effect of polymer extrusion temperature on poly(vinylidene fluoride) hollow fiber membranes: properties and performance used as gas–liquid membrane contactor for CO2 absorption, Separ. Purif. Technol. 99 (2012) 91–103.

[140] S. Rajabzadeh, C. Liang, Y. Ohmukai, T. Maruyama, H. Matsuyama, Effect of additives on the morphology and properties of poly(vinylidene fluoride) blend hollow fiber membrane prepared by the thermally induced phase separation method, J. Membr. Sci. 423–424 (2012) 189–194.

[141] G.R. Guillen, Y. Pan, M. Li, E.M.V. Hoek, Preparation and characterization of membranes formed by nonsolvent induced phase separation: a review, Ind. Eng. Chem. Res. 50 (2011) 3798–3817.

[142] A.F. Ismail, L.P. Yean, Review on the development of defect-free and ultrathin-skinned asymmetric membranes for gas separation through manipulation of phase inversion and rheological factors, J. Appl. Polym. Sci. 88 (2003) 442–451.

[143] S.S. Shojaie, W.B. Krantz, A.R. Greenberg, Dense polymer film and membrane formation via the dry-cast process part I. Model development, J. Membr. Sci. 94 (1994) 255–280.

[144] S.S. Shojaie, W.B. Krantz, A.R. Greenberg, Dense polymer film and membrane formation via the dry-cast process part II. Model validation and morphological studies, J. Membr. Sci. 94 (1994) 281–298.

[145] H. Matsuyama, M. Teramoto, T. Uesaka, Membrane formation and structure development by dry-cast process, J. Membr. Sci. 135 (1997) 271–288.

[146] H. Matsuyama, M. Nishiguchi, Y. Kitamura, Phase separation mechanism during membrane formation by dry-cast process, J. Appl. Polym. Sci. 77 (2000) 776–783.

[147] S.A. Altinkaya, B. Ozbas, Modeling of asymmetric membrane formation by dry-casting method, J. Membr. Sci. 230 (2004) 71–89.

[148] S.A. Altinkaya, H. Yenal, B. Ozbas, Membrane formation by dry-cast process: model validation through morphological studies, J. Membr. Sci. 249 (2005) 163–172.

[149] C.S. Tsay, A.J. McHugh, Mass transfer dynamics of the evaporation step in membrane formation by phase inversion, J. Membr. Sci. 64 (1991) 81–92.

[150] W. Li, A.J. Ryan, I.K. Meier, Morphology development via reaction-induced phase separation in flexible polyurethane foam, Macromolecules 35 (2002) 5034–5042.

[151] K. Matsuzaka, H. Jinnai, T. Koga, T. Hashimoto, Effect of oscillatory shear deformation on demixing processes of polymer blends, Macromolecules 30 (1997) 1146–1152.

[152] C.S. Tsay, A.J. Mchugh, Mass transfer modeling of asymmetric membrane formation by phase inversion, J. Polym. Sci. B Polym. Phys. 28 (1990) 1327–1365.

[153] P. Radovanovic, S.W. Thiel, S.-T. Hwang, Formation of asymmetric polysulfone membranes by immersion precipitation. Part I. Modelling mass transport during gelation, J. Membr. Sci. 65 (1992) 213–229.

[154] L.-P. Cheng, Y.S. Soh, A.-H. Dwan, C.C. Gryte, An improved model for mass transfer during the formation of polymeric membranes by the immersion-precipitation process, J. Polym. Sci. B Polym. Phys. 32 (1994) 1413–1425.

[155] L.-P. Cheng, A.-H. Dwan, C.C. Gryte, Membrane formation by isothermal precipitation in polyamide-formic acid-water systems II. Precipitation dynamics, J. Polym. Sci. B Polym. Phys. 33 (1995) 223–235.

[156] A.M.W. Bulte, E.M. Naafs, F. van Eeten, M.H.V. Mulder, C.A. Smolders, H. Strathmann, Equilibrium thermodynamics of the ternary membrane-forming system nylon, formic acid and water, Polymer 37 (1996) 1647–1655.

[157] H. Matsuyama, M. Teramoto, R. Nakatani, T. Maki, Membrane formation via phase separation induced by penetration of nonsolvent from vapor phase. I. Phase diagram and mass transfer process, J. Appl. Polym. Sci. 74 (1999) 159–170.

[158] R.M. Boom, I.M. Wienk, T. van den Boomgaard, C.A. Smolders, Microstructures in phase inversion membranes. Part 2. The role of a polymeric additive, J. Membr. Sci. 73 (1992) 277–292.

[159] R.M. Boom, T. van den Boomgaard, C.a. Smolders, Mass transfer and thermodynamics during immersion precipitation for a two-polymer system: evaluation with the system PES—PVP—NMP—water, J. Membr. Sci. 90 (1994) 231–249.

[160] J. Barzin, B. Sadatnia, Theoretical phase diagram calculation and membrane morphology evaluation for water/solvent/polyethersulfone systems, Polymer 48 (2007) 1620–1631.

[161] Y. Yip, A.J. McHugh, Modeling and simulation of nonsolvent vapor-induced phase separation, J. Membr. Sci. 271 (2006) 163–176.

[162] M. Karimi, W. Albrecht, M. Heuchel, T. Weigel, A. Lendlein, Determination of solvent/polymer interaction parameters of moderately concentrated polymer solutions by vapor pressure osmometry, Polymer 49 (2008) 2587–2594.

[163] H. Tompa, Polymer solutions, Academic Press, New York, 1956.

[164] H.J. Lee, B. Jung, Y.S. Kang, H. Lee, Phase separation of polymer casting solution by nonsolvent vapor, J. Membr. Sci. 245 (2004) 103–112.

[165] P. van de Witte, P.J. Dijkstra, J.W.A. van den Berg, J. Feijen, Phase separation processes in polymer solutions in relation to membrane formation, J. Membr. Sci. 117 (1996) 1–31.

[166] W. Lu, Z. Yuan, Y. Zhao, H. Zhang, H. Zhang, X. Li, Porous membranes in secondary battery technologies, Chem. Soc. Rev. 46 (2017) 2199–2236.

[167] H. Matsuyama, M. Teramoto, R. Nakatani, T. Maki, Membrane formation via phase separation induced by penetration of nonsolvent from vapor phase. II. Membrane morphology, J. Appl. Polym. Sci. 74 (1999) 171–178.

[168] R.J. Bearman, Statistical mechanical theory of the diffusion coefficients in binary liquid solutions, J. Chem. Phys. 32 (1960) 1308–1313.

[169] A. Venault, Y. Chang, D.-M. Wang, D. Bouyer, A review on polymeric membranes and hydrogels prepared by vapor-induced phase separation process, Polym. Rev. 53 (2013) 568–626.

[170] J. Vrentas, J. Duda, Diffusion of large penetrant molecules in amorphous polymers, J. Polym. Sci. Polym. Phys. Ed 17 (1979) 1085–1096.

[171] P.E. Price Jr., I.H. Romdhane, Multicomponent diffusion theory and its applications to polymer-solvent systems, AIChE J. 49 (2003) 309–322.

[172] S. Alsoy, J.L. Duda, Modeling of multicomponent drying of polymer films, AIChE J. 45 (1999) 896–905.

[173] J.M. Zielinski, B.F. Hanley, Practical friction-based approach to modeling multicomponent diffusion, AIChE J. 45 (1999) 1–12.

[174] D. Bouyer, C. Pochat-Bohatier, Validation of mass-transfer model for VIPS process using in situ measurements performed by near-infrared spectroscopy, AIChE J. 59 (2013) 671–686.

[175] F.P. Incropera, A.S. Lavine, T.L. Bergman, D.P. DeWitt, Fundamentals of Heat and Mass Transfer, Wiley, 2007.

[176] Y.-h. Tang, Y.-d. He, X.-l. Wang, Three-dimensional analysis of membrane formation via thermally induced phase separation by dissipative particle dynamics simulation, J. Membr. Sci. 437 (2013) 40–48.

[177] M. Hideto, T. Masaaki, N. Ryo, M. Taisuke, Membrane formation via phase separation induced by penetration of nonsolvent from vapor phase. II. Membrane morphology, J. Appl. Polym. Sci. 74 (1999) 171–178.

[178] N. Peng, T.-S. Chung, M.L. Chng, W. Aw, Evolution of ultra-thin dense-selective layer from single-layer to dual-layer hollow fibers using novel Extem® polyetherimide for gas separation, J. Membr. Sci. 360 (2010) 48–57.

[179] L. Gao, B. Tang, P. Wu, An experimental investigation of evaporation time and the relative humidity on a novel positively charged ultrafiltration membrane via dry–wet phase inversion, J. Membr. Sci. 326 (2009) 168–177.

[180] M. Bodzek, J. Bohdziewicz, Porous polycarbonate phase-inversion membranes, J. Membr. Sci. 60 (1991) 25–40.

[181] H. Matsuyama, M. Teramoto, R. Nakatani, T. Maki, membrane formation via phase separation induced by penetration of nonsolvent from vapor phase. I. Phase diagram and mass transfer process, J. Appl. Polym. Sci. 74 (1999) 159–170.

[182] Y. Peng, H. Fan, J. Ge, S. Wang, P. Chen, Q. Jiang, The effects of processing conditions on the surface morphology and hydrophobicity of polyvinylidene fluoride membranes prepared via vapor-induced phase separation, Appl. Surf. Sci. 263 (2012) 737–744.

[183] A.B.D. Cassie, S. Baxter, Wettability of porous surfaces, Trans. Faraday Soc. 40 (1944) 546–551.

[184] Q. Wang, Z. Wang, Z. Wu, Effects of solvent compositions on physicochemical properties and anti-fouling ability of PVDF microfiltration membranes for wastewater treatment, Desalination 297 (2012) 79–86.

[185] M. Gironès, I.J. Akbarsyah, W. Nijdam, C.J.M. van Rijn, H.V. Jansen, R.G. H. Lammertink, M. Wessling, Polymeric microsieves produced by phase separation micromolding, J. Membr. Sci. 283 (2006) 411–424.

[186] M. Ulbricht, O. Schuster, W. Ansorge, M. Ruetering, P. Steiger, Influence of the strongly anisotropic cross-section morphology of a novel polyethersulfone microfiltration membrane on filtration performance, Separ. Purif. Technol. 57 (2007) 63–73.

[187] N. Widjojo, T.S. Chung, W.B. Krantz, A morphological and structural study of Ultem/P84 copolyimide dual-layer hollow fiber membranes with delamination-free morphology, J. Membr. Sci. 294 (2007) 132–146.

[188] D.-M. Wang, F.-C. Lin, J.-C. Chiang, J.-Y. Lai, Control of the porosity of asymmetric TPX membranes, J. Membr. Sci. 141 (1998) 1–12.

[189] H. Strathmann, K. Kock, P. Amar, R.W. Baker, The formation mechanism of asymmetric membranes, Desalination 16 (1975) 179–203.

[190] M.A. Frommer, D. Lancet, The mechanism of membrane formation: membrane structures and their relation to preparation conditions, in: H.K. Lonsdale, H. E. Podall (Eds.), Reverse Osmosis Membrane Research: Based on the Symposium on "Polymers for Desalination" Held at the 162nd National Meeting of the American Chemical Society in Washington, D.C., September 1971, Springer US, Boston, MA, 1972, pp. 85–110.

[191] C.-L. Li, D.-M. Wang, A. Deratani, D. Quémener, D. Bouyer, J.-Y. Lai, Insight into the preparation of poly(vinylidene fluoride) membranes by vapor-induced phase separation, J. Membr. Sci. 361 (2010) 154–166.

[192] T. Marino, F. Galiano, A. Molino, A. Figoli, New frontiers in sustainable membrane preparation: cyrene™ as green bioderived solvent, J. Membr. Sci. (2019) 580.

[193] T. Marino, S. Blefari, E. Di Nicolò, A. Figoli, A more sustainable membrane preparation using triethyl phosphate as solvent, in: Green Processing and Synthesis, 2017, p. 295.

[194] M.B. Thürmer, P. Poletto, M. Marcolin, J. Duarte, M. Zeni, Effect of non-solvents used in the coagulation bath on morphology of PVDF membranes, Mater. Res. 15 (2012) 884–890.

[195] S.P. Deshmukh, K. Li, Effect of ethanol composition in water coagulation bath on morphology of PVDF hollow fibre membranes, J. Membr. Sci. 150 (1998) 75–85.

[196] A.L. Ahmad, W.K.W. Ramli, W.J.N. Fernando, W.R.W. Daud, Effect of ethanol concentration in water coagulation bath on pore geometry of PVDF membrane for Membrane Gas Absorption application in CO2 removal, Separ. Purif. Technol. 88 (2012) 11–18.

[197] Y.L. Thuyavan, N. Anantharaman, G. Arthanareeswaran, A.F. Ismail, Impact of solvents and process conditions on the formation of polyethersulfone membranes and its fouling behavior in lake water filtration, J. Chem. Technol. Biotechnol. 91 (2016) 2568–2581.

[198] G. Arthanareeswaran, V.M. Starov, Effect of solvents on performance of polyethersulfone ultrafiltration membranes: investigation of metal ion separations, Desalination 267 (2011) 57–63.

[199] T. Marino, F. Galiano, S. Simone, A. Figoli, DMSO EVOL™ as novel non-toxic solvent for polyethersulfone membrane preparation, Environ. Sci. Pollut. Control Ser. 26 (2019) 14774–14785.

[200] S.P. Sun, K.Y. Wang, N. Peng, T.A. Hatton, T.-S. Chung, Novel polyamide-imide/cellulose acetate dual-layer hollow fiber membranes for nanofiltration, J. Membr. Sci. 363 (2010) 232–242.

[201] A. Venault, A.J. Jumao-as-Leyba, Z.-R. Yang, S. Carretier, Y. Chang, Formation mechanisms of low-biofouling PVDF/F127 membranes prepared by VIPS process, J. Taiwan Inst. Chem. Eng. 62 (2016) 297–306.

[202] Q. Ye, L. Cheng, L. Zhang, L. Xing, H. Chen, Preparation of symmetric network PVDF membranes for protein adsorption via vapor-induced phase separation, J. Macromol. Sci., Part B 50 (2011) 2004–2022.

[203] M.-J. Han, S.-T. Nam, Thermodynamic and rheological variation in polysulfone solution by PVP and its effect in the preparation of phase inversion membrane, J. Membr. Sci. 202 (2002) 55–61.

[204] S. Zhao, Z. Wang, X. Wei, X. Tian, J. Wang, S. Yang, S. Wang, Comparison study of the effect of PVP and PANI nanofibers additives on membrane formation mechanism, structure and performance, J. Membr. Sci. 385–386 (2011) 110–122.

[205] M. Bikel, I.G.M. Pünt, R.G.H. Lammertink, M. Wessling, Micropatterned polymer films by vapor-induced phase separation using permeable molds, ACS Appl. Mater. Interfaces 1 (2009) 2856–2861.

[206] W. Doyen, W. Mues, B. Molenberghs, B. Cobben, Spacer fabric supported flat-sheet membranes: a new era of flat-sheet membrane technology, Desalination 250 (2010) 1078–1082.

[207] M. Bikel, P.Z. Çulfaz, L.A.M. Bolhuis-Versteeg, J.G. Pérez, R.G.H. Lammertink, M. Wessling, Polymeric microsieves via phase separation microfabrication: process and design optimization, J. Membr. Sci. 347 (2010) 93–100.

[208] S.S. Madaeni, N.T. Hasankiadeh, A.R. Kurdian, A. Rahimpour, Modeling and optimization of membrane fabrication using artificial neural network and genetic algorithm, Separ. Purif. Technol. 76 (2010) 33–43.

[209] N.A. Ochoa, P. Prádanos, L. Palacio, C. Pagliero, J. Marchese, A. Hernández, Pore size distributions based on AFM imaging and retention of multidisperse polymer solutes: characterisation of polyethersulfone UF membranes with dopes containing different PVP, J. Membr. Sci. 187 (2001) 227–237.

[210] A. Venault, Y. Chang, D.-M. Wang, D. Bouyer, A. Higuchi, J.-Y. Lai, PEGylation of anti-biofouling polysulfone membranes via liquid- and vapor-induced phase separation processing, J. Membr. Sci. 403–404 (2012) 47–57.

[211] A. Venault, Y. Chang, Surface hydrophilicity and morphology control of anti-biofouling polysulfone membranes via vapor-induced phase separation processing, J. Nanosci. Nanotechnol. 13 (2013) 2656–2666.

[212] H. Susanto, M. Ulbricht, Characteristics, performance and stability of polyethersulfone ultrafiltration membranes prepared by phase separation method using different macromolecular additives, J. Membr. Sci. 327 (2009) 125–135.

[213] J.-H. Kim, K.-H. Lee, Effect of PEG additive on membrane formation by phase inversion, J. Membr. Sci. 138 (1998) 153–163.

[214] J.-J. Shieh, T.-S. Chung, R. Wang, M.P. Srinivasan, D.R. Paul, Gas separation performance of poly(4-vinylpyridine)/polyetherimide composite hollow fibers, J. Membr. Sci. 182 (2001) 111–123.

[215] S.M. Mousavi, A. Zadhoush, Investigation of the relation between viscoelastic properties of polysulfone solutions, phase inversion process and membrane morphology: the effect of solvent power, J. Membr. Sci. 532 (2017) 47–57.

[216] R.E. Kesting, A.K. Fritzsche, M.K. Murphy, C.A. Cruse, A.C. Handermann, R. F. Malon, M.D. Moore, The second-generation polysulfone gas-separation membrane. I. The use of lewis acid: base complexes as transient templates to increase free volume, J. Appl. Polym. Sci. 40 (1990) 1557–1574.

[217] S. Doi, K. Hamanaka, Pore size control technique in the spinning of polysulfone hollow fiber ultrafiltration membranes, Desalination 80 (1991) 167–180.

[218] C.A. Smolders, A.J. Reuvers, R.M. Boom, I.M. Wienk, Microstructures in phase-inversion membranes. Part 1. Formation of macrovoids, J. Membr. Sci. 73 (1992) 259–275.

[219] S.K. Yong, J.K. Hyo, Y.K. Un, Asymmetric membrane formation via immersion precipitation method. I. Kinetic effect, J. Membr. Sci. 60 (1991) 219–232.

[220] I.-C. Kim, K.-H. Lee, T.-M. Tak, Preparation and characterization of integrally skinned uncharged polyetherimide asymmetric nanofiltration membrane, J. Membr. Sci. 183 (2001) 235–247.

[221] D.-M. Wang, T.-T. Wu, F.-C. Lin, J.-Y. Hou, J.-Y. Lai, A novel method for controlling the surface morphology of polymeric membranes, J. Membr. Sci. 169 (2000) 39–51.

[222] S.-J. Shin, J.-P. Kim, H.-J. Kim, J.-H. Jeon, B.-R. Min, Preparation and characterization of polyethersulfone microfiltration membranes by a 2-methox-yethanol additive, Desalination 186 (2005) 1–10.

[223] H. Sun, S. Liu, B. Ge, L. Xing, H. Chen, Cellulose nitrate membrane formation via phase separation induced by penetration of nonsolvent from vapor phase, J. Membr. Sci. 295 (2007) 2–10.

[224] I. Soroko, M. Makowski, F. Spill, A. Livingston, The effect of membrane formation parameters on performance of polyimide membranes for organic solvent nanofiltration (OSN). Part B: analysis of evaporation step and the role of a co-solvent, J. Membr. Sci. 381 (2011) 163–171.

[225] A.K. Hołda, I.F.J. Vankelecom, Integrally skinned PSf-based SRNF-membranes prepared via phase inversion—Part B: influence of low molecular weight additives, J. Membr. Sci. 450 (2014) 499–511.

[226] P. Vandezande, X. Li, L.E.M. Gevers, I.F.J. Vankelecom, High throughput study of phase inversion parameters for polyimide-based SRNF membranes, J. Membr. Sci. 330 (2009) 307–318.

[227] A.K. Hołda, B. Aernouts, W. Saeys, I.F.J. Vankelecom, Study of polymer concentration and evaporation time as phase inversion parameters for polysulfone-based SRNF membranes, J. Membr. Sci. 442 (2013) 196–205.

[228] M. Mulder, Basic Principles of Membrane Technology, Kluwer Academic Publisher, Dordrecht, The Netherlands, 2003.

[229] A. Dehban, A. Kargari, F. Zokaee Ashtiani, Preparation and characterization of an antifouling poly (phenyl sulfone) ultrafiltration membrane by vapor-induced phase separation technique, Separ. Purif. Technol. 212 (2019) 986–1000.

[230] Z. Chen, M. Deng, Y. Chen, G. He, M. Wu, J. Wang, Preparation and performance of cellulose acetate/polyethyleneimine blend microfiltration membranes and their applications, J. Membr. Sci. 235 (2004) 73–86.

[231] T. Marino, F. Russo, A. Figoli, The formation of polyvinylidene fluoride membranes with tailored properties via vapour/non-solvent induced phase separation, Membranes 8 (2018) 71.

[232] J. Dai, X.-l. Xu, J.-h. Yang, N. Zhang, T. Huang, Y. Wang, Z.-w. Zhou, C.-l. Zhang, Greatly enhanced porosity of stretched polypropylene/graphene oxide composite membrane achieved by adding pore-forming agent, RSC Adv. 5 (2015) 20663–20673.

[233] L.-J. Zhu, H.-M. Song, G. Wang, Z.-X. Zeng, C.-T. Zhao, Q.-J. Xue, X.-P. Guo, Microstructures and performances of pegylated polysulfone membranes from an in situ synthesized solution via vapor induced phase separation approach, J. Colloid Interface Sci. 515 (2018) 152–159.

[234] L. Zhu, H. Song, G. Wang, Z. Zeng, Q. Xue, Symmetrical polysulfone/poly(acrylic acid) porous membranes with uniform wormlike morphology and pH responsibility: preparation, characterization and application in water purification, J. Membr. Sci. 549 (2018) 515–522.

[235] S.P. Sun, T.A. Hatton, S.Y. Chan, K.-L. Chung, Novel thin-film composite nanofiltration hollow fiber membranes with double repulsion for effective removal of emerging organic matters from water, J. Membr. Sci. 401–402 (2012) 152–162.

[236] H. Fan, Y. Peng, Z. Li, P. Chen, Q. Jiang, Shaobin Wang, Preparation and characterization of hydrophobic PVDF membranes by vapor-induced phase separation and application in vacuum membrane distillation, J. Polym. Res. 20 (2013).

[237] F.A. AlMarzooqi, M.R. Bilad, H.A. Arafat, Development of PVDF membranes for membrane distillation via vapour induced crystallisation, Eur. Polym. J. 77 (2016) 164–173.

[238] M.-J. Han, D. Bhattacharyya, Changes in morphology and transport characteristics of polysulfone membranes prepared by different demixing conditions, J. Membr. Sci. 98 (1995) 191–200.

[239] C. Alexowsky, M. Bojarska, M. Ulbricht, Porous poly(vinylidene fluoride) membranes with tailored properties by fast and scalable non-solvent vapor induced phase separation, J. Membr. Sci. 577 (2019) 69–78.

[240] C. H, M. P, D. A, D. C, Influence of the relative humidity on film formation by vapor induced phase separation, Polym. Eng. Sci. 43 (2003) 798–808.

[241] D.-J. Lin, K. Beltsios, T.-H. Young, Y.-S. Jeng, L.-P. Cheng, Strong effect of precursor preparation on the morphology of semicrystalline phase inversion poly (vinylidene fluoride) membranes, J. Membr. Sci. 274 (2006) 64–72.

[242] X. Wang, X. Wang, L. Zhang, Q. An, H. Chen, Morphology and formation mechanism of poly(vinylidene fluoride) membranes prepared with immerse precipitation: effect of dissolving temperature, J. Macromol. Sci., Part B 48 (2009) 696–709.

[243] A. Gugliuzza, E. Drioli, New performance of hydrophobic fluorinated porous membranes exhibiting particulate-like morphology, Desalination 240 (2009) 14–20.

[244] M. Benz, W.B. Euler, O.J. Gregory, The role of solution phase water on the deposition of thin films of poly(vinylidene fluoride), Macromolecules 35 (2002) 2682–2688.

[245] H. Matsuyama, Y. Takida, T. Maki, M. Teramoto, Preparation of porous membrane by combined use of thermally induced phase separation and immersion precipitation, Polymer 43 (2002) 5243–5248.

[246] J.T. Jung, J.F. Kim, H.H. Wang, E. di Nicolo, E. Drioli, Y.M. Lee, Understanding the non-solvent induced phase separation (NIPS) effect during the fabrication of microporous PVDF membranes via thermally induced phase separation (TIPS), J. Membr. Sci. 514 (2016) 250–263.

[247] Y. Liu, T. Xiao, C. Bao, Y. Fu, X. Yang, Fabrication of novel Janus membrane by nonsolvent thermally induced phase separation (NTIPS) for enhanced performance in membrane distillation, J. Membr. Sci. 563 (2018) 298–308.

[248] F.G. Paulsen, S.S. Shojaie, W.B. Krantz, Effect of evaporation step on macrovoid formation in wet-cast polymeric membranes, J. Membr. Sci. 91 (1994) 265–282.

[249] H. Julian, P.D. Sutrisna, A.N. Hakim, H.O. Harsono, Y.A. Hugo, I.G. Wenten, Nano-silica/polysulfone asymmetric mixed-matrix membranes (MMMs) with high CO2 permeance in the application of CO2/N2 separation, Polym. Plast. Technol. Mater. 58 (2019) 678–689.

[250] Y. Dai, Q. Li, X. Ruan, Y. Hou, X. Jiang, X. Yan, G. He, F. Meng, Z. Wang, Fabrication of defect-free Matrimid® asymmetric membranes and the elevated temperature application for N2/SF6 separation, J. Membr. Sci. 577 (2019) 258–265.

[251] T.-S. Chung, Z.-L. Xu, W. Lin, Fundamental understanding of the effect of air-gap distance on the fabrication of hollow fiber membranes, J. Appl. Polym. Sci. 72 (1999) 379–395.

[252] L. Jiang, T.-S. Chung, D.F. Li, C. Cao, S. Kulprathipanja, Fabrication of Matrimid/ polyethersulfone dual-layer hollow fiber membranes for gas separation, J. Membr. Sci. 240 (2004) 91–103.

[253] D. Li, T.-S. Chung, J. Ren, R. Wang, Thickness dependence of macrovoid evolution in wet phase-inversion asymmetric membranes, Ind. Eng. Chem. Res. 43 (2004) 1553–1556.

[254] S. Bonyadi, T.S. Chung, W.B. Krantz, Investigation of corrugation phenomenon in the inner contour of hollow fibers during the non-solvent induced phase-separation process, J. Membr. Sci. 299 (2007) 200–210.

[255] T. Marino, E. Blasi, S. Tornaghi, E. Di Nicolò, A. Figoli, Polyethersulfone membranes prepared with Rhodiasolv®Polarclean as water soluble green solvent, J. Membr. Sci. 549 (2018) 192–204.

[256] R.G. Chapman, E. Ostuni, S. Takayama, R.E. Holmlin, L. Yan, G.M. Whitesides, Surveying for surfaces that resist the adsorption of proteins, J. Am. Chem. Soc. 122 (2000) 8303–8304.

[257] R.G. Chapman, E. Ostuni, M.N. Liang, G. Meluleni, E. Kim, L. Yan, G. Pier, H. S. Warren, G.M. Whitesides, Polymeric thin films that resist the adsorption of proteins and the adhesion of bacteria, Langmuir 17 (2001) 1225–1233.

[258] S. Chen, L. Li, C. Zhao, J. Zheng, Surface hydration: principles and applications toward low-fouling/nonfouling biomaterials, Polymer 51 (2010) 5283–5293.

[259] D. Rana, T. Matsuura, Surface modifications for antifouling membranes, Chem. Rev. 110 (2010) 2448–2471.

[260] L.-J. Zhu, H-M. Song, C. Li, G. Wang, Z.-X. Zeng, Q.-J. Xue, Surface wormlike morphology control of polysulfone/poly(N-isopropylacrylamide) membranes by tuning the two-stage phase separation and their thermo-responsive permselectivity, J. Membr. Sci. 555 (2018) 290–298.

[261] Y.-C. Chiag, Y. Chang, W.-Y. Chen, R.-c. Ruaan, Biofouling resistance of ultrafiltration membranes controlled by surface self-assembled coating with PEGylated copolymers, Langmuir 28 (2012) 1399–1407.

[262] N.-J. Lin, H.-S. Yang, Y. Chang, K.-L. Tung, W.-H. Chen, H.-W. Cheng, S.-W. Hsiao, P. Aimar, K. Yamamoto, J.-Y. Lai, Surface self-assembled PEGylation of fluoro-based PVDF membranes via hydrophobic-driven copolymer anchoring for ultra-stable biofouling resistance, Langmuir 29 (2013) 10183–10193.

[263] A. Venault, J.-R. Wu, Y. Chang, P. Aimar, Fabricating hemocompatible bi-continuous PEGylated PVDF membranes via vapor-induced phase inversion, J. Membr. Sci. 470 (2014) 18–29.

[264] A. Venault, M.R.B. Ballad, Y.-T. Huang, Y.-H. Liu, C.-H. Kao, Y. Chang, Antifouling PVDF membrane prepared by VIPS for microalgae harvesting, Chem. Eng. Sci. 142 (2016) 97–111.

[265] S. Carretier, L.-A. Chen, A. Venault, Z.-R. Yang, P. Aimar, Y. Chang, Design of PVDF/PEGMA-b-PS-b-PEGMA membranes by VIPS for improved biofouling mitigation, J. Membr. Sci. 510 (2016) 355–369.

[266] G.V. Dizon, A. Venault, Direct in-situ modification of PVDF membranes with a zwitterionic copolymer to form bi-continuous and fouling resistant membranes, J. Membr. Sci. 550 (2018) 45–58.

[267] A. Venault, C.-H. Hsu, K. Ishihara, Y. Chang, Zwitterionic bi-continuous membranes from a phosphobetaine copolymer/poly(vinylidene fluoride) blend via VIPS for biofouling mitigation, J. Membr. Sci. 550 (2018) 377–388.

[268] K. Ishihara, H. Hanyuda, N. Nakabayashi, Synthesis of phospholipid polymers having a urethane bond in the side chain as coating material on segmented polyurethane and their platelet adhesion-resistant properties, Biomaterials 16 (1995) 873–879.

[269] O. Benhabiles, F. Galiano, T. Marino, H. Mahmoudi, H. Lounici, A. Figoli, Preparation and characterization of TiO2-PVDF/PMMA blend membranes using an alternative non-toxic solvent for UF/MF and photocatalytic application, Molecules (2019) 24.

[270] H. Fan, Y. Peng, Application of PVDF membranes in desalination and comparison of the VMD and DCMD processes, Chem. Eng. Sci. 79 (2012) 94–102.

[271] F. Abdulla AlMarzooqi, M. Roil Bilad, H. Ali Arafat, Improving liquid entry pressure of polyvinylidene fluoride (PVDF) membranes by exploiting the role of fabrication parameters in vapor-induced phase separation VIPS and non-solvent-induced phase separation (NIPS) processes, Appl. Sci. 7 (2017) 181.

[272] A. Alkhudhiri, N. Darwish, N. Hilal, Membrane distillation: a comprehensive review, Desalination 287 (2012) 2–18.

[273] G.-d. Kang, Y.-m. Cao, Application and modification of poly(vinylidene fluoride) (PVDF) membranes – a review, J. Membr. Sci. 463 (2014) 145–165.

[274] Y.-S. Park, C.-K. Lee, S.-K. Kim, H.-J. Oh, S.-H. Lee, J.-S. Choi, Effect of temperature difference on performance of membrane crystallization-based membrane distillation system, Desal. Water Treat. 51 (2013) 1362–1365.

[275] A. Venault, A.J. Jumao-as-Leyba, F.-C. Chou, D. Bouyer, I.J. Lin, T.-C. Wei, Y. Chang, Design of near-superhydrophobic/superoleophilic PVDF and PP membranes for the gravity-driven breaking of water-in-oil emulsions, J. Taiwan Inst. Chem. Eng. 65 (2016) 459–471.

[276] W. Zhang, Z. Shi, F. Zhang, X. Liu, J. Jin, L. Jiang, Superhydrophobic and superoleophilic PVDF membranes for effective separation of water-in-oil emulsions with high flux, Adv. Mater. 25 (2013) 2071–2076.

[277] A. Venault, C.-H. Chiang, H.-Y. Chang, W.-S. Hung, Y. Chang, Graphene oxide/ PVDF VIPS membranes for switchable, versatile and gravity-driven separation of oil and water, J. Membr. Sci. 565 (2018) 131–144.

[278] A. Venault, C.-Y. Chang, T.-C. Tsai, H.-Y. Chang, D. Bouyer, K.-R. Lee, Y. Chang, Surface zwitterionization of PVDF VIPS membranes for oil and water separation, J. Membr. Sci. 563 (2018) 54–64.

[279] F. Tasselli, J.C. Jansen, F. Sidari, E. Drioli, Morphology and transport property control of modified poly(ether ether ketone) (PEEKWC) hollow fiber membranes prepared from PEEKWC/PVP blends: influence of the relative humidity in the air gap, J. Membr. Sci. 255 (2005) 13–22.

[280] F. Wu, Z. Xu, Z. Wang, Y. Shi, L. Li, Z. Zhang, Membrane-based air separation for catalytic oxidation of isolongifolene, Chem. Eng. J. 158 (2010) 426–430.

[281] A. Montembault, C. Viton, A. Domard, Rheometric study of the gelation of chitosan in aqueous solution without cross-linking agent, Biomacromolecules 6 (2005) 653–662.

[282] C. Pochat-Bohatier, A. Venault, D. Bouyer, L. Vachoud, L. David, C. Faur, Development and characterization of composite chitosan/active carbon hydrogels for a medical application, J. Appl. Polym. Sci. 128 (2013) 2945–2953.

[283] Y. Chakrabandhu, C. Pochat-Bohatier, L. Vachoud, D. Bouyer, J.P. Desfours, Control of elaboration process to form chitin-based membrane for biomedical applications, Desalination 233 (2008) 120–128.

[284] D. Bouyer, L. Vachoud, Y. Chakrabandhu, C. Pochat-Bohatier, Influence of mass transfer on gelation time using VIPS-gelation process for chitin dissolved in LiCl/ NMP solvent—modelling and experimental study, Chem. Eng. J. 157 (2010) 605–619.

[285] A. Venault, D. Bouyer, C. Pochat-Bohatier, L. Vachoud, C. Faur, Investigation of chitosan gelation mechanisms by a modeling approach coupled to local experimental measurement, AIChE J. 58 (2012) 2226–2240.

[286] A. Venault, D. Bouyer, C. Pochat-Bohatier, L. Vachoud, C. Faur, Preparation of composite hydrogels for medical applications: experimental study and modeling of mass transfers, in: International Journal of Chemical Reactor Engineering, 2010.

[287] A. Venault, D. Bouyer, C. Pochat-Bohatier, C. Faur, L. Vachoud, Modeling the mass transfers during the elaboration of chitosan-activated carbon composites for medical applications, AIChE J. 56 (2010) 1593–1609.

[288] D. Ma, A.J. McHugh, The interplay of phase inversion and membrane formation in the drug release characteristics of a membrane-based delivery system, J. Membr. Sci. 298 (2007) 156–168.

[289] L. Vachoud, D. Bouyer, C. Pochat-Bohatier, C. Faur, Rheometric study of chitosan/activated carbon composite hydrogels for medical applications using an experimental design, J. Appl. Polym. Sci. 120 (2011) 808–820.

[290] M. Skyllas-Kazacos, M.H. Chakrabarti, S.A. Hajimolana, F.S. Mjalli, M. Saleem, Progress in flow battery research and development, J. Electrochem. Soc. 158 (2011) R55–R79.

[291] W. Wang, Q. Luo, B. Li, X. Wei, L. Li, Z. Yang, Recent progress in redox flow battery research and development, Adv. Funct. Mater. 23 (2013) 970–986.

[292] A.Z. Weber, M.M. Mench, J.P. Meyers, P.N. Ross, J.T. Gostick, Q. Liu, Redox flow batteries: a review, J. Appl. Electrochem. 41 (2011) 1137.

[293] T. Liu, X. Li, H. Zhang, J. Chen, Progress on the electrode materials towards vanadium flow batteries (VFBs) with improved power density, J. Energy Chem. 27 (2018) 1292–1303.

[294] A. Parasuraman, T.M. Lim, C. Menictas, M. Skyllas-Kazacos, Review of material research and development for vanadium redox flow battery applications, Electrochim. Acta 101 (2013) 27–40.

[295] M.-s.J. Jung, J. Parrondo, C.G. Arges, V. Ramani, Polysulfone-based anion exchange membranes demonstrate excellent chemical stability and performance for the all-vanadium redox flow battery, J. Mater. Chem. 1 (2013) 10458–10464.

[296] S. Zhang, B. Zhang, D. Xing, X. Jian, Poly(phthalazinone ether ketone ketone) anion exchange membranes with pyridinium as ion exchange groups for vanadium redox flow battery applications, J. Mater. Chem. 1 (2013) 12246–12254.

[297] S. Winardi, S.C. Raghu, M.O. Oo, Q. Yan, N. Wai, T.M. Lim, M. Skyllas-Kazacos, Sulfonated poly (ether ether ketone)-based proton exchange membranes for vanadium redox battery applications, J. Membr. Sci. 450 (2014) 313–322.

[298] T. Luo, O. David, Y. Gendel, M. Wessling, Porous poly(benzimidazole) membrane for all vanadium redox flow battery, J. Power Sources 312 (2016) 45–54.

[299] Z. Yuan, Y. Duan, H. Zhang, X. Li, H. Zhang, I. Vankelecom, Advanced porous membranes with ultra-high selectivity and stability for vanadium flow batteries, Energy Environ. Sci. 9 (2016) 441–447.

[300] T. Luo, B. Dreusicke, M. Wessling, Tuning the ion selectivity of porous poly(2,5-benzimidazole) membranes by phase separation for all vanadium redox flow batteries, J. Membr. Sci. 556 (2018) 164–177.

[301] P. Leung, A.A. Shah, L. Sanz, C. Flox, J.R. Morante, Q. Xu, M.R. Mohamed, C. Ponce de León, F.C. Walsh, Recent developments in organic redox flow batteries: a critical review, J. Power Sources 360 (2017) 243–283.

[302] Z. Yang, L. Tong, D.P. Tabor, E.S. Beh, M.-A. Goulet, D. De Porcellinis, A. Aspuru-Guzik, R.G. Gordon, M.J. Aziz, Alkaline benzoquinone aqueous flow battery for large-scale storage of electrical energy, Adv. Energy Mater. 8 (2018) 1702056.

[303] Z. Yang, L. Tong, D.P. Tabor, E.S. Beh, M.-A. Goulet, D. De Porcellinis, A. Aspuru-Guzik, R.G. Gordon, M.J. Aziz, Flow batteries: alkaline benzoquinone aqueous flow battery for large-scale storage of electrical energy (adv. Energy mater. 8/2018), Adv. Energy Mater. 8 (2018) 1870034.

[304] X. Huang, Separator technologies for lithium-ion batteries, J. Solid State Electrochem. 15 (2011) 649–662.

[305] A. Deratani, D. Quemener, D. Bouyer, B.C. Pochat, C.L. Li, J.Y. Lai, D.M. Wang, PVDF membranes has superhydrophobic surface, in: U.d.M.I. Centre National de la Recherche Scientifique CNRS, Arkema France (Ed.), France, 2010.

[306] N. Jabeen, A. Hussain, Q. Xia, S. Sun, J. Zhu, H. Xia, High-performance 2.6 V aqueous asymmetric supercapacitors based on in situ formed Na0.5MnO2 nanosheet assembled nanowall arrays, Adv. Mater. 29 (2017) 1700804.

[307] P. Simon, Y. Gogotsi, Materials for electrochemical capacitors, Nat. Mater. 7 (2008) 845.

[308] Q. Xue, J. Sun, Y. Huang, M. Zhu, Z. Pei, H. Li, Y. Wang, N. Li, H. Zhang, C. Zhi, Recent progress on flexible and wearable supercapacitors, Small 13 (2017) 1701827.

[309] W. Dong, X. Niu, X. Ji, Y. Chen, L.-B. Kong, L. Kang, F. Ran, Transferring electrochemically active nanomaterials into a flexible membrane electrode via slow phase separation method induced by water vapor, ACS Sustain. Chem. Eng. 7 (2019) 4295–4306.

[310] Y.-D. He, Y.-H. Tang, X.-L. Wang, Dissipative particle dynamics simulation on the membrane formation of polymer–diluent system via thermally induced phase separation, J. Membr. Sci. 368 (2011) 78–85.

[311] Y.-h. Tang, Y.-d. He, X.-l. Wang, Investigation on the membrane formation process of polymer–diluent system via thermally induced phase separation accompanied with mass transfer across the interface: dissipative particle dynamics simulation and its experimental verification, J. Membr. Sci. 474 (2015) 196–206.

[312] Y.-h. Tang, H.-h. Lin, T.-y. Liu, H. Matsuyama, X.-l. Wang, Multiscale simulation on the membrane formation process via thermally induced phase separation accompanied with heat transfer, J. Membr. Sci. 515 (2016) 258–267.

[313] J.F. Hester, P. Banerjee, A.M. Mayes, Preparation of protein-resistant surfaces on poly(vinylidene fluoride) membranes via surface segregation, Macromolecules 32 (1999) 1643–1650.

[314] S. Chen, S. Jiang, An new avenue to nonfouling materials, Adv. Mater. 20 (2008) 335–338.

[315] Y.-W. Chen, A. Venault, J.-F. Jhong, H.-T. Ho, C.-C. Liu, R.-H. Lee, G.-H. Hsiue, Y. Chang, Developing blood leukocytes depletion membranes from the design of bio-inert PEGylated hydrogel interfaces with surface charge control, J. Membr. Sci. 537 (2017) 209–219.